

**CHARACTERIZING THE REGULATION AND FUNCTION OF THE
SUMO-SPECIFIC ISOPEPTIDASE SENP2**

by
Hana' M. Odeh

A dissertation submitted to Johns Hopkins University in conformity with the
requirements for the degree of Doctor of Philosophy

Baltimore, Maryland
September 2018

© 2018 Hana' M. Odeh
All Rights Reserved

ABSTRACT

The small ubiquitin-related modifier (SUMO) protein is post-translationally and covalently attached to a multitude of other proteins, regulating a plethora of essential cellular functions in the nucleus and the cytoplasm. Recent evidence links SUMO to membrane-associated functions, however, the mechanism of SUMO regulation at membranes remains largely unknown. To look at SUMO regulation, we focused on characterizing the subcellular localizations and functions of the SUMO-specific isopeptidases, collectively known as SENPs, since they comprise the largest family of SUMO proteases and are major regulators of SUMO dynamics. SENPs share a conserved C-terminal catalytic domain, but have divergent N-terminal domains containing targeting signals that determine their unique subcellular localizations and substrate specificities. In this thesis, we characterized the N-terminal domain of the mammalian SUMO-specific protease SENP2. We found that SENP2 can directly interact with intracellular membranes via a unique N-terminal amphipathic α -helix. We also show that SENP2-membrane interaction is directly regulated by Karyopherin- α (Kap- α). Furthermore, we identified SENP2 interacting proteins using BioID, which revealed that SENP2 interacts with a subset of ER-, Golgi-, and inner nuclear membrane-associated proteins. We also developed a new technique to identify SENP2 substrates. Collectively, our findings demonstrate the critical role N-terminal targeting signals play in the differential regulation of SUMO proteases, and indicate that SENP2 may play a role in regulating sumoylation at membranes.

Advisor: Dr. Michael J. Matunis

Primary Readers:

Dr. Carolyn Machamer, Dr. Daniel Raben, Dr. Valeria Culotta, and Dr. Sean Prigge

Secondary Readers:

Dr. Philip Jordan, and Dr. Conor McMeniman

ACKNOWLEDGEMENTS

It is a privilege to be a trainee in the Matunis lab. Because of Mike, I can finally say that I am equipped with the tools to become a scientist. I've gained new perspectives on the meaning and importance of basic research. I've learned that yesterday's control is not today's control. I've learned how to carefully plan experiments, and that repetition is a vital part of RE-search! Mike's precision, attention to detail, dedication and support are unmatched. I am in debt for all your generosity, your time, and patience. Thank you, Mike. Now, it's finally my turn to say: Thank you for the opportunity.

My lab members, past and current, thank you for all the fruitful discussions, the encouragement, the support, the coffee, and the donuts.

To my committee members who have been so helpful in steering me towards the finish line: Carolyn, Dan, Valeria, and Pierre, thank you for being my strongest advocates.

To the rest of my BMB family, from staff, faculty, classmates and colleagues, thank you for fostering an environment that is welcoming, inclusive, and friendly. A shout out to Lyle for the wings and noodles, and to Mindy for keeping lunch club alive and well. After 8 years, with all the complicated feelings that come with this place, I will miss being at Hopkins, and will always carry a part of East Baltimore with me.

Many, many thanks go to my extended family, my community, my friends: Mindy, Kaete, Juliet, Jay, Gaddis, Aleks, Kareshma, Saba, and many more! Whether in commiseration or in celebration, they never failed to be there for me. I am lucky to be part of such a big, yet close, community of like-minded people that are truly inspiring.

To say thank you to my partner and my best friend Jeremy, is to put many feelings of appreciation and gratitude into words that will never suffice. But I will say this: Thank you for putting up with me. Thank you for all the love and all the proof-readings and everything in between.

Last, but certainly not least, my family, my truest backbone and my no.1 support. To my parents, Amal and Mahmoud, who truly led by example. To say that I appreciate your unwavering support and unconditional love is an understatement. Thank you for instilling in me the power and importance of education. Thank you for all the sacrifices you've taken to provide me with the best education and opportunities. And thank you for paving the way for me to pursue my passion and to find my true self.

To my sister Hanin, who continues to be my role model, thank you for setting the bar high since day 1! I wouldn't be where I am today without following your footsteps. And to my brother Mustafa, thank you for proving to me that running an SDS-PAGE doesn't take 5 years of training! And thank you for always keeping me proud.

My final thanks and biggest gratitude goes to my aunts Khuloud and Huda. Thank you for being a source of comfort and motivation throughout the years. Thank you for adopting me and providing me with all the meals, and all the meats! You quickly made me feel at home. This journey would've been a lot more difficult without you.

Thank you, thank you, thank you.

DEDICATION

To Faten

TABLE OF CONTENTS

ABSTRACT	ii
ACKNOWLEDGEMENTS	iv
DEDICATION	vi
TABLE OF CONTENTS	vii
LIST OF TABLES	ix
LIST OF FIGURES	x
ABBREVIATIONS	xii
CHAPTER I: INTRODUCTION	1
POST-TRANSLATIONAL MODIFICATIONS.....	2
SUMO AS A DIVERSE SIGNAL	3
THE SUMOYLATION PROCESS – SUMO CONJUGATION AND DE- CONJUGATION	5
SUMO REGULATION – A CLOSER LOOK AT SENPs	8
SUMO AT INTRACELLULAR MEMBRANES – THINKING OUTSIDE THE NUCLEUS	10
THESIS RATIONALE	14
TABLES	16
FIGURES AND FIGURE LEGENDS	17
CHAPTER II: SENP2 TARGETING TO INTRACELLULAR MEMBRANES	20
ABSTRACT	21
INTRODUCTION	22
MATERIALS AND METHODS.....	26
RESULTS	35
DISCUSSION	44
FIGURES AND FIGURE LEGENDS	52

CHAPTER III: THE SUMO CAPTURE	75
ABSTRACT	76
MATERIALS AND METHODS.....	80
RESULTS	83
DISCUSSION.....	88
FIGURES AND FIGURE LEGENDS	92
APPENDIX I: TRIALS AND TRIBULATIONS:	102
INTRODUCTION	103
RESULTS AND DISCUSSION.....	108
FIGURES AND FIGURE LEGENDS	115
OVERVIEW AND FUTURE DIRECTIONS	127
OVERVIEW	128
SEN2-MEMBRANE INTERACTION	129
SEN2 SUBSTRATES AND FUNCTIONAL SIGNIFICANCE.....	130
IS MEMBRANE ASSOCIATION REGULATORY?	132
BIBLIOGRAPHY	134
CURRICULUM VITAE.....	147

LIST OF TABLES

Table I-1..... 16

LIST OF FIGURES

Figure I-1.	17
Figure I-2.	18
Figure I-3.	19
Figure II-1.	53
Figure II-2.	55
Figure II-3.	57
Figure II-4.	58
Figure II-5.	59
Figure II-6.	60
Figure II-7.	61
Figure II-8.	62
Figure II-9.	64
Figure II-10.	66
Figure II-11.	68
Figure II-12.	70
Figure II-13.	71
Figure II-14.	73
Figure II-15.	74
Figure III-1.	93
Figure III-2.	95
Figure III-3.	96
Figure III-4.	97
Figure III-5.	99
Figure III-6.	101
Figure A-1.	116
Figure A-2.	118
Figure A-3.	121

Figure A-4.....	123
Figure A-5.....	125
Figure A-6.....	126

ABBREVIATIONS

ALPS	ArfGAP1 lipid-packing sensor
AP-MS	Affinity purification - mass spectrometry
BAC	Bacterial artificial chromosome
CFTR	Cystic fibrosis transmembrane conductance regulator
Co-IP	Co-immunopurification
DeSI	De-sumoylating isopeptidase
DMEM	Dulbecco modified eagle medium
Drp1	Dynamin-related protein 1
DTT	Dithiothreitol
EDTA	Ethylenediaminetetraacetic acid
Elk-1	E twenty six-like 1
EMC	ER membrane protein complex
ERAD	ER-associated degradation
FDC	Familial dilated cardiomyopathy
FPLD	Familial partial lipodystrophy
GFP	Green fluorescent protein
GLUT	Glucose transporter
GM130	Golgi matrix protein 130
GRP78	Glucose-regulated protein 78
GSV	GLUT-storage vesicle
IPTG	Isopropyl β -D-1-thiogalactopyranoside

Kap- α	Karyopherin alpha
LAP2	Lamin-associated polypeptide 2
LAS	Lamin-associated sequence
MAPL	Mitochondrial anchored protein ligase
MBP	Maltose binding protein
NEBD	Nuclear envelope breakdown
NEM	N-Ethylmaleimide
NLS	Nuclear localization signal
NPC	Nuclear pore complex
NUP	Nucleoporin
PAGE	Polyacrylamide gel electrophoresis
PBS	Phosphate buffered saline
PC	Phosphatidylcholine
PCNA	Proliferating cell nuclear antigen
PE	Phosphatidylethanolamine
PIAS	Protein inhibitor of activated STAT
PML	Promyelocytic leukemia protein
PMSF	Phenylmethylsulfonyl fluoride
PTM	Post-translational modification
RanGAP1	Ran-GTPase-activating protein
RING	Really interesting new gene
RNAi	RNA interference
RNF4	Ring finger protein 4

RT-qPCR	Real time-quantitative polymerase chain reaction
SAINT	Significance analysis of interactomes
SDS	Sodium dodecyl sulfate
SENP	Sentrin-specific protease
SIM	SUMO-interacting motif
SUMO	Small ubiquitin-related modifier
TDG	Thymine DNA glycosylase
TCIS	Tagged chromosomal insertion site
TET	Tetracycline
Ubl	Ubiquitin-like protein
Ulp	Ubiquitin-like protease
USPL1	Ubiquitin-specific peptidase-like protein 1
YY1	Ying-yang 1

CHAPTER I
INTRODUCTION

POST-TRANSLATIONAL MODIFICATIONS

Post-translational modifications (PTMs) add a level of functional diversity and complexity to our proteome. They are inducible and reversible in nature, providing means for our cells to rapidly regulate protein activity, localization, and interactions with other proteins, nucleic acids, and lipids. PTMs involve the covalent addition of a small protein or a functional group onto proteins. Among the many PTMs, one widely studied modification is ubiquitination. Ubiquitin is a highly conserved, 76 amino acid protein that gets covalently added onto lysine residues of a plethora of other proteins. Although ubiquitin is most widely known as a signal for degradation, the complexity and different topologies of mono- and poly-ubiquitin chains allow ubiquitin to function as a diverse signal and thereby regulate nearly all essential cellular functions, including cell cycle progression, chromatin remodeling, and DNA repair (Pickart and Eddins, 2004; Hochstrasser, 2009; Tanaka, 2009). Many ubiquitin-like proteins (Ubls) that share a similar structural fold with ubiquitin have been identified, including the small ubiquitin-related modifier SUMO, ISG15, Fat10, NEDD8, and Atg8 (Kerscher *et al.*, 2006). This thesis will particularly focus on SUMO and its regulation and potential functions at intracellular membranes.

Our interest in studying SUMO as a post-translational modification stems from its wide implications in human health and disease, including 7 diseases that are among the top 10 leading causes of death in the U.S. (CDC, 2017). For example, many studies have shown that the sumoylation machinery is enhanced in numerous cancers, including breast, colorectal, lung, and prostate cancers (Seeler and Dejean, 2017; Yang *et al.*, 2017). SUMO is also important for proper cardiac development and function, where any

misregulation in sumoylation can result in cardiac fibrosis or arrest (Da Silva-Ferrada *et al.*, 2016; Liu *et al.*, 2017; Yang *et al.*, 2017). Furthermore, perturbations in neuronal sumoylation can contribute to numerous neurodegenerative diseases, including Huntington's, Parkinson's, and Alzheimer's disease (Dorval and Fraser, 2006; Guerra de Souza *et al.*, 2016; Martins *et al.*, 2016; Ochaba *et al.*, 2016; Yang *et al.*, 2017). Collectively, SUMO is involved in every cellular function that is essential for normal physiology, and can present a promising therapeutic target for the treatment of many diseases. Therefore, understanding the molecular dialogues between SUMO and other proteins can unveil the next wave of therapeutics for the advancement of public health.

SUMO AS A DIVERSE SIGNAL

SUMO is a ~100 amino acid protein that is post-translationally and covalently attached to a multitude of other proteins in all eukaryotic cells. It was first discovered as a signal that regulates the localization of Ran-GTPase-activating protein RanGAP1. More specifically, the sumoylation of RanGAP1 directs its localization to the nuclear pore complexes (NPCs) (Matunis *et al.*, 1996; Mahajan *et al.*, 1997). Since then, studies on SUMO elucidated other essential roles for this small yet powerful protein. It has been shown to be involved in regulating transcription, DNA repair, stress response, nucleocytoplasmic trafficking, chromosome segregation, and chromatin remodeling (Johnson, 2004; Hay, 2005; Makhnevych *et al.*, 2009). The misregulation of SUMO is implicated in a variety of diseases, including cardiac disease, neurodegenerative disease and cancers (Yang *et al.*, 2017). Therefore, understanding the molecular mechanisms behind SUMO regulation is of crucial importance for the advancement of public health.

Yeast and invertebrates express one SUMO, while vertebrates express three functional paralogs: SUMO1, SUMO2, and SUMO3. Mammalian SUMO2 and SUMO3 are 95% identical and are often referred to as SUMO2/3. However, SUMO1 is only 50% identical to SUMO2/3 and therefore may have distinct functions. SUMO1 and SUMO2/3 primarily have unique substrates dictated, in part, by the SUMO conjugation machinery. Substrates can be mono-sumoylated, poly-sumoylated, or modified by hybrid SUMO-ubiquitin chains. Besides ubiquitin, SUMO can also act in combination with other PTMs, further diversifying the signaling cascade and downstream biological consequences (Saitoh and Hinchey, 2000; Tatham *et al.*, 2001; Johnson, 2004; Guzzo *et al.*, 2012).

Once a protein is sumoylated, it can interact non-covalently with other proteins containing SUMO-interacting motifs (SIMs). A SIM is usually defined as a short hydrophobic patch (V/I-X-V/I-V/I) flanked by an acidic patch (Song *et al.*, 2004; Hecker *et al.*, 2006; Kerscher, 2007). SUMO-SIM interactions play an important role in defining the consequences of sumoylation and can have a variety of effects. First, SUMO-SIM interactions enhance protein-protein interactions and can result in the formation of large protein complexes. A well-characterized example includes the sumoylation of a known tumor suppressor called promyelocytic leukemia protein (PML). In addition to containing sites for covalent sumoylation, PML also contains multiple SIMs. Once sumoylated, PML binds to other sumoylated PML proteins via its SIMs, thereby forming PML-nuclear bodies that are able to recruit other sumoylated proteins or proteins containing SIMs (Matunis *et al.*, 2006). The SUMO-dependent formation of PML-nuclear bodies plays an important role in genome maintenance, stress response, and DNA repair. Secondly, SUMO-SIM interactions can facilitate the targeting of sumoylated proteins for

proteasomal degradation via the recruitment of SUMO-targeted ubiquitin ligases that contain tandem SIMs, like ring finger protein 4 (RNF4). Furthermore, changes in structural conformations, or efficient SUMO conjugation can also be facilitated by SUMO-SIM interactions (Matunis *et al.*, 2006; Shen *et al.*, 2006; Tatham *et al.*, 2008). One example includes the conformational change of thymine DNA glycosylase (TDG). TDG enzyme removes mismatched thymine and uracil bases, creating abasic sites in double-stranded DNA. The covalent SUMO modification of TDG, and non-covalent interactions via SIMs facilitate the conformational change required to release TDG from the abasic site, allowing subsequent repair (Hardeland *et al.*, 2002; Baba *et al.*, 2005; Steinacher and Schar, 2005; Kerscher, 2007). Collectively, from multiple SUMO paralogs, to many unique substrates, to various chain formations and SIMs, sumoylation provides a diversity of signals that regulate many essential cellular processes.

THE SUMOYLATION PROCESS – SUMO CONJUGATION AND DE-CONJUGATION

The mechanism of SUMO conjugation is closely related to that of ubiquitin, involving an ATP-dependent enzymatic cascade of SUMO-specific E1-activating, E2-conjugating and E3-ligating enzymes (Figure I-1) (Johnson, 2004; Cappadocia and Lima, 2017). SUMO is initially synthesized as an immature precursor protein that requires cleavage by sentrin-specific proteases (SENPs), exposing the di-glycine motif at its C-terminus (Hickey *et al.*, 2012). The mature form of SUMO can then be activated by the ATP-dependent heterodimeric E1 enzyme called Aos1/Uba2. E1 catalyzes the adenylation of the C-terminus of SUMO and subsequently forms a thioester linkage

between its catalytic cysteine and the C-terminus of SUMO (Johnson *et al.*, 1997). Through a transesterification reaction, SUMO is then transferred from E1 to the SUMO-conjugating enzyme, E2 (Ubc9). Ubc9 can recognize SUMO consensus sites on target proteins, which entail a hydrophobic residue (Ψ), an acceptor lysine residue (K) followed by any amino acid (X), and ending with an aspartate or a glutamate (Ψ -K-X-D/E) (Johnson and Blobel, 1997). Notably, charged Ubc9 can also recognize target proteins via their SIM motifs, and facilitate SUMO conjugation on a nearby lysine residue (Johnson, 2004). Ultimately, Ubc9 mediates the transfer of SUMO to the substrate where the C-terminal glycine of SUMO covalently binds to the ϵ -amino group of the acceptor lysine residue in the target protein forming an isopeptide linkage (Johnson and Blobel, 1997). The E1 and E2 enzymes can catalyze the reaction of SUMO conjugation independently from SUMO E3 ligases. However, a number of E3 ligases can contribute to the conjugation process, and perhaps more importantly, to substrate selectivity and SUMO paralog specificity (Desterro *et al.*, 1997; Johnson and Blobel, 1997; Johnson *et al.*, 1997; Li and Hochstrasser, 1999; Bernier-Villamor *et al.*, 2002; Mikolajczyk *et al.*, 2007).

There are three major classes of SUMO E3 ligases: the protein inhibitor of activated STAT (PIAS) family, the vertebrate-specific NPC protein Nup358/RanBP2, and the polycomb group member Pc2 (Johnson, 2004; Kerscher *et al.*, 2006). The PIAS family is the best-characterized group of E3 ligases. They contain an SP-RING (Siz/PIAS RING) domain that is similar to the RING domain of ubiquitin E3 ligases. Yeast encodes three PIAS E3 ligases, Siz1, Siz2, and Mms21, while mammals encode five (PIAS1, PIAS3, PIAS α , PIAS β , and PIASy) (Pichler *et al.*, 2002; Kagey *et al.*, 2003; Rytinki *et al.*, 2009). While ubiquitin E3 ligases are essential players in determining substrate

specificity, SUMO E3 ligases play a peripheral role since they are not required for modification. Nevertheless, some SUMO modifications are E3-dependent, a well-characterized example being the proliferating cell nuclear antigen protein (PCNA) (Yunus and Lima, 2009).

Like other PTMs, the sumoylation process is dynamic and reversible. SUMO de-conjugation is carried out by a family of SUMO-specific proteases that cleave at the C-terminus of SUMO (Figure I-1). SUMO proteases not only play a role in de-conjugation, but also are required for SUMO precursor maturation, hence directly affecting SUMO conjugation (Johnson, 2004; Hickey *et al.*, 2012). The first de-sumoylating enzymes were identified in yeast, the ubiquitin-like protease 1 and 2 (Ulp1 and Ulp2) (Li and Hochstrasser, 1999, 2003). Later on, six different SUMO-specific proteases were discovered in vertebrates, SENP1-3, and SENP5-7 (Table I-1). This class of SUMO proteases belongs to the CE class of cysteine proteases, containing a catalytic triad of cysteine, aspartate, and histidine (Drag and Salvesen, 2008). All six SENPs share a conserved catalytic domain and have divergent N-terminal domains, which are critical in determining their respective subcellular localizations (Figure I-2) (Mukhopadhyay and Dasso, 2007; Nayak and Muller, 2014). The subcellular localization of SUMO proteases greatly influences their substrate specificity. Thus, determining the location of each specific protease is a crucial step towards elucidating their function. Table I-1 summarizes the known subcellular localizations of each protease, their SUMO isoform preference, and their generic mode of action (Hickey *et al.*, 2012). Notably, non-classical SUMO proteases have also been discovered, including the mammalian DeSI (de-sumoylating isopeptidase) and USPL1 (ubiquitin-specific peptidase-like protein 1)

families, however, their functional significances still remain to be elucidated (Schulz *et al.*, 2012; Shin *et al.*, 2012).

The balance between the rapid SUMO conjugation and de-conjugation is what results in the “SUMO enigma” (Hay, 2005); that is, at steady state level, a very low percentage of any substrate is found sumoylated, yet that pool of sumoylated substrate can have profound functional consequences, demonstrating the power of such a small protein modification on the state of the cell.

SUMO REGULATION – A CLOSER LOOK AT SENPs

All SENPs characterized thus far are essential for survival. This serves as a testament for the crucial role SENPs play in regulating the sumoylation pathway. It also shows that each SENP plays a distinct, non-redundant role and may be acting on a unique subset of sumoylated proteins, subsequently regulating a different set of cellular functions. SENP1 and SENP2 for example, regulate cell cycle progression. SENP3 and SENP5 are involved in ribosome biogenesis, while SENP6 and SENP7 can edit poly-SUMO-2/3 chains (Cubenas-Potts *et al.*, 2013; Nayak and Muller, 2014). The question of how SENPs recognize different substrates is of major interest in the field. In yeast, it has been demonstrated that subcellular localization, dictated by the divergent N-terminal domains of Ulp1 and Ulp2, plays a major role in conferring substrate specificity (Li and Hochstrasser, 2000). Restricting protease access to a subset of sumoylated proteins could be one way to determine which substrates are being regulated, however, it is also possible that the divergent N-terminal domains of proteases directly mediate the binding to a specific set of substrates. The latter mechanism is yet to be fully investigated.

Similarly to yeast, SENPs divergent N-terminal domains also dictate unique subcellular localizations in mammals. However, their specific role in defining substrate specificity is yet to be fully elucidated. Thus far, SENP1 and SENP2 are known to localize at NPCs with the ability to shuttle in and out of the nucleus. SENP3 and SENP5 localize to the nucleolus, while SENP6 and SENP7 are found in the nucleoplasm (Hang and Dasso, 2002; Zhang *et al.*, 2002; Bailey and O'Hare, 2004; Gong and Yeh, 2006; Yun *et al.*, 2008). Besides having unique subcellular localizations, SENPs also exhibit differences in their enzymatic activities. SENP1 and SENP2 have the highest endopeptidase and isopeptidase activity. SENP1 preferentially processes SUMO1 precursor proteins, while SENP2 processes SUMO2 precursors more efficiently. Both SENP1 and SENP2 can deconjugate SUMO1 and SUMO2/3 modified proteins. In contrast, SENP3 and SENP5 preferentially deconjugate SUMO2/3, and SENP6 and SENP7 function more efficiently as poly-SUMO2/3 chain editors (Mikolajczyk *et al.*, 2007). SENP1 and SENP2 are among the best studied SENPs and the two SUMO proteases investigated in our lab.

Although SENP1 and SENP2 both localize to NPCs during interphase, they still exhibit divergent, non-redundant functions. This may suggest that their N-terminal domains not only contain elements for localization but also contribute to substrate specificity by directly binding to sumoylated substrates. Consistent with this, SENP1 binds to Reptin, a tumor suppressor protein, while SENP2 cannot (Kim *et al.*, 2006). Another possibility is that there are other elements or targeting signals at the N-terminus, beyond NPC-targeting, that contribute to the regulation and substrate specificity of SENP1 and SENP2 but have yet to be discovered. It is also worthy to note that SENP1

and SENP2 can be modified by other PTMs, like phosphorylation, that could contribute to their divergent functions, localization, and regulation. Also, the presence of multiple splice variants with different N-termini increases the regulatory repertoire of SENPs. Taken together, it is clear that the diverse N-terminal region of SENPs plays a crucial role in determining their specificity and regulation, however, more work is required to decipher those differences. This thesis focuses on exploring a novel N-terminal targeting signal in SENP2 that may contribute to substrate specificity.

SUMO AT INTRACELLULAR MEMBRANES – THINKING OUTSIDE THE NUCLEUS

Many of the best-studied sumoylated proteins identified thus far localize to the nucleus. SUMO is known to play a central role in regulating transcription, DNA repair, RNA processing and chromatin remodeling, among many other functions (Johnson, 2004; Hay, 2013; Hendriks and Vertegaal, 2016). However, there is a rapidly growing body of work that provides evidence for SUMO functions outside the nucleus, more specifically in the cytoplasm, the endoplasmic reticulum, Golgi, mitochondria, and the plasma membrane (Figure I-3). Proteomic analyses, for example, have identified multiple non-nuclear targets for sumoylation (Wasik and Filipek, 2014). Additionally, it has been well established that the sumoylation machinery is not confined to the nucleus. In fact, SENP1 and SENP2 can shuttle in and out of the nucleus (Goeres *et al.*, 2011). Taken together, this provides evidence that SUMO has non-nuclear functions that require further exploration.

The first evidence for SUMO outside the nucleus included the regulation of the glucose transporter type 4 (GLUT4) (Giorgino *et al.*, 2000; Sadler *et al.*, 2013). In the absence of insulin, only about 1% of GLUT4 is present at the plasma membrane, with the majority being localized to GLUT4-storage vesicles (GSVs). It has been shown that sumoylation of GLUT4 mediates its sorting and transport to GSVs as well as increases its protein expression and stability, showing that SUMO has a direct role in regulating the localization and expression of a plasma membrane protein. Another glucose transporter, GLUT1, responsible for basal glucose transport, is also sumoylated (Giorgino *et al.*, 2000; Benson *et al.*, 2017). Biochemical analyses showed that a higher molecular weight form of GLUT1 immunopurifies with Ubc9, however, the functional consequences of GLUT1 sumoylation needs further characterization.

Besides its role in directly regulating glucose transport, SUMO has an expansive role in regulating ion channels (Benson *et al.*, 2017). To date, at least four ion channels have been reported to be sumoylated. The potassium leak channel K2P1 was one of the first to be identified as a SUMO substrate. In fact, unlike the majority of sumoylated proteins, K2P1 is mostly present in its sumoylated form at the plasma membrane. Sumoylation appears to maintain the channel in its inactive form, however, once SUMO is de-conjugated, the channel is active and a K⁺ current is readily detected (Rajan *et al.*, 2005). This suggests that sumoylation is acutely controlling the function of ion channels at the plasma membrane. Other examples include the voltage-gated potassium channels Kv1.5 and Kv7.2, both of which are sumoylated. Kv1.5 sumoylation modulates its biophysical properties, where any alterations in sumoylation alters the action potential duration or the resting membrane potential, subsequently affecting the excitability of

atrial myocytes and vascular smooth muscle cells (Benson *et al.*, 2017). Finally, sumoylation of the Kv7.2 channel, expressed mainly in the cardiac and nervous systems, diminishes the M-current leading to an increased excitability of hippocampal neurons (Qi *et al.*, 2014). Together, these reports identify an emerging role for SUMO modification of ion channels at the plasma membrane.

Switching to a different domain, SUMO is also involved in regulating mitochondrial functions. The mitochondrion is constantly undergoing cycles of fission and fusion, a process that is highly regulated by sumoylation. More specifically, SUMO1 modification of the dynamin-related protein 1 (Drp1) increases its activity by enhancing the binding of Drp1 to the outer mitochondrial membrane, leading to mitochondrial fission (Anderson and Blackstone, 2013). Interestingly, and in contrast to SUMO1 modification, the modification of Drp1 by SUMO2/3 is thought to prevent the protein from associating with the mitochondria, thereby inhibiting mitochondrial fission (Anderson and Blackstone, 2013). This contrast between SUMO1 and SUMO2/3 exemplifies how different SUMO paralogs can have different functional outcomes. The misregulation of Drp1 sumoylation drastically affects mitochondrial division and is associated with brain ischemia, demonstrating the important role SUMO plays in regulating mitochondrial function (Fu *et al.*, 2014).

One common theme that brings together the non-nuclear functions of SUMO, from glucose transport to ion channel regulation to mitochondrial division, is that they all are membrane-associated functions, which triggers the question: how are membrane-associated proteins recognized and regulated by the sumoylation machinery? It is reasonable to suggest that the sumoylation machinery itself can associate with

intracellular membranes, where it directly interacts with membrane-associated proteins and regulates their modifications and functions. Consistent with this, fractionation studies showed that Ubc9 is found in the plasma membrane fraction (Giorgino *et al.*, 2000), however, further studies that characterize the subcellular localization of SUMO E3 ligases and SENPs is required in order to understand the additional layers of SUMO regulation at membranes. Thus far, the SUMO E3 mitochondrial anchored protein ligase (MAPL) has been shown to not only associate with the mitochondrial membrane but also is the E3 ligase responsible for Drp1 sumoylation (Braschi *et al.*, 2009). Furthermore, SENP2, SENP3, and SENP5 overexpression affects Drp1 sumoylation, however, how and whether these enzymes are targeted to mitochondria is virtually unknown (Harder *et al.*, 2004; Mandler *et al.*, 2016). Of particular interest is the role of SENP2 in regulating the sumoylation of the voltage-gated potassium channel Kv7.2. Reduced expression of SENP2 in mice results in the hyper-sumoylation of Kv7.2 in hippocampal neurons, leading to increased neuronal excitability, seizures and sudden death (Qi *et al.*, 2014). Thus, SENP2 is linked to a pathophysiological process involving sumoylation at membranes. This raises the intriguing question: does SENP2 directly recognize and regulate membrane-associated proteins? This thesis will address in depth the subcellular localization of SENP2, particularly at intracellular membranes.

Adding onto the intracellular membranes theme, several lines of evidence also suggest a pivotal role for SUMO modifications in the regulation of inner nuclear membrane-associated proteins. For example, emerin and lamin A, major constituents of the inner nuclear membrane are both regulated by sumoylation. Importantly, decreased sumoylation of lamin A is implicated in familial partial lipodystrophy (FPLD), and

familial dilated cardiomyopathy (FDC). Furthermore, sumoylation has been tied with chromatin repression and transcriptional regulation, a function that is also related to the nuclear membrane (Zhang and Sarge, 2008; Yip *et al.*, 2012; Neyret-Kahn *et al.*, 2013; Simon *et al.*, 2013). Collectively, the current data suggests an essential role for SUMO at the nuclear periphery. However, the regulation of sumoylation within this domain is unclear.

In summary, SUMO modification is an important and widespread regulatory mechanism that is present both in and out of the nucleus, and at intracellular membranes. It can have a significant impact on the functions of the cell. Further research is required to address SUMO regulation in the cytoplasm, particularly at membranes.

THESIS RATIONALE

The roles of SUMO in the cell are rapidly expanding. Whether it is in the nucleus or in the cytoplasm, almost every essential function in the cell is touched by SUMO. Every time a new SUMO substrate is discovered, one begs to ask the question: What regulates the regulator? In other words, how is the sumoylation machinery itself being regulated? To answer these questions, one must turn to the characterization of important master regulators: the SUMO isopeptidases.

This body of work seeks to answer many questions related to the SUMO isopeptidase SENP2 and the regulation of sumoylation at intracellular membranes. Given that SENP1 and SENP2 are functionally non-redundant yet are both localized to the NPCs, is it possible that there are yet undiscovered targeting signals in their N-terminal domains that allow them to be functionally distinguishable? Furthermore, given that

SENP2 can directly regulate the voltage-gated potassium channel Kv7.2 (Qi *et al.*, 2014), could it be that SENP2 has a targeting signal that allows it to interact with intracellular membranes? To answer these questions, I searched for novel targeting signals in the N-terminal domain of SENP2. Chapter II will discuss how SENP2 is in fact targeted to intracellular membranes via a unique N-terminal amphipathic α -helix. Chapter III is focused on the development of new and unique tools for identifying and characterizing SENP2-specific substrates. Attempting to identify the functional consequences of SENP2 regulation at intracellular membranes, I have studied multiple potential membrane-associated protein targets at the inner nuclear membrane, ER, and the plasma membrane, which are all described in Appendix I. Overall, our findings illustrate that SENP2 is a unique isopeptidase when it comes to regulating the sumoylation of membrane proteins, and implicate SENP2 as an important factor in regulating membrane-associated functions.

TABLES

Name	Subcellular localization	Isoform preference	Precursor processing	Deconjugation	Chain editing
<i>Saccharomyces cerevisiae</i>					
Ulp1	Nuclear pore	Smt3	Yes	Yes	No
Ulp2	Nucleoplasm	Smt3	No	Yes	Yes
<i>Mammals</i>					
SENP1	Nuclear pore and nuclear foci	SUMO-1 and SUMO-2/3	Yes	Yes	No
SENP2	Nuclear pore and nuclear foci; cytoplasm	SUMO-2/3 and SUMO-1	Yes	Yes	No
SENP3	Nucleolus	SUMO-2/3	Unknown	Yes	No
SENP5	Nucleolus and mitochondria	SUMO-2/3	Yes	Yes	No
SENP6	Nucleoplasm	SUMO-2/3	No	Yes	Yes
SENP7	Nucleoplasm	SUMO-2/3	No	Yes	Yes

Table I-1. Identified *S. cerevisiae* and mammalian SUMO proteases. The primary location of each SUMO protease, its SUMO isoform preference, and its mode of action, is listed.

FIGURES AND FIGURE LEGENDS

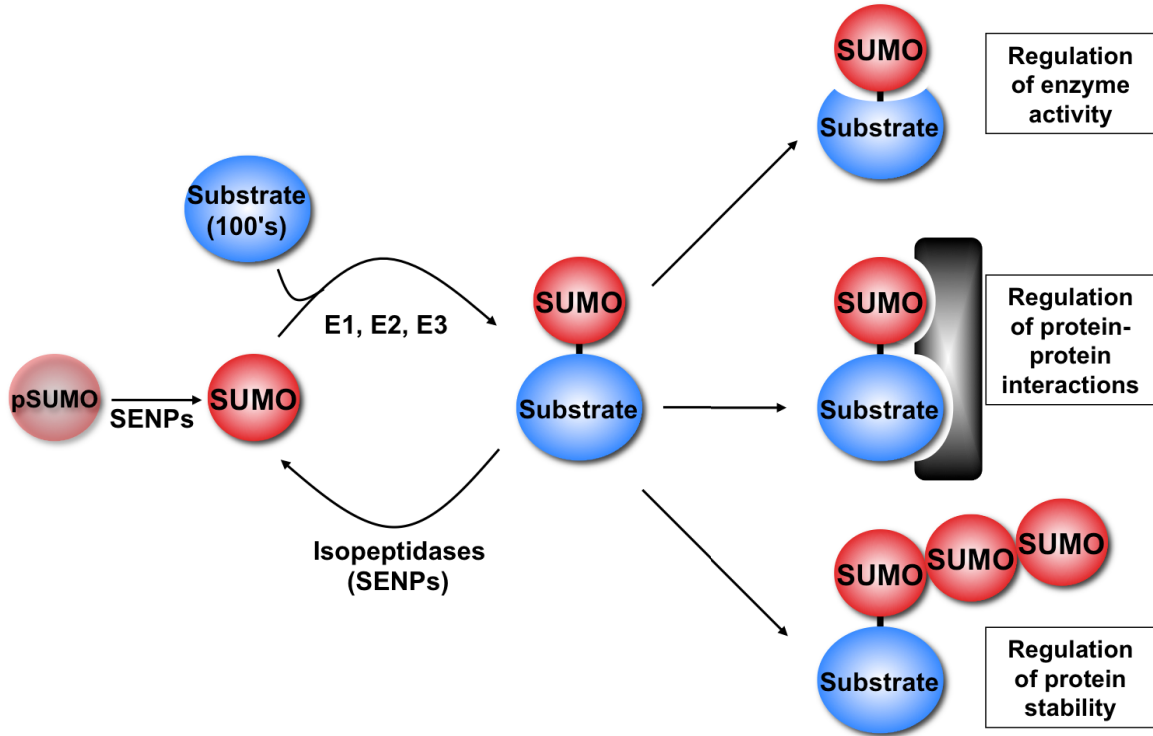


Figure I-1. Schematic representation of the SUMO conjugation and de-conjugation cycle. SUMO proteases are required for SUMO precursor processing. Mature SUMO is then conjugated to substrates through an ATP-dependent enzymatic cascade. E1-activating enzyme is required for the ATP-dependent activation of SUMO, which is then transferred to E2-conjugating enzyme forming a thioester intermediate. SUMO is then bound covalently to lysine residues, in an E3 ligase dependent or independent fashion, forming an isopeptide linkage. SUMO can have a variety of effects on its substrates, from changing enzyme activity, interaction with other proteins, to regulation of protein stability. SUMO proteases are responsible for the de-conjugation process.

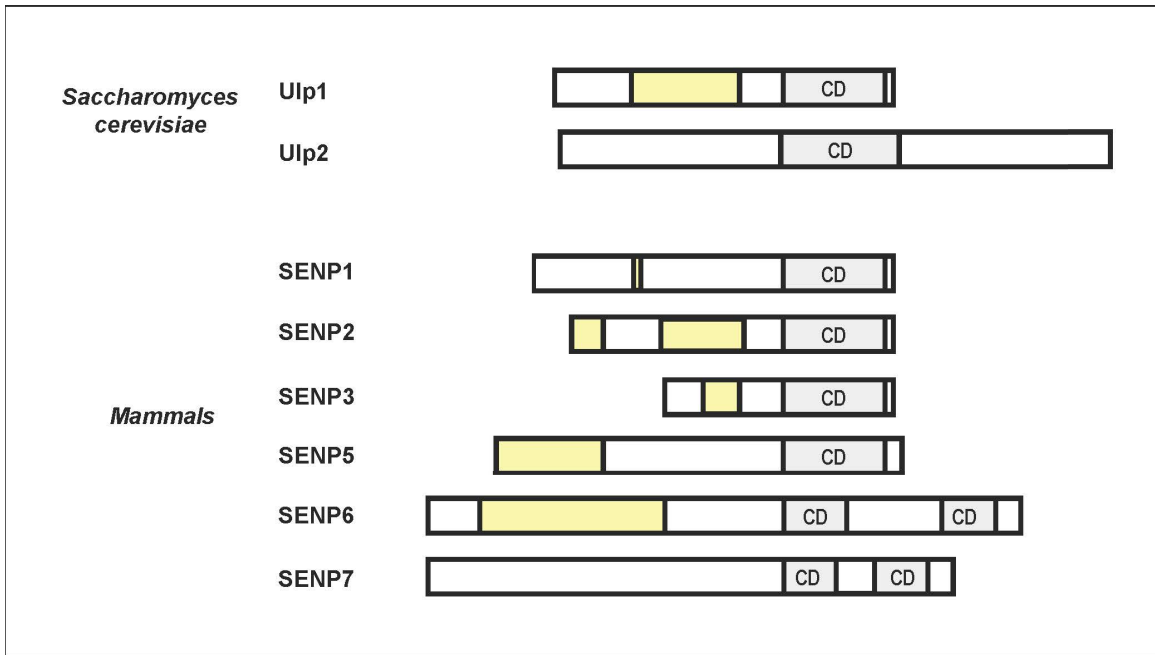


Figure I-2. Schematic representation of *S. cerevisiae* and mammalian SUMO proteases. The conserved catalytic domain (CD) is highlighted in grey. N-terminal regions shown to be important for subcellular localization of the protease are highlighted in yellow.

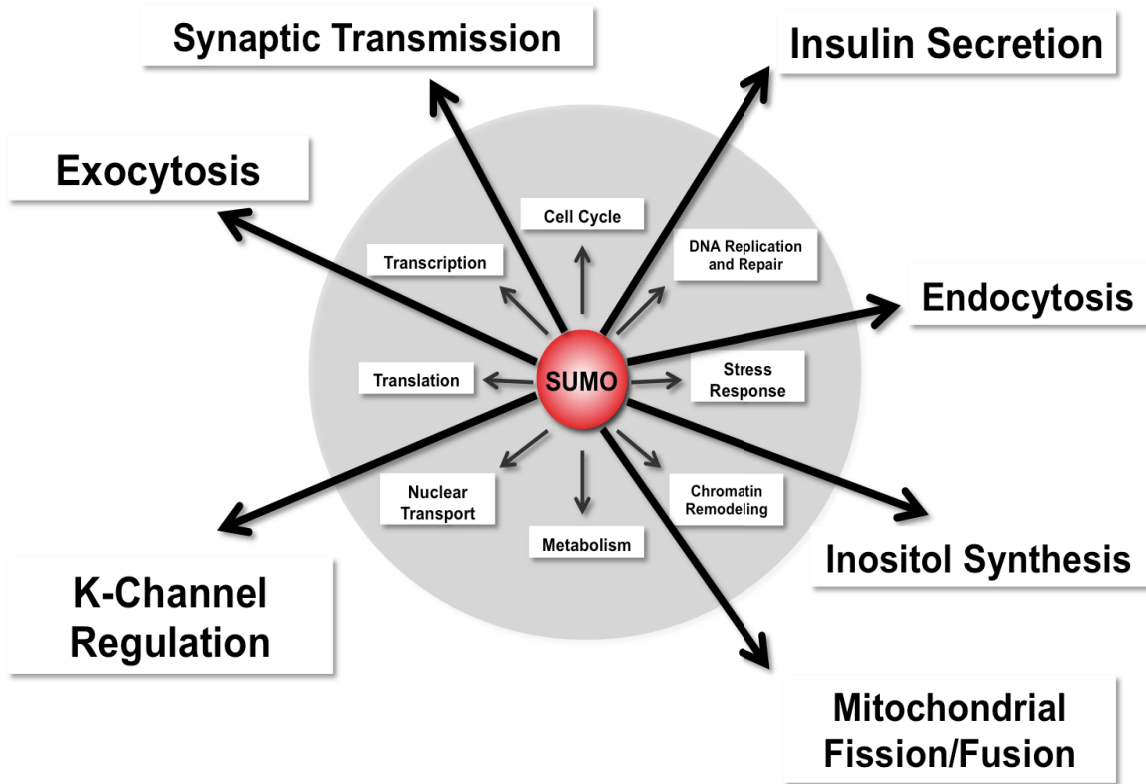


Figure I-3. Schematic diagram representing the emerging evidence of SUMO functions outside the nucleus. The best studied functions of SUMO are associated with the nucleus, however, there is emerging evidence for SUMO-mediated regulation of mitochondrial fission and fusion, ion channel regulation, insulin secretion, and other non-nuclear functions, most of which are also associated with intracellular membranes.

CHAPTER II
SENP2 TARGETING TO INTRACELLULAR MEMBRANES

ABSTRACT

Sumoylation regulates a wide range of essential cellular functions, many of which are associated with activities in the nucleus. Although there is also emerging evidence for the involvement of SUMO at intracellular membranes, the mechanisms by which sumoylation is regulated at membranes is largely unexplored. In this study, we report that the SUMO-specific isopeptidase, SENP2, uniquely associates with intracellular membranes. Using *in vivo* analyses and *in vitro* binding assays, we show that SENP2 is targeted to intracellular membranes via a predicted N-terminal amphipathic α -helix that promotes direct membrane binding. Furthermore, we demonstrate that SENP2 binding to intracellular membranes is regulated by interactions with the nuclear import receptor karyopherin- α (Kap- α). Consistent with membrane association, BioID revealed interactions between SENP2 and ER, Golgi and inner nuclear membrane-associated proteins. Collectively, our findings indicate that SENP2 binds to intracellular membranes where it interacts with membrane-associated proteins and has the potential to regulate their sumoylation and membrane-associated functions.

INTRODUCTION

The small ubiquitin-related modifier (SUMO) is a highly conserved 100 amino acid protein that is post-translationally and covalently attached to a multitude of other proteins (Wilson, 2017). Similar to other ubiquitin-like proteins, sumoylation adds another level of regulation to protein activity, stability, and localization. Yeast and invertebrates express one SUMO protein, while vertebrates express several functional paralogs, including SUMO1, SUMO2, and SUMO3. Mammalian SUMO2 and SUMO3 are 95% identical and thought to be functionally related. However, SUMO1 is only 50% identical to SUMO2/3 and may have unique functions (Citro and Chiocca, 2013). The mechanism of SUMO conjugation is closely related to ubiquitin. In brief, a SUMO-activating enzyme (E1) is required for the ATP-dependent activation of SUMO, which is then transferred to SUMO-conjugating enzyme (E2) forming a thioester intermediate. Ultimately, SUMO is transferred to substrate proteins, in some cases through the action of E3 ligases, where its C-terminal glycine is covalently linked to the ϵ -amino group of lysine residues in the target protein forming an isopeptide linkage (Cappadocia and Lima, 2017). In addition to its action through covalent conjugation, SUMO can also interact non-covalently with downstream effector proteins that contain SUMO-interacting motifs (SIMs) (Hay, 2013).

A wide range of essential cellular functions are regulated by sumoylation, many of which are associated with activities in the nucleus, including transcription, chromatin remodeling and DNA repair (Hendriks and Vertegaal, 2016). However, there is growing evidence for the involvement of SUMO in the cytoplasm, most notably at intracellular

membranes (Wasik and Filipek, 2014). For example, SUMO plays an important role in regulating the dynamin-related GTPase Drp1, which mediates mitochondrial fission once recruited to the outer mitochondrial membrane (Anderson and Blackstone, 2013). The misregulation of Drp1 sumoylation subsequently affects mitochondrial division and is associated with brain ischemia (Fu *et al.*, 2014). Another important SUMO substrate at membranes is the cystic fibrosis transmembrane conductance regulator (CFTR). In normal conditions, this multi-domain membrane protein resides in the plasma membrane. However, the most common mutant form of CFTR associated with cystic fibrosis contains a destabilizing phenylalanine deletion at position 508 ($\Delta F508$) that causes the protein to be degraded at the ER membrane (Meng *et al.*, 2017). The degradation of $\Delta F508$ is mediated by the ubiquitin-proteasome pathway, but has also recently been shown to involve sumoylation (Gong *et al.*, 2016). Lastly, sumoylation controls the activity of multiple ion channels, including Kv7 potassium channels in hippocampal neurons linked to epilepsy and sudden death (Qi *et al.*, 2014). Despite these and other rapidly expanding roles for sumoylation at membranes, what remains to be elucidated is how the sumoylation machinery itself is targeted to membranes to control the modification of these proteins.

To investigate SUMO regulation at membranes more closely, we have focused our attention on the SUMO de-conjugation machinery. The dynamic and reversible nature of sumoylation depends on the action of a variety of SUMO-specific proteases that cleave the isopeptide bond formed between the C-terminus of SUMO and its substrates. SUMO proteases also mediate SUMO precursor maturation, hence indirectly affecting SUMO conjugation. To date, there are three families of structurally distinct SUMO

proteases: the SENP (senptrin-specific protease) family, the DeSI (de-sumoylating isopeptidase) family, and USPL1 (ubiquitin-specific peptidase-like protein 1) (Nayak and Muller, 2014). In mammalian cells, SENPs represent the largest family of SUMO proteases, with a total of six encoded SENPs (SEN1-3 and SEN5-7), all of which share a conserved C-terminal catalytic domain and variable N-terminal domains (Hickey *et al.*, 2012).

The subcellular localization of individual SENPs is determined by distinct targeting signals within their N-terminal domains. Consequently, each SENP exhibits a unique subcellular localization that is believed to affect function by determining accessibility to specific substrates. SENP2, for example, localizes to the nuclear pore complexes (NPCs) in interphase and to kinetochores in mitosis (Goeres *et al.*, 2011; Cubenas-Potts *et al.*, 2013). SENP2 localization depends on multiple N-terminal targeting signals, including a Nup107-160 subcomplex binding domain, and a bipartite nuclear localization signal (NLS) that facilitates interactions with karyopherins and FG-repeat nucleoporins. Disrupting these signals affects not only SENP2 localization but also its functions in regulating the sumoylation of kinetochore-associated proteins and chromosome segregation in mitosis (Itahana *et al.*, 2006; Goeres *et al.*, 2011; Cubenas-Potts *et al.*, 2013).

In addition to its association with NPCs and kinetochores, there is also evidence supporting a role for SENP2 in regulating the sumoylation of membrane-associated proteins. First, SENP2 regulates the sumoylation of Drp1, hence playing a role in mitochondrial fission (Fu *et al.*, 2014). In addition, SENP2 has been implicated in controlling the sumoylation of the potassium channel Kv7.2 at the plasma membrane.

More specifically, reduced expression of SENP2 in mice results in hyper-sumoylation of Kv7.2 in hippocampal neurons, leading to increased neuronal excitability, seizures and sudden death (Qi *et al.*, 2014). Thus, SENP2 is linked to pathophysiological processes involving sumoylation at membranes. How SENP2 is specifically targeted to protein substrates at membranes, however, is unknown.

In this study, we discovered a new signal within SENP2 that specifies a unique subcellular localization to intracellular membranes. We show that SENP2 has a predicted amphipathic α -helix at its extreme N-terminus that allows it to directly interact with membranes. We also present evidence that the binding of Kap- α to an adjacent NLS regulates membrane interaction. Consistent with these findings, we found using BioID that SENP2 interacts with a subset of ER, Golgi and inner nuclear membrane-associated proteins. Together, our findings have identified SENP2 as a SUMO protease with the potential to regulate sumoylation at membranes.

MATERIALS AND METHODS

Antibodies

SENP2 and lamin B rabbit polyclonal antibodies were produced as previously described (Chaudhary and Courvalin, 1993; Goeres *et al.*, 2011). Remaining antibodies were obtained from the following sources: anti-GFP (Clontech, Mountain View, CA); anti-tubulin (Sigma-Aldrich, St. Louis, MO); anti-calnexin (Enzo Life Sciences, Inc., Farmingdale, NY); anti-MBP (GenScript, Piscataway, NJ); anti-FLAG M2 (Sigma-Aldrich, St. Louis, MO); anti-His (Sigma-Aldrich, St. Louis, MO); anti-GM130 (BD Biosciences, San Jose, CA); anti-GRP78 (Santa Cruz Biotechnology, Inc., Dallas, TX); and mAb414 recognizing p62, Nup153, Nup214, and Nup358 (Abcam, Cambridge, MA).

Plasmid constructs

SENP2 cDNA was obtained as previously described (Zhang *et al.*, 2002). Full-length SENP2 and SENP2 deletion constructs (1-63, 143-350, and 10-63) were PCR amplified and cloned into pEGFP-C1 as described (Goeres *et al.*, 2011), and cloned into pEGFP-N1, using standard cloning procedures. SENP2 NLS mutation (R29A/R49A) and/or amphipathic α -helix mutation (I8D) were introduced using PCR based, site-directed mutagenesis. SENP1 cDNA was a gift from Mary Dasso (National Institute of Health, Bethesda, MD). Full-length SENP1 was cloned into pmCherry-C2 vector. MBP and MBP-SENP2 fusion proteins, SENP2(1-63)^{WT} and SENP2(1-63)^{I8D}, were cloned into a pRSF vector obtained from Jürgen Bosch (Johns Hopkins, Baltimore, MD) for bacterial expression. Kap- α_2 cDNA was obtained from a mouse fetal liver cDNA library and

cloned into pET21a vector (EMD Biosciences, Gibbstown, NJ) as previously described (Goeres *et al.*, 2011).

Cell culture, and transfection

HeLa cells were maintained in DMEM supplemented with 10% fetal bovine serum, at 37°C and 5% CO₂. Cells were grown at a confluency of 40-50% for transfection with the indicated plasmids using Lipofectamine 2000 according to manufacturer's protocol (Invitrogen, Carlsbad, CA). Cells were harvested either at 24 or 48 hours post-transfection, as indicated, for immunoblotting, or immunofluorescence microscopy.

Immunoblotting

Immunoblot analysis was performed using either enzyme-linked chemiluminescence ECL-Prime reagent (GE Healthcare, Silver Spring, MD) and developed with film, or using IRDye®-conjugated secondary antibodies and imaged using Odyssey infrared imager (LI-COR).

Immunofluorescence microscopy

HeLa cells were cultured on glass coverslips. Cells were fixed with 2% formaldehyde in 1X phosphate-buffered saline (PBS) for 30 minutes at room temperature, then permeabilized in 0.2% Triton-X 100 in 1X PBS for 6 minutes at room temperature. Immunostaining was carried out as previously described (Matunis *et al.*, 1996). For ER and Golgi staining, cells were fixed as described above, and then

permeabilized using 0.05% digitonin for 6 minutes. Zeiss Observer Z1 fluorescence microscope with an Apotome VH optical sectioning grid (Carl Zeiss, Jena, Germany) was used to acquire images.

Immunoelectron microscopy

HeLa cells were processed for indirect immunolabeling of ultrathin cryosections essentially as previously described (McCaffery and Farquhar, 1995). Briefly, cells were fixed in a monolayer at 4°C in 100mM PO₄ (pH 7.4), 2.5% sucrose, and containing 4% formaldehyde. The cells were harvested, pelleted and cryo-protected in 2.3M sucrose containing 30% polyvinyl pyrrolidone. Cell pellets were mounted onto aluminum cryopins and frozen in liquid nitrogen. Ultrathin cryosections were then cut on a Leica UCT ultramicrotome equipped with an FCS cryostage and sections were collected onto 300 mesh, formvar/carbon coated nickel grids. Grids were washed, blocked in 10% FCS and incubated overnight with primary chicken anti-GFP antibody (10µg/ml). After washing, grids were incubated with 6 or 12nm Au-conjugated donkey anti-chicken antibody (Jackson ImmunoResearch Labs, Ft. Washington, PA) for 2 hours, washed and subsequently embedded in a mixture containing 3.2% polyvinyl alcohol (10,000 MW), 0.2% methyl cellulose (400 centipoises), and 0.2% uranyl acetate. Sections were analyzed on a Tecnai 12 transmission electron microscope and images collected with a Soft Imaging System Megaview III digital camera.

Recombinant protein expression and purification

MBP-tagged SENP2(1-63)^{WT}, SENP2(1-63)^{I8D}, or MBP construct alone were

transformed into *Escherichia coli* Rosetta competent cells. Expression was induced using 0.5mM isopropylthiogalactoside (IPTG) at 20°C overnight. Cells were pelleted and resuspended in ice-cold lysis buffer (50mM Tris-HCl (pH 7.5), 150mM NaCl, 1mM EDTA, 1mM phenylmethylsulfonyl fluoride (PMSF), 5mg/ml leupeptin and pepstatin A, 1mM dithiothreitol (DTT) and 1mg/ml lysozyme). Suspensions were sonicated for a total of 1 minute, 0.5-second intervals, and then centrifuged at 30,000 x g for 30 minutes at 4°C. The supernatant was incubated with equilibrated amylose resin (New England Biolabs, Ipswich, MA) for 2 hours at 4°C, with end-to-end rotation. Bound protein was eluted in buffer containing 50mM Tris-HCl (pH 7.5), 150mM NaCl, 1mM EDTA, 1mM DTT, and 20mM maltose.

His-tagged mouse Kap- α_2 was expressed in *Escherichia coli* Rosetta competent cells as described above and purified using Ni-NTA agarose affinity column chromatography, according to manufacturer's protocol (Qiagen). For expression and purification of MBP-SEN2(1-63)^{WT} in complex with His-tagged Kap- α_2 , both protein expression constructs were co-transformed in *Escherichia coli* Rosetta competent cells. Co-expression was induced using 0.5mM IPTG at 20°C overnight. Complex purification was performed as described above. A final concentration of 20mM maltose was added to co-elute the protein complex.

In vitro liposome co-sedimentation assay

Lipids dissolved in chloroform, purchased from Avanti Polar Lipids (Alabaster, AL), were mixed together in a glass tube to make the following lipid composition: 79 mol% phosphatidylcholine (PC), 20 mol% phosphatidylethanolamine (PE), and 1 mol%

NBD-labeled phosphatidylethanolamine (NBD-PE). Lipid vesicles were prepared essentially as previously described (Tu-Sekine and Raben, 2012). Briefly, the homogenous lipid mixture was dried under dry nitrogen stream and stored under vacuum for 2-20 hours to remove residual chloroform. Lipid films were rehydrated with hydration buffer (50mM Tris-HCl (pH 7.5), 150mM NaCl, 1mM EDTA, and 176mM sucrose) at 37°C for 30 minutes. During hydration, and in 10-minute intervals, samples were vortexed and then sonicated in a water bath sonicator for 30 seconds, until the lipid films were completely resuspended. Vesicles were formed by extrusion through a 100nm polycarbonate membrane, using an Avanti mini-extruder and following manufacturer's protocol. Sucrose-filled liposomes were then diluted with binding buffer (50mM Tris-HCl (pH 7.5), 150mM NaCl, and 1mM EDTA) at a 1:4 ratio, then spun down at 186,000 x g in a tabletop ultracentrifuge at 22°C for 1 hour. Pellets were resuspended with binding buffer and concentrations were determined using a spectrophotometer. A fresh liposomes batch was prepared for each experiment. For liposome co-sedimentation assays, 1.5mM, 3mM, 6mM, or 12mM liposomes were mixed with 0.7µg of protein prepared in binding buffer, in a total volume of 100µL per reaction. Liposomes and protein were incubated for 30 minutes at room temperature. The reaction was pelleted at 186,000 x g in a tabletop ultracentrifuge at 22°C for 1 hour. Equal volumes of pellet and supernatant were analyzed by SDS-PAGE, followed by immunoblotting. It should be noted that apparent maximal protein binding varied between individual experiments, but that variability within experimental replicates was low.

Subcellular fractionation

Isolation of ER membranes was performed as previously described (Bozidis *et al.*, 2007). Briefly, HeLa cells were seeded in 55cm² plates and either untreated, or transfected with GFP-SEN2(1-63)^{mNLS} or GFP-SEN2(1-63)^{mNLS/18D}. After 24 hours, cells were harvested and pelleted by centrifugation at 200 x g for 10 minutes at 4°C. Cells were lysed in 1X MTE buffer (270mM D-mannitol, 10mM Tris-base (pH 7.4), 0.1mM EDTA). Lysate was sonicated for a total of 30 seconds, 10-second intervals, and then centrifuged at 1400 x g for 15 minutes at 4°C. To separate crude ER from crude mitochondria, supernatant was centrifuged at 15,000 x g for 15 minutes. To purify ER membranes, supernatant was layered on top of a discontinuous sucrose gradient (from bottom to top: 2mL of 2.0M sucrose, 3mL of 1.5M sucrose, 3mL of 1.3M sucrose) in a polyallomer ultracentrifuge tube (Beckman Coulter, Indianapolis, IN). ER sucrose gradients were centrifuged for 70 minutes at 152,000 x g. Banded ER membranes at the 1.3M sucrose interface were collected using an 18 Gauge needle then transferred to a new polyallomer tube and pelleted at 126,000 x g for 45 minutes. Pellets containing ER membranes were resuspended in 1X MTE buffer. Fractions collected were analyzed by SDS-PAGE followed by immunoblotting.

Stable cell lines and biotin-streptavidin affinity purification for BioID

Stable cell lines for BioID analysis were established essentially as previously described (Gupta *et al.*, 2015). In brief, the full-length human SEN2 (BC040609) coding sequence was amplified by PCR, and cloned into pcDNA5 FRT/TO FLAG-BirA* expression vector. Using the Flp-In system (Invitrogen, Carlsbad, CA), 293T-REx Flp-In

cells stably expressing FLAG-BirA* alone, FLAG-BirA*-SEN2^{WT}, or FLAG-BirA*-SEN2^{I8D} were generated. 10 x 150 cm² plates of sub-confluent (60%) cells were incubated for 24 hours in complete media supplemented with 1µg/ml tetracycline (Sigma-Aldrich, St. Louis, MO) and 50µM biotin (BioShop Canada Inc., Ontario, Canada). Cells were collected and pelleted (200 x g, for 3 minutes), the pellet was washed twice with PBS, and dried pellets were snap frozen.

Cell pellets were resuspended in 10mL of lysis buffer (50mM Tris-HCl (pH 7.5), 150 mM NaCl, 1mM EDTA, 1mM EGTA, 1% Triton X-100, 0.1% SDS, 1:500 protease inhibitor cocktail (Sigma-Aldrich, St. Louis, MO), 1:1000 benzonase nuclease (Novagen)) and incubated on an end-to-end rotator at 4°C for 1 hour, briefly sonicated to disrupt any visible aggregates, then centrifuged at 45,000 x g for 30 minutes at 4°C. Supernatant was transferred to a fresh 15mL conical tube. 30µL of packed, pre-equilibrated streptavidin sepharose beads (GE Healthcare, Silver Spring, MD) were added and the mixture incubated for 3 hours at 4°C with end-to-end rotation. Beads were pelleted by centrifugation at 2000 x g for 2 minutes and transferred with 1mL of lysis buffer to a fresh microcentrifuge tube. Beads were washed once with 1mL lysis buffer and twice with 1mL of 50mM ammonium bicarbonate (pH 8.3). Beads were transferred in ammonium bicarbonate to a fresh centrifuge tube, and washed two more times with 1mL ammonium bicarbonate buffer. Tryptic digestion was performed by incubating the beads with 1µg MS-grade TPCK trypsin (Promega, Madison, WI) dissolved in 200µL of 50mM ammonium bicarbonate (pH 8.3) overnight at 37°C. The following morning, 0.5µg MS-grade TPCK trypsin was added, and beads were incubated 2 additional hours at 37°C. Beads were pelleted by centrifugation at 2000 x g for 2 minutes, and the

supernatant was transferred to a fresh microcentrifuge tube. Beads were washed twice with 150 μ L of 50mM ammonium bicarbonate, and washes were pooled with the eluate. The sample was lyophilized and resuspended in buffer A (0.1% formic acid). 1/5th of the sample was analyzed per MS run.

Mass spectrometry

Analytical columns (75 μ m inner diameter) and pre-columns (150 μ m inner diameter) were made in-house from fused silica capillary tubing from InnovaQuartz (Phoenix, AZ) and packed with 100 Å C18-coated silica particles (Magic, Michrom Bioresources, Auburn, CA). Peptides were subjected to liquid chromatography (LC)-electrospray ionization-tandem mass spectrometry, using a 120-minute reversed-phase (100% water–100% acetonitrile, 0.1% formic acid) buffer gradient running at 250ml/min on a Proxeon EASY-nLC pump in-line with a hybrid LTQ-Orbitrap Velos mass spectrometer (Thermo Fisher Scientific, Waltham, MA). A parent ion scan was performed in the Orbitrap using a resolving power of 60,000, then up to the twenty most intense peaks were selected for MS/MS (minimum ion count of 1000 for activation), using standard collision induced dissociation fragmentation. Fragment ions were detected in the LTQ. Dynamic exclusion was activated such that MS/MS of the same m/z (within a range of 15 ppm; exclusion list size = 500) detected twice within 15 seconds were excluded from analysis for 30 seconds. For protein identification, Thermo .RAW files were converted to .mzXML format using Proteowizard (Kessner *et al.*, 2008), then searched using X!Tandem (Craig and Beavis, 2004) against the human (Human RefSeq Version 45) database. X!Tandem search parameters were: 15ppm parent mass error; 0.4

Da fragment mass error; complete modifications, none; cysteine modifications, none; potential modifications, +16@M and W, +32@M and W, +42@N-terminus, +1@N and Q. Data were analyzed using the trans-proteomic pipeline (Deutsch *et al.*, 2010; Pedrioli, 2010) via the ProHits software suite (Liu *et al.*, 2010). Proteins identified with a Protein Prophet cut-off of 0.9 and at least two unique peptides were analyzed with the SAINT express algorithm (v3.6.1) (Teo *et al.*, 2014). Sixteen control runs (consisting of twelve FLAG-BirA*only and four samples with no bait expressed) were collapsed to the two highest spectral counts for each prey, and the SAINT score cut-off value was set to a BFDR<0.01 (1% FDR). A network of high confidence interactors was assembled using Cytoscape (3.4.0).

RESULTS

SEN2 associates with NPCs and with the inner nuclear membrane

SEN2 has previously been shown to associate with NPCs, based on fluorescence microscopy and mass spectrometry-based identification of interacting proteins (Hang and Dasso, 2002; Zhang *et al.*, 2002; Goeres *et al.*, 2011). In addition to punctate NPC localization, however, we have also observed that SEN2 can be more generally detected as a continuous staining of the inner nuclear membrane (Figure II-1). To explore this localization more closely, we transiently expressed GFP-SEN2 in HeLa cells and examined the co-localization with either mAb414 (a NPC marker) or lamin B (an inner nuclear membrane marker). Consistent with previous findings, SEN2 co-localized with NPCs, but even more closely co-localized with lamin B (Figure II-1, A and B). We then compared the localization of SEN2 with that of SENP1, a second SUMO isopeptidase also associated with NPCs (Chow *et al.*, 2012; Cubenas-Potts *et al.*, 2013). Transient co-transfection of GFP-SEN2 with mCherry-SENP1 showed that SEN2 and SENP1 have distinct localization patterns. SEN2 displayed a more continuous staining at the nuclear envelope, whereas SENP1 was detected as punctae resembling NPC staining (Figure II-1C). These results revealed that SEN2 associates with NPCs and also with the inner nuclear membrane. To elucidate the molecular basis of SEN2 localization in greater detail, we further explored the signals that target it to the inner nuclear membrane.

The extreme N-terminus of SENP2 contains both NPC and membrane-targeting signals

SENP2 contains multiple N-terminal signals specifying localization, including two signals that mediate interactions with NPCs. One signal within amino acids 1-63 consists of a bipartite NLS that mediates interactions with FG repeat nucleoporins through high affinity karyopherin binding. A second signal, within amino acids 143-350, interacts with the Nup107-160 subcomplex of the NPC (Goeres *et al.*, 2011). To determine whether one or the other of these signals also directs SENP2 to the inner nuclear membrane, we closely examined the localization of GFP-tagged fusion proteins (Figure II-2). GFP-SENP2(1-63) showed a continuous staining of the inner nuclear membrane similar to full-length SENP2 (Figure II-2, A and B). In contrast, GFP-SENP2(143-350) showed a punctate pattern similar to NPC staining (Figure II-2C). This result suggested that the first 63 amino acids of SENP2, in addition to promoting interactions with FG-repeat nucleoporins, might also have an additional signal that facilitates associations with the inner nuclear membrane. To explore this prediction, we deleted the first 9 amino acids and analyzed the localization of GFP-SENP2(10-63) (Figure II-2D). Consistent with the presence of a second, membrane targeting signal, GFP-SENP2(10-63) was no longer concentrated at the nuclear periphery but instead showed a diffuse nucleoplasmic localization. Thus, the extreme N-terminus of SENP2 contains both NPC and inner nuclear membrane targeting signals.

The extreme N-terminus of SENP2 contains a predicted amphipathic α -helix

To explore how residues in the extreme N-terminus of SENP2 may function in targeting to the inner nuclear membrane, we performed secondary structure analysis and identified a predicted amphipathic α -helix that could serve as an in-plane membrane anchor (Figure II-3, A and D). Sequence alignment of the first 52 amino acids of SENP2 demonstrated that the predicted amphipathic α -helix is highly conserved within mammals (Figure II-3B). Interestingly, although the extreme N-terminus of zebrafish SENP2 is not conserved at the amino acid sequence level with mammalian SENPs, it nonetheless contains a predicted amphipathic α -helix (Figure II-3C). This suggests that the predicted amphipathic α -helix has an essential role in the overall function of SENP2.

To test whether the targeting of SENP2 to the inner nuclear membrane is dependent on this predicted amphipathic α -helix, we generated a mutant GFP-SENP2 expression construct with isoleucine 8 mutated to aspartic acid (I8D) in the hydrophobic face of the predicted amphipathic α -helix (Figure II-3D). Wild type or I8D mutant GFP-SENP2 proteins were transiently expressed in HeLa cells and their localization analyzed using fluorescence microscopy. Compared to wild type SENP2, the I8D mutant showed reduced targeting to the inner nuclear membrane and enhanced nucleoplasmic localization (Figure II-3E, upper panel). The SENP2 I8D mutant retains the 143-350 NPC targeting signal, explaining the observed residual membrane localization. To more clearly assess the ability of the predicted amphipathic α -helix to target SENP2 to the inner nuclear membrane, we evaluated the localization of wild type and I8D mutant GFP-SENP2(1-63). In contrast to wild type GFP-SENP2(1-63), the I8D mutant showed only diffuse nucleoplasmic localization comparable to that observed with GFP-SENP2(10-63)

(Figures II-3E and II-2D). These results are consistent with the predicted N-terminal amphipathic α -helix acting as an in-plane membrane anchor that tethers SENP2 to the inner nuclear membrane.

Overproduction of SENP2 induces the formation of intranuclear membranes

In addition to localization at the nuclear membrane, GFP-SENP2 is also detected in intranuclear foci, whose number and intensity correlate with levels of SENP2 expression (Figure II-1). Notably, the amphipathic α -helices of several other proteins, including Nup153 and Nbp1, form membranous intranuclear inclusions upon overexpression (Bastos *et al.*, 1996; Kupke *et al.*, 2011). To investigate whether GFP-SENP2 overexpression also induces the formation of intranuclear membranes, we performed immunoelectron microscopy on ultrathin cryosections of transfected HeLa cells (Figure II-4). We found that intranuclear labeling was concentrated within densely stained inclusions containing membranous structures reminiscent of those detected in cells overexpressing the amphipathic α -helix of Nup153. Cells expressing GFP-SENP2^{18D} did not show similar membranous structures (Figure II-5). These results are consistent with interactions between SENP2 and the inner nuclear membrane and suggest an ability to stimulate membrane formation.

The N-terminal amphipathic α -helix of SENP2 mediates direct membrane binding

Although predicted to interact directly with membranes, the N-terminus of SENP2 may also promote indirect binding to the inner nuclear membrane through interactions with other membrane-associated proteins. To test for direct membrane

interaction, we expressed and purified recombinant wild type and I8D mutant SENP2(1-63) as maltose binding protein (MBP) fusion proteins. The purified proteins were incubated with in vitro synthesized liposomes, and membrane binding was evaluated using a co-sedimentation assay. Wild type MBP-SENP2(1-63)^{WT} co-sedimented with liposomes in a dose-dependent manner, consistent with direct membrane binding (Figure II-6, A and C). In contrast, the I8D mutant MBP-SENP2(1-63)^{I8D} did not pellet with liposomes, revealing an essential role for the amphipathic α -helix in membrane binding (Figure II-6, A and C). As a negative control, liposomes were incubated with purified recombinant MBP, which showed no direct membrane interaction (Figure II-6A). As an additional control, recombinant proteins failed to sediment in the absence of liposomes (Figure II-6B). Thus, our results demonstrate that the predicted N-terminal amphipathic α -helix of SENP2 binds directly to membranes.

SENP2 interactions with membranes can be modulated by Kap- α binding

SENP2 contains a bipartite NLS in close proximity to the predicted N-terminal amphipathic α -helix. This NLS binds with high affinity to Kap- α and mediates its import to the nucleus and association with FG-repeat nucleoporins (Goeres *et al.*, 2011). Studies of other nuclear proteins containing N-terminal amphipathic α -helices in close proximity to functional NLSs, including Nbp1, Pom33, and Nup153, have found that karyopherin binding inhibits interactions with cytoplasmic membranes prior to delivery to the nucleus (Kupke *et al.*, 2011; Floch *et al.*, 2015; Vollmer *et al.*, 2015). To investigate whether Kap- α binding similarly controls the membrane interactions of SENP2, we performed liposome binding assays in the presence or absence of recombinant purified Kap- α . MBP-

SEN2(1-63) alone, or in a 1:1 complex with Kap- α -6xHis (Figure II-7D) was incubated in the presence or absence of membranes and sedimentation was evaluated by centrifugation. As previously observed, ~80% of MBP-SEN2(1-63) co-sedimented with liposomes. In contrast, liposome binding of MBP-SEN2(1-63) was reduced by >50% in the presence of Kap- α and only ~10% of Kap- α itself associated with the liposome pellet (Figure II-7, A and C). Because Kap- α alone has limited membrane affinity (Figure II-8), its membrane association in these experiments likely represents levels of MBP-SEN2(1-63)-Kap- α complexes bound to liposomes. Therefore, levels of Kap- α binding may more closely reflect its effects on MBP-SEN2(1-63) membrane interaction. Thus, our results reveal that SEN2 membrane interaction can be regulated by Kap- α binding. Next, we wanted to investigate Kap- α regulation in an in vivo setting.

Disrupting the SEN2 N-terminal NLS facilitates targeting to cytoplasmic membranes

To investigate the effect of Kap- α binding on SEN2 localization in vivo, we analyzed the localization of a mutant GFP-SEN2(1-63) in which the NLS had been mutated at two residues (mNLS: R29A/R49A), thereby disrupting the Kap- α interaction (Goeres *et al.*, 2011). The effect of this NLS mutation on localization was first analyzed by fluorescence microscopy. In contrast to the nuclear membrane localization of GFP-SEN2(1-63), the NLS mutant protein showed a reticular-like staining pattern in the cytoplasm that partially co-localized with the ER marker, calnexin, and co-localized with the Golgi marker GM130 (Figure II-9A). To further verify membrane localization in the cytoplasm, we isolated a fraction enriched for ER membranes by sucrose gradient

sedimentation and performed immunoblot analysis. Consistent with the calnexin co-localization, GFP-SEN2(1-63)^{mNLS} was detected in the membrane fraction together with calnexin (Figure II-9B, left panel). In contrast, when we combined the I8D and NLS mutations and performed the same fractionation analysis, we found that GFP-SEN2(1-63)^{mNLS/I8D} was dramatically reduced in the membrane fraction, and was mostly found in the soluble fraction with tubulin (Figure II-9B, right panel). Our findings show that the N-terminus of SEN2 has the ability to associate with intracellular membranes in the cytoplasm, and this association is negatively regulated by Kap- α binding.

Endogenous SEN2 isoforms associate with intracellular membranes

Immunoblot analysis of endogenous SEN2 expressed in cultured mammalian cells reveals multiple isoforms ranging from 55 to 27 kDa that are thought to be derived through alternative splicing. Moreover, endogenous SEN2 is detected at the nuclear envelope but also in the nucleus and cytoplasm by immunofluorescence microscopy, suggesting differential localization of these isoforms (Goeres *et al.*, 2011). To explore possible associations of endogenous SEN2 with membranes, HeLa cells were fixed, permeabilized with digitonin and then co-labeled with antibodies recognizing SEN2 and the ER protein marker, GRP78 (Figure II-10A). Consistent with ER membrane association, the cytoplasmic SEN2 signal co-localized with GRP78. To further validate this finding, we again isolated a fraction enriched for ER membranes by sucrose gradient sedimentation and performed immunoblot analysis (Figure II-10B). Multiple SEN2 isoforms migrating at 50, 40 and 27 kDa co-purified with the membrane fraction. However, one isoform migrating at ~48 kDa was uniquely detected in the soluble

fraction. This isoform may correspond to a splice variant identified in mice that lacks the 50 N-terminal amino acids, including the predicted amphipathic α -helix (Figure II-10C) (Nishida *et al.*, 2001). To investigate whether the co-purification of endogenous SENP2 isoforms with membranes may be due to interactions with NPCs, we probed fractions with mAb414, which recognizes multiple nucleoporins (Figure II-10D). Nup358, Nup214, and Nup153 largely co-purified with the soluble fraction, whereas p62 showed an equal distribution between soluble and membrane fractions. Thus, although it is unlikely that membrane interaction is due to binding to NPC filament proteins, NPC binding in general cannot be ruled out.

SENP2 interacts with membrane-associated proteins

Our results thus far provide evidence that SENP2 associates with the inner nuclear membrane, ER, and Golgi membranes. However, the sumoylated proteins regulated by SENP2 at these membranes remain largely unknown. We previously used an affinity purification-mass spectrometry (AP-MS) based approach to isolate stable SENP2-interacting proteins and identified proteins of the nuclear pore complex (nucleoporins) and soluble nuclear transport receptors (Goeres *et al.*, 2011). In order to identify more transiently associated or less abundant SENP2-interacting proteins, including potential substrates, we turned to the proximity-dependent biotin identification (BioID) approach (Roux *et al.*, 2013). Stable cell lines for inducible expression of full-length wild type SENP2 fused to the biotin ligase variant, BirA*, or the BirA* ligase alone were generated. Expression levels and localization of FLAG-BirA*-SENP2 were compared to endogenous SENP2 via immunofluorescence microscopy and immunoblot analysis

(Figure II-11). Following induction, cells were cultured in the presence of biotin for 24 hours and biotinylated proteins were purified by streptavidin affinity chromatography and analyzed by mass spectrometry (a full list of identified proteins can be found in the supplemental materials of the following paper: Odeh *et al.*, 2018). This list of proteins was analyzed using the Significance Analysis of INTeractomes (SAINT) approach to identify high-confidence SENP2-interacting partners (Choi *et al.*, 2012). Consistent with previous AP-MS analysis (Goeres *et al.*, 2011), NPC-associated proteins were detected (Figure II-12A and supplemental materials in Odeh *et al.*, 2018). Of particular interest, and consistent with immunofluorescence microscopy, subcellular fractionation, and *in vitro* binding results, we also detected interactions with proteins of the inner nuclear membrane, ER, and Golgi that were not previously identified (Figure II-12A and supplemental materials in Odeh *et al.*, 2018). To test whether these unique interactions with SENP2 are dependent on its predicted amphipathic α -helix, we performed the BioID analysis using stably-expressed FLAG-BirA*-SENP2^{I8D}. Similar to the wild type SENP2, SENP2^{I8D} interacted with NPC-associated proteins (Figure II-12B), indicating that these interactions are independent on SENP2-membrane association. However, the SENP2^{I8D} mutant lost association with most of the membrane-associated proteins compared to the wild type protein, consistent with the N-terminal predicted amphipathic α -helix being responsible for SENP2-membrane binding (Figure II-12B and supplemental materials in Odeh *et al.*, 2018). Given the diffuse nucleoplasmic localization of SENP2^{I8D}, the mutant protein also gained new interactions with soluble nuclear proteins that did not interact with SENP2^{WT}.

DISCUSSION

As the functions of SUMO rapidly expand beyond the nucleus, evidence for SUMO regulation at multiple intracellular membranes continues to emerge. However, very little is known about how SUMO is affecting membrane-associated functions, or how sumoylation is regulated at membranes. In this study, we have identified a novel interaction between SENP2, an essential regulator of SUMO dynamics, and intracellular membranes. We showed that SENP2 has a unique N-terminal amphipathic α -helix, absent in other SUMO proteases, which allows it to directly interact with membranes under the regulation of Kap- α . We also identified a unique subset of membrane-associated proteins that interact with SENP2, providing further insights into the potential roles SUMO can play in regulating membrane-associated functions.

SENP2 predicted amphipathic α -helix and membrane interaction

Our previous study showed that SENP2 associates dynamically with NPCs (Goeres *et al.*, 2011). However, our immunofluorescence microscopy data reported here indicate that SENP2 not only associates with NPCs, but also co-localizes with the inner nuclear membrane. Apparent differences in localization could be explained by GFP-SENP2 expression levels. At low expression levels, GFP-SENP2 showed punctate staining, closely resembling NPC staining. In contrast, the signal for moderate to high expression levels of GFP-SENP2 revealed localization to both the NPCs and the nuclear membrane (Figure II-13). Thus, SENP2 may have higher affinity for NPCs compared to the inner nuclear membrane itself. However, endogenous SENP2 localizes to membranes,

including ER and Golgi, evident from subcellular fractionation and colocalization with GRP78. We performed colocalization studies with various Golgi marker proteins and endogenous SENP2 but were unable to detect obvious Golgi enrichment either due to the low level of SENP2 expression or transient interactions between SENP2 and Golgi-associated proteins and membranes. Nevertheless, consistent with membrane localization, in our BioID analysis we identified membrane-associated proteins that interact with SENP2 giving us further reason to explore this newly discovered SENP2-membrane interaction.

Sequence analysis and secondary structural predictions revealed that SENP2 has a unique N-terminal amphipathic α -helix, absent in other SUMO proteases. Our *in vivo* and *in vitro* analyses further demonstrated that this predicted amphipathic α -helix directly associates with membranes. Studies have shown that there are two classes of amphipathic α -helices, one that senses membrane curvature, and one that induces membrane curvature (Drin and Antony, 2010). For instance, proteins with the ArfGAP1 lipid-packing sensor (ALPS)-like motif, composed of polar, uncharged residues, mainly serine and threonine, are more suitable for sensing membrane curvature (Drin *et al.*, 2007). Examples include: the Golgi protein golgin GMAP-210 (Drin *et al.*, 2007), and nucleoporin Nup133 (Drin *et al.*, 2007). In contrast, amphipathic α -helices with basic, charged residues are thought to induce membrane curvature. Given that SENP2 has a stretch of basic, charged residues (refer to Figure II-3D), we predict that its amphipathic α -helix is more suitable for inducing membrane curvature, however, further investigation is still required. Notably, multiple NPC-associated proteins with ALPS-like motifs (Nup120, Nup85, Nup170, and Nup188) or with a basic stretch of amino acids in their amphipathic α -helix (Nup1/Nup60

in yeast) have an important role in pore complex insertion into the nuclear membrane (Alber *et al.*, 2007; Doucet and Hetzer, 2010; Doucet *et al.*, 2010; Drin and Antonny, 2010; Meszaros *et al.*, 2015; Souquet and Doye, 2015). SENP2 has also been reported to play a role in NPC homeostasis, more specifically, when SENP1 and SENP2 are co-depleted, the expression levels of certain nucleoporins decreases and are mislocalized (Chow *et al.*, 2014). Thus, it would be interesting to explore whether these effects are attributed to the ability of SENP2 to bind to membranes through its predicted amphipathic α -helix.

Another aspect of SENP2 that is shared with other proteins with amphipathic α -helices associated with the inner nuclear membrane, like yeast Nbp1 and Nup1/Nup60 (Nup153 in humans), is its ability to induce the formation of intranuclear membranes upon overexpression (Bastos *et al.*, 1996; Kupke *et al.*, 2011; Meszaros *et al.*, 2015). The overexpression of Nup1 for example, results in the de novo synthesis of ‘expansion’ membranes that are thought to arise as a secondary response to the physical stress imposed on the nuclear envelope (Meszaros *et al.*, 2015). We also noticed the formation of intranuclear membranes upon SENP2 overexpression, seen by immuno-EM as arrays of membranous structures. Although likely an artifact of overexpression, it is possible that the formation of intranuclear membranes is a product of a normal function of SENP2 amphipathic α -helix and its predicted ability to induce membrane curvature.

It is interesting to note that Nup1 overexpression results in the enlargement of cells indicating a mitotic defect, which was attributed to its amphipathic α -helix and its induction of membrane formation (Meszaros *et al.*, 2015). Similarly, it has been previously shown that SENP2 overexpression causes cell cycle arrest in mitosis (Zhang *et*

al., 2008). We asked whether this mitotic arrest is dependent on SENP2 amphipathic α -helix and induction of intranuclear membranes, and we found that the overexpression of either SENP2^{WT} or SENP2^{I8D} resulted in a similar mitotic phenotype (Figure II-14). Collectively, we found that the SENP2 predicted amphipathic α -helix shares many properties with amphipathic α -helices described for other proteins, suggesting important consequences for SENP2 function.

SENP2 and Kap- α regulation

Using *in vitro* and *in vivo* methods, we showed that the predicted amphipathic α -helix of SENP2 is regulated by its interactions with Kap- α . Kap- α binds to the NLS in close proximity to the amphipathic α -helix, thereby impeding interactions with cytoplasmic membranes. We propose that once SENP2 is transported into the nucleus and Kap- α is released, the helix is free to bind to the inner nuclear membrane, hence explaining the preferential localization of SENP2 (Figure II-15). Regulation of localization has been previously described for other proteins with predicted amphipathic α -helices and a proximal NLS, including Nbp1 (Kupke *et al.*, 2011), Nup60 (Meszaros *et al.*, 2015), Pom33 (Floch *et al.*, 2015), and Nup153 (Vollmer *et al.*, 2015). Based on our findings, we propose that karyopherin binding may serve as a common mechanism to regulate the relative distribution of these proteins between nuclear and cytoplasmic membranes.

Kap- α binding to SENP2 could be regulated at multiple levels. First, phosphorylation of SENP2 at amino acids within or in close proximity to the NLS could regulate the binding of Kap- α . Second, alternative splicing could result in protein variants

lacking a functional NLS. Consistent with this latter mechanism, the bipartite NLS of SENP2 is split between two exons, exon 1 and exon 2. Collectively, either mechanism could explain our detection of endogenous SENP2 at both nuclear and cytoplasmic membranes.

It is also possible that alternative splicing could affect SENP2 localization by the presence or absence of the amphipathic α -helix itself. In fact, studies in mice have identified an alternatively spliced SENP2 variant lacking the first 50 N-terminal amino acids (Nishida *et al.*, 2001). Consistently, we identified two SENP2 variants of ~50kDa and ~48kDa that were detected in the membrane and soluble fractions, respectively (refer to Figure II-10, B and C). Similar to the SENP2 isoform identified in mice, we predict that the lower molecular weight variant lacks the amphipathic α -helix.

Sumoylation at intracellular membranes

Using BioID, we found that SENP2 interacts with a subset of membrane-associated proteins in the ER, Golgi and inner nuclear membrane. These interactions are dependent on the presence of the predicted amphipathic α -helix. Notably, we did not capture those interactions in our previous AP-MS analysis (Goeres *et al.*, 2011), likely reflecting the ability of BioID to more effectively capture dynamic, transient protein-protein interactions (Roux *et al.*, 2013). Since proteins are covalently modified, harsher lysis methods can be employed enabling us to identify membrane or poorly soluble proteins. Additionally, weak interactors can be retained since protein-protein interactions do not have to be maintained post-lysis (Coyaud *et al.*, 2015). One caveat however, is that the BioID does not differentiate between SENP2 substrates and interacting proteins.

Nonetheless, the interacting proteins that were identified suggest new functions for sumoylation at membranes that must be further explored.

Closer analysis of the functions of the ER- and Golgi-associated proteins identified, we found that a significant number of these proteins are involved in vesicle-mediated transport, for example YKT6, SAR1B, YIF1A, and PREB. Interestingly, studies in yeast also showed that SUMO interacts with a subset of proteins involved in vesicle transport, suggesting a role for sumoylation in regulating this process (Makhnevych *et al.*, 2009). Together, we hypothesize that SENP2 may have a role in regulating vesicle-mediated transport, by directly regulating the sumoylation of vesicle trafficking proteins.

In addition to vesicle-mediated transport, sumoylation also plays a role in regulating the nuclear export and subsequent translation of mRNAs encoding secreted, or membrane-targeted proteins. More specifically, a previous study showed that the SUMO E3 ligase, RanBP2/Nup358, located at the cytoplasmic face of the NPC, directly binds with the signal sequence coding regions of mRNAs, potentially coupling sumoylation with the biogenesis of membrane-targeted proteins (Mahadevan *et al.*, 2013). Given the interactions between SENP2 and ER-associated proteins, it will be valuable to explore the role of SENP2 in this process.

It is also worth noting that our BioID analysis identified multiple subunits of the ER membrane protein complex (EMC), including EMC1 through EMC5 (also known as MGMT1), and EMC7-9 (refer to Figure II-12A). EMC is a multifunctional 10-subunit protein complex involved in ER-associated degradation (ERAD), protein folding, cellular response to ER stress, lipid homeostasis, and the efficient insertion of tail-anchored

proteins into ER membranes (Jonikas *et al.*, 2009; Christianson *et al.*, 2011; Richard *et al.*, 2013; Lahiri *et al.*, 2014; Satoh *et al.*, 2015; Wideman, 2015; Guna *et al.*, 2018). Since sumoylation is involved in regulating many of the same processes (Enserink, 2015), it is reasonable to suggest that SENP2 interaction with EMC subunits allows it to directly regulate those functions. It is also possible that the EMC complex itself may facilitate the binding of the SENP2 amphipathic α -helix to the ER membrane, but this requires further investigation.

Besides ER- and Golgi-associated proteins, a subset of proteins at the inner nuclear membrane was also found to interact with SENP2. Among those proteins, lamins stood out, as they are well-studied SUMO substrates. Lamin A, for example, is known to be sumoylated at several lysine residues: K201, K420, and K486. Multiple mutations within the SUMO sites of lamin A result in decreased sumoylation and are associated with disease (laminopathies), more specifically, familial dilated cardiomyopathy or familial partial lipodystrophy (Zhang and Sarge, 2008; Simon *et al.*, 2013). How the sumoylation of lamin A is regulated is still unknown, however, based on the interactions we have identified between lamins and SENP2, we suggest that SENP2 may be playing a role in regulating the sumoylation process of lamins, particularly lamin A, and therefore regulating its functions.

In conclusion, our study opens doors to further explore the roles of sumoylation at membranes. As a crucial next step, SENP2 substrates, including potential candidates identified through BioID, need to be further characterized. Overall, our findings further illustrate the importance of the unique targeting signals in the N-termini of SENPs and their role in defining localization and function. Additionally, based on Kap- α regulation

of the amphipathic- α helix, we predict that the N-terminal signals themselves may be differentially regulated in response to the physiological needs of the cell.

FIGURES AND FIGURE LEGENDS

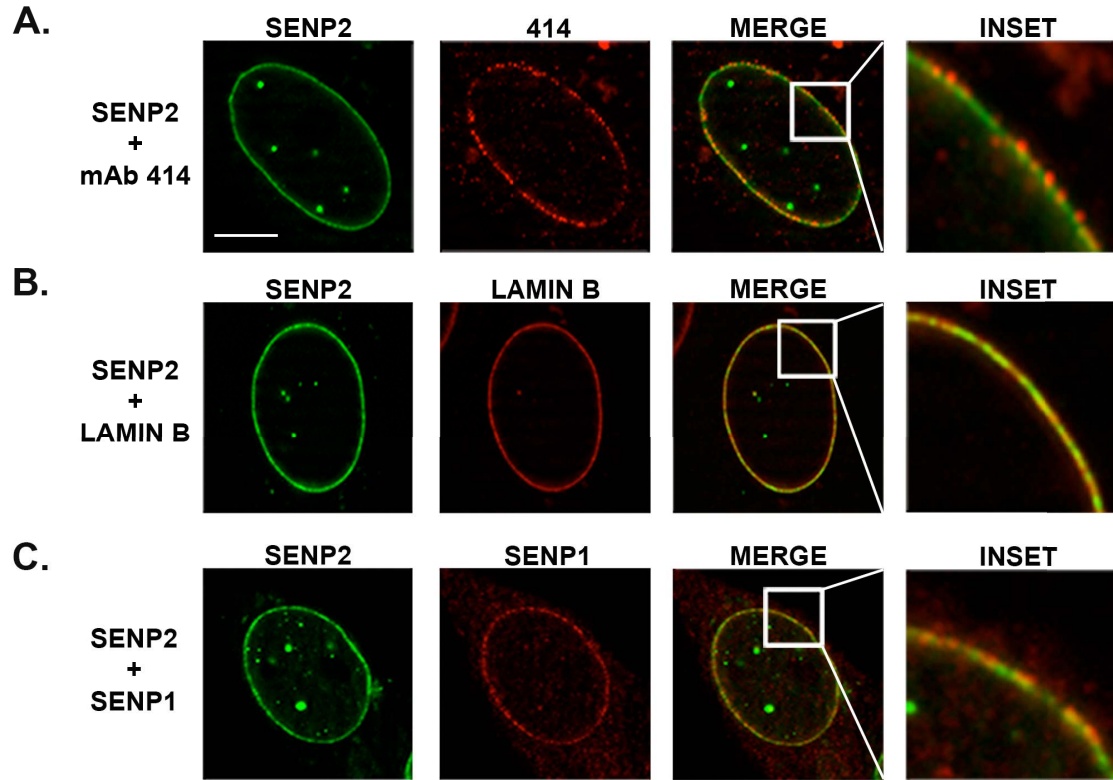


Figure II-1. SENP2 localizes to NPCs and the inner nuclear membrane. HeLa cells were transiently transfected with full length GFP-SENP2 and co-localization with NPCs, nuclear lamina or mCherry-SENP1 was assessed by fluorescence microscopy. (A) Cells were stained with mAb 414, an antibody specific for nucleoporins. GFP-SENP2 partially co-localized with the punctate NPC staining. (B) Cells were stained with an antibody specific for lamin B, a marker for the inner nuclear membrane. GFP-SENP2 co-localized with the continuous lamin B nuclear rim staining. (C) Cells were co-transfected with mCherry-SENP1. SENP1 and SENP2 co-localized at NPCs. Continuous rim staining and localization to the inner nuclear membrane is unique to SENP2. Scale bar = 5 μ m.

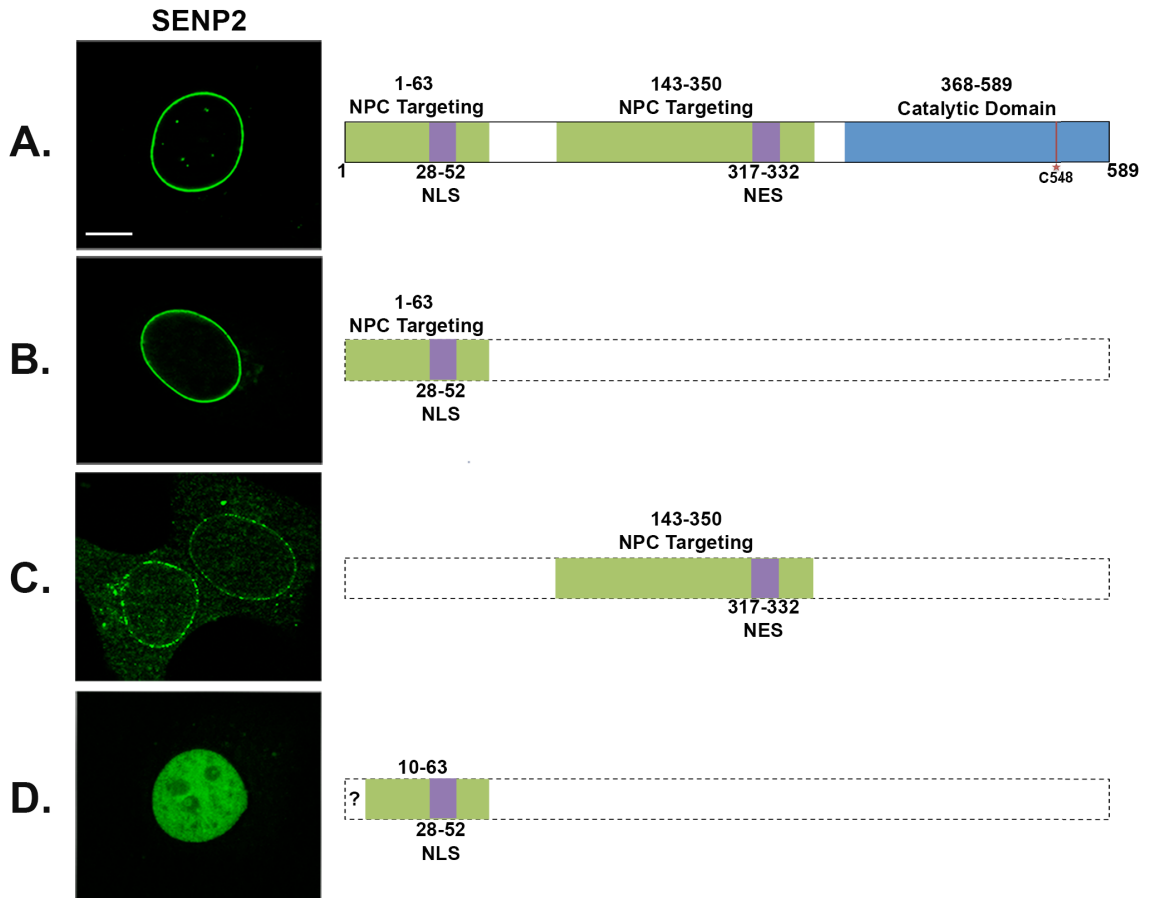
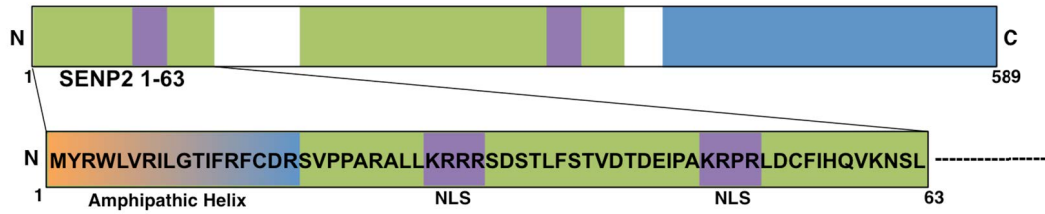
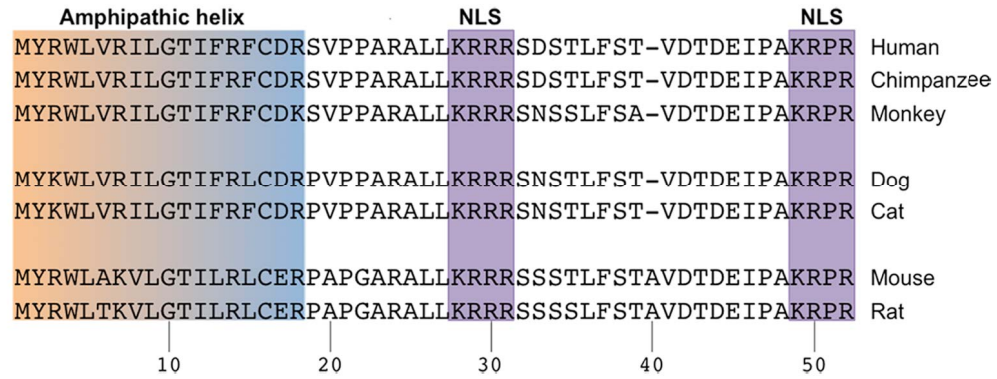


Figure II-2. The extreme N-terminus of SENP2 directs localization to the inner nuclear membrane. HeLa cells were transiently transfected with full length GFP-SENP2 or the indicated SENP2 deletion constructs and analyzed by fluorescence microscopy. (A) GFP-SENP2 localizes to NPCs and the inner nuclear membrane. (B) GFP-SENP2(1-63), containing a bi-partite NLS, localizes to NPCs and the inner nuclear membrane similarly to full-length SENP2. (C) GFP-SENP2(143-350), containing a nuclear export signal (NES) and a signal that binds the Nup107-160 subcomplex of the NPC, localizes only to NPCs. (D) GFP-SENP2(10-63) localizes to the nucleoplasm, suggesting the presence of an extreme N-terminal signal that targets SENP2 to the inner nuclear membrane. Scale bar = 5 μ m.

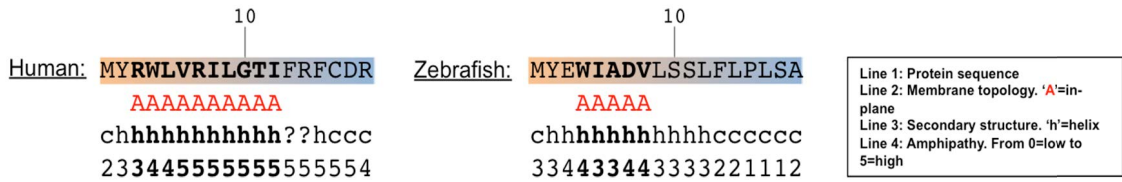
A.



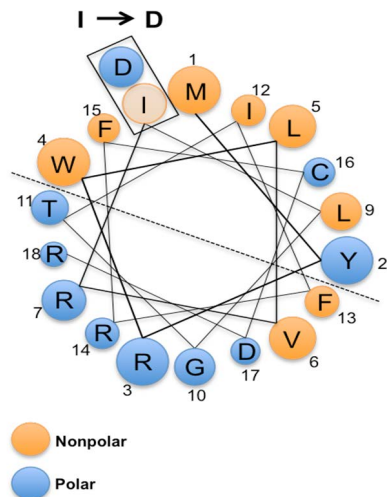
B.



C.



D.



E.

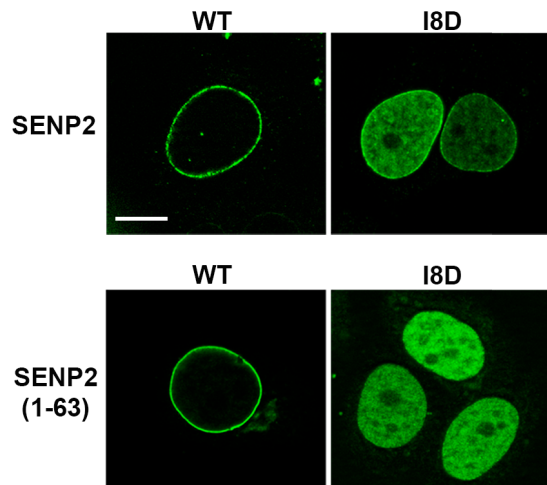


Figure II-3. SENP2 has a predicted amphipathic α -helix at the extreme N-terminus. (A) Schematic diagram of full length SENP2. Sequence and structure prediction analyses of the first 63 amino acids revealed that SENP2 has a predicted N-terminal amphipathic α -helix, highlighted in orange and blue. Analysis was performed using the AmphipaseeK prediction method (Sapay *et al.*, 2006). (B) Sequence alignment of the first 52 amino acids of SENP2. The sequence of the predicted amphipathic α -helix is highly conserved among mammals. (C) Amphipathic in-plane membrane anchor predictions of SENP2 in human and zebrafish. Lines 1 through 4 show the first 18 amino acid sequence of SENP2, membrane topology, secondary structure, and level of amphipathy, respectively. Although not conserved at the sequence level, human and zebrafish SENP2 share a predicted amphipathic α -helix at the extreme N-terminus. (D) Helical wheel representation of the predicted amphipathic α -helix. Orange indicates non-polar residues, and blue indicates polar residues. The position of the isoleucine 8 to aspartic acid substitution (I8D) is indicated. (E) HeLa cells were transiently transfected with wild type (WT) GFP-SENP2, GFP-SENP2(1-63) or the equivalent I8D mutants and analyzed by fluorescence microscopy. The I8D mutation resulted in a diffuse nucleoplasmic localization and reduced membrane targeting, suggesting that the predicted amphipathic α -helix serves as in-plane membrane anchor that tethers SENP2 to the inner nuclear membrane. Scale bar = 5 μ m.

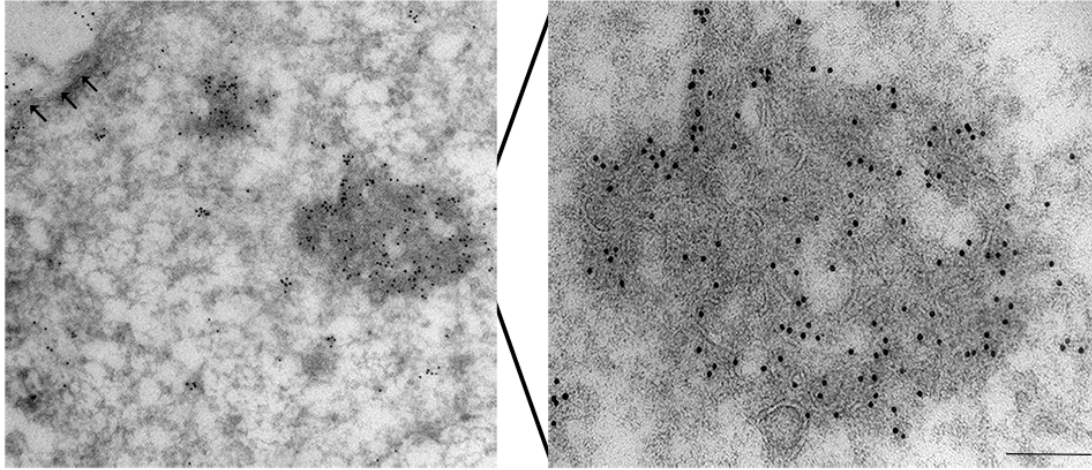


Figure II-4. SENP2 overexpression results in the formation of intranuclear membrane arrays. HeLa cells were transiently transfected with full length GFP-SENP2 and analyzed by immunoelectron microscopy using anti-GFP antibody. Micrographs reveal the presence of intra-nuclear membrane arrays upon SENP2 overexpression. Arrows indicate the inner nuclear membrane. Scale bar = 200nm.

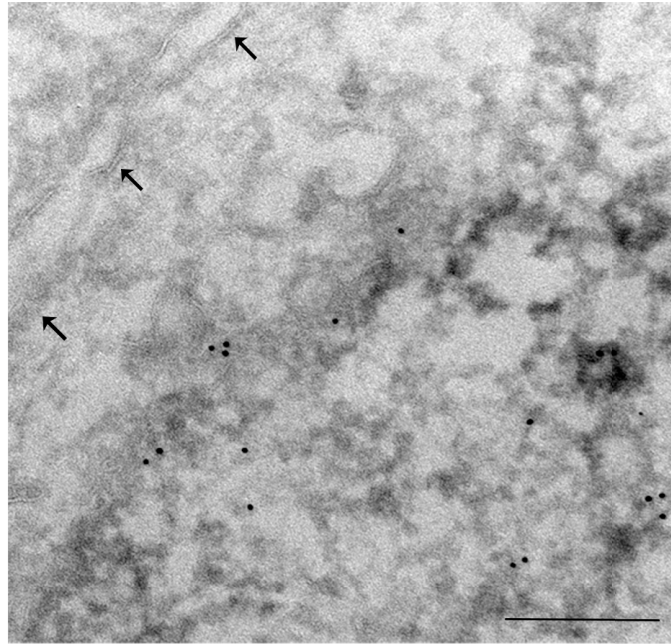


Figure II-5. Overexpression of the mutant GFP-SEN2^{I8D} does not cause the formation of intranuclear membranes. HeLa cells were transiently transfected with full length GFP-SEN2^{I8D} and analyzed by immunoelectron microscopy using anti-GFP antibody. Unlike the overexpression of wild type SENP2, the I8D mutant does not induce the formation of membranous structures. Arrows indicate the inner nuclear membrane. Scale bar = 500nm.

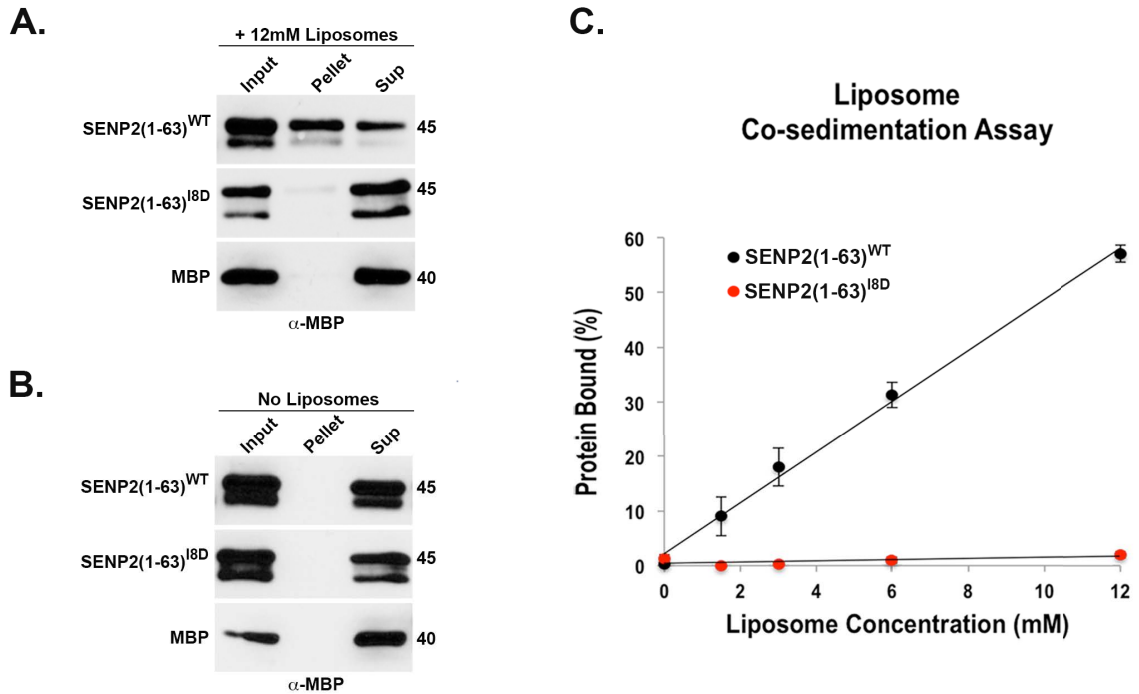


Figure II-6. The N-terminus of SENP2 interacts directly with membranes. (A) Recombinant MBP-SEN2(1-63)^{WT} or MBP-SEN2(1-63)^{I8D} were incubated with liposomes and membrane binding was evaluated using a co-sedimentation assay. Input, pellet and supernatant fractions were analyzed by SDS-PAGE and immunoblotting using an anti-MBP antibody. MBP-SEN2(1-63)^{WT} co-sedimented with liposomes, whereas the I8D mutant and MBP alone did not. (B) Control sedimentation assays were performed in the absence of liposomes. Proteins were only detected in the soluble fractions. (C) Quantitative analysis from three independent co-sedimentation experiments performed in the presence of increasing concentrations of liposomes. MBP-SEN2(1-63)^{WT} bound to liposomes in a dose-dependent manner, whereas the I8D mutant showed negligible binding even at high liposome concentrations. Error bars indicate standard deviations from three independent experiments.

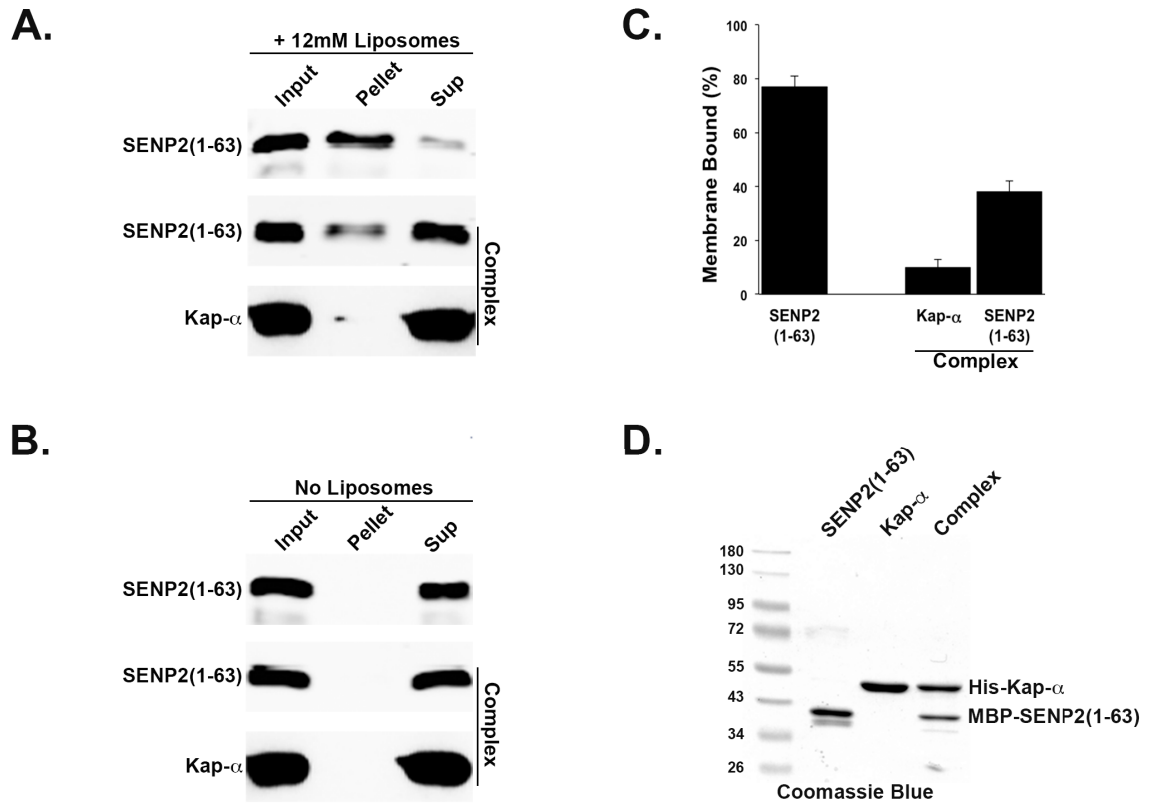


Figure II-7. SENP2-membrane interaction is inhibited by Kap- α . (A) Recombinant MBP-SENP2(1-63) alone, or in a 1:1 complex with Kap- α -6xHis was incubated with liposomes and membrane binding was evaluated using a co-sedimentation assay. Input, pellet and supernatant fractions were analyzed by SDS-PAGE and immunoblotting using anti-MBP and anti-His antibodies. When complexed with Kap- α , SENP2(1-63) membrane binding was inhibited. (B) Control sedimentation assays were performed in the absence of liposomes. (C) Quantification of SENP2(1-63) liposome binding alone or in the presence of Kap- α . Error bars indicate standard deviations from three independent experiments. (D) SDS-PAGE analysis of purified proteins and protein complexes used in the liposome co-sedimentation assays.

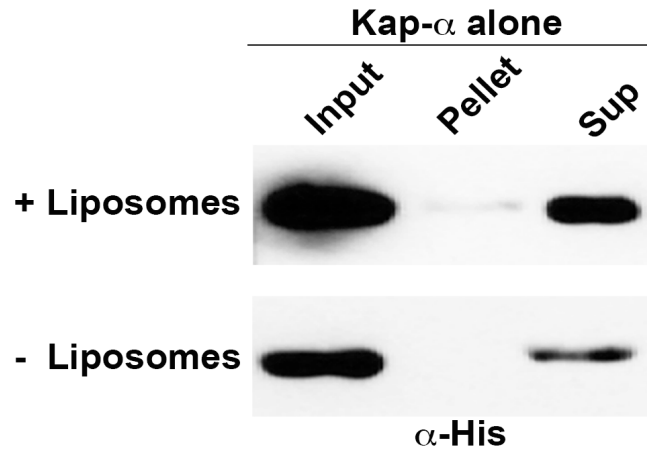
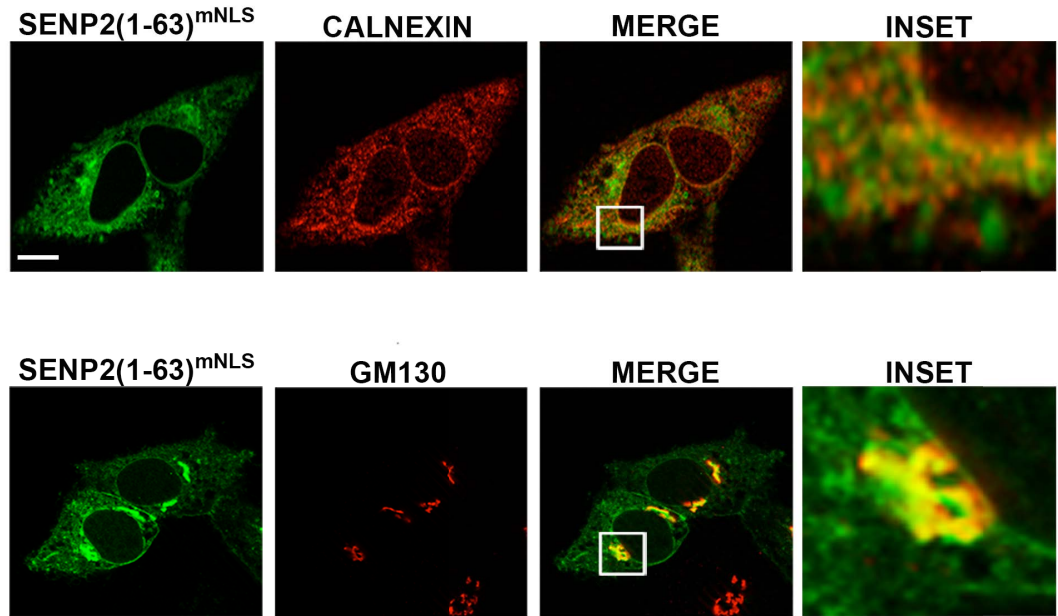


Figure II-8. Kap- α has no membrane binding affinity. Recombinant Kap- α -6xHis was incubated in the presence or absence of liposomes, and membrane binding was evaluated using a co-sedimentation assay. Input, pellet, and supernatant fractions were analyzed by SDS-PAGE and immunoblotting using anti-His antibody. Kap- α showed negligible binding to liposomes indicated by the weak signal detected in the pellet fraction. Control sedimentation was performed in the absence of liposomes, where Kap- α was only detected in the supernatant.

A.



B.

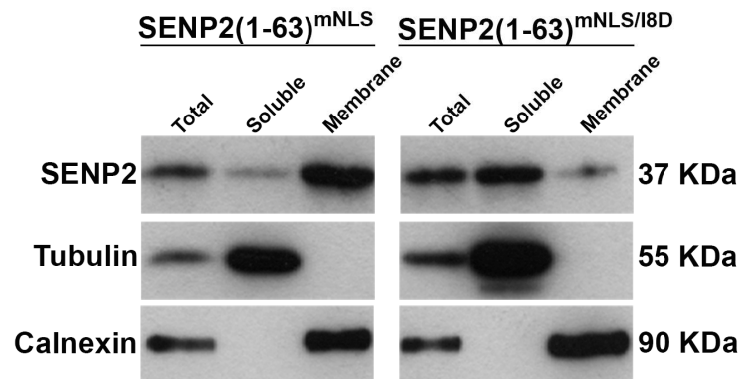


Figure II-9. Disrupting the SENP2 N-terminal NLS enables targeting to ER and Golgi membranes. Using site-directed mutagenesis, alanine substitutions were generated at positions R29 and R49 within the SENP2 N-terminal NLS (designated mNLS) in both wild type and I8D GFP-SENP2(1-63) expression constructs. (A) HeLa cells were transfected with GFP-SENP2(1-63)^{mNLS} and analyzed by indirect immunofluorescence microscopy. Cells were either stained using an anti-calnexin antibody (upper panel) or an anti-GM130 antibody (lower panel) to label ER and Golgi membranes, respectively. GFP-SENP2(1-63)^{mNLS} partially co-localized with calnexin and co-localized with GM130. Scale bar = 5 μ m. (B) HeLa cells were transfected with wild type and I8D mutant GFP-SENP2(1-63)^{mNLS} and fractions enriched in ER membranes were isolated using sucrose gradient sedimentation. Soluble and membrane fractions were analyzed by immunoblotting. Tubulin and calnexin were detected as markers for soluble and membrane fractions, respectively. GFP-SENP2(1-63)^{mNLS} was concentrated in the membrane fraction, whereas GFP-SENP2(1-63)^{mNLS/I8D} was predominantly soluble.

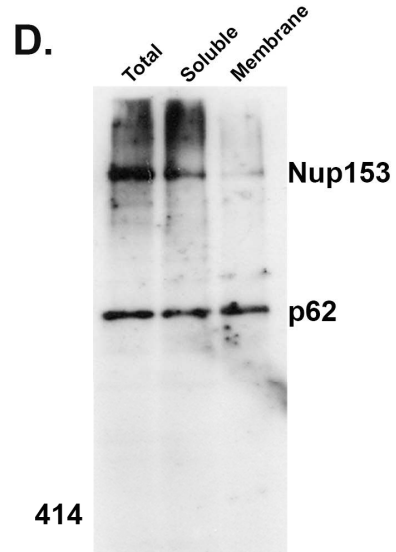
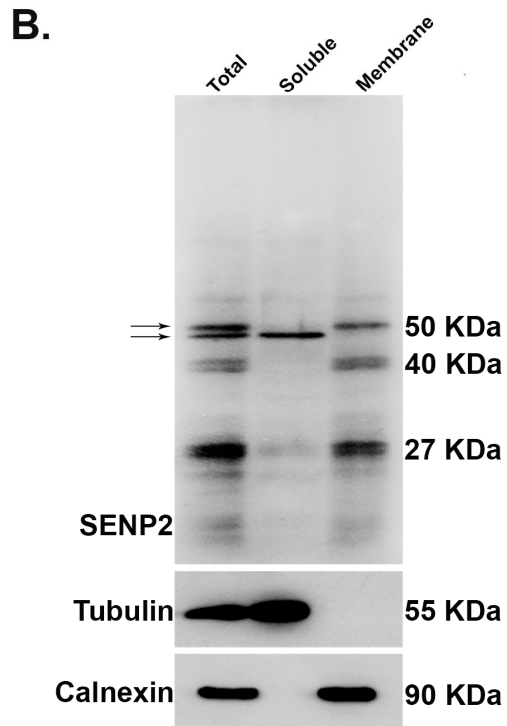
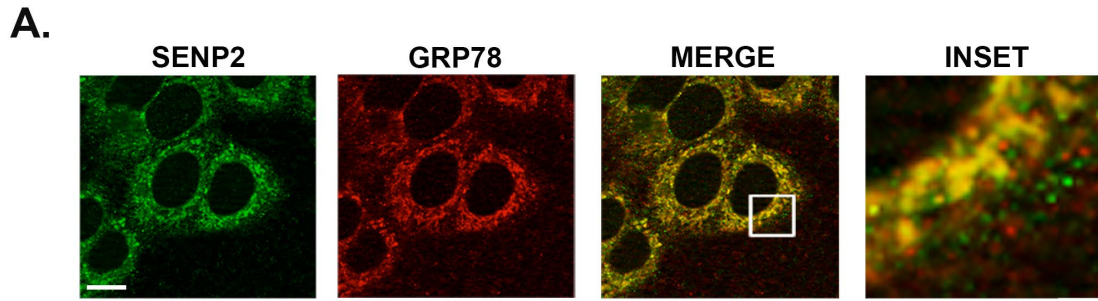
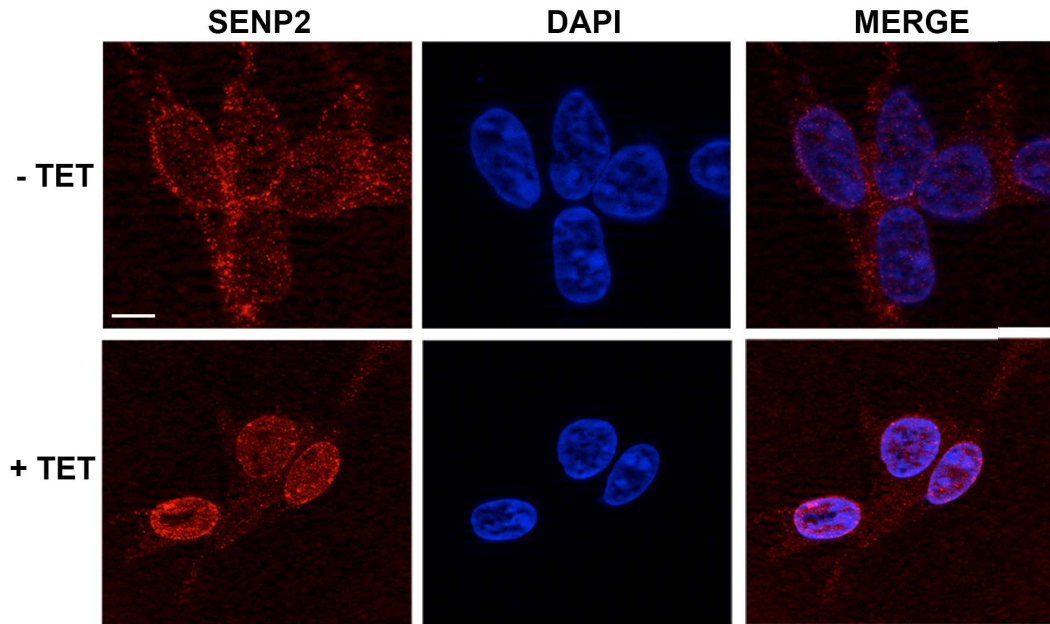


Figure II-10. Endogenous SENP2 isoforms associate with intracellular membranes. (A) HeLa cells were fixed then permeabilized with digitonin. Cells were co-stained with anti-SENP2 and anti-GRP78 antibodies, and then analyzed by indirect immunofluorescence microscopy. Endogenous SENP2 co-localized with GRP78, demonstrating ER membrane association. Scale bar = 5 μ m. (B) HeLa cells were fractionated by sucrose gradient sedimentation and fractions enriched in ER membranes were isolated and analyzed by immunoblotting. Anti-tubulin and anti-calnexin were used as markers for soluble and membrane fractions, respectively. SENP2 isoforms migrating at 50, 40 and 27 kDa were found in the membrane fraction. One of the two isoforms migrating at ~48 kDa, both indicated by black arrows, was present in the soluble fraction, suggesting the absence of the predicted amphipathic α -helix. (C) A schematic diagram representing the two potential SENP2 isoforms migrating at ~50 kDa, one lacking the first 50 amino acids. (D) Immunoblot using mAb414 showing the distribution of nucleoporins after HeLa cell fractionation. Nucleoporin p62 was equally distributed between the soluble and membrane fractions, while nucleoporin Nup153 was mostly soluble.

A.



B.

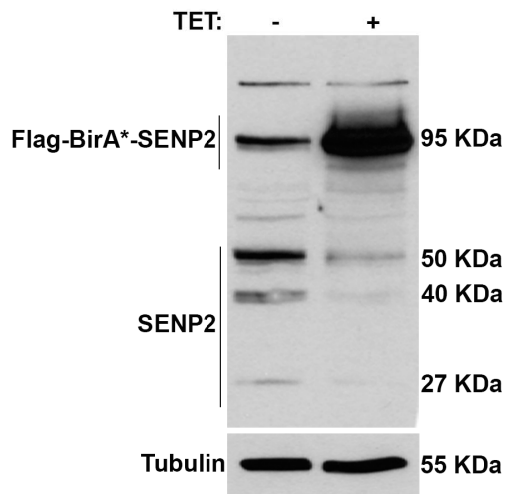


Figure II-11. FLAG-BirA*-SEN2^{WT} expression in 293T-REx Flp-In cells. Cells were incubated for 24 hours with complete media supplemented with 1µg/ml tetracycline (+ TET), or with no tetracycline as a control (- TET). (A) Cells were harvested and stained with anti-SEN2 antibody and analyzed by indirect immunofluorescence microscopy. Scale bar = 5µm. (B) Cells were harvested and analyzed by immunoblotting. Anti-SEN2 antibody was used to detect the expression levels of endogenous SEN2 and FLAG-BirA*-SEN2, as indicated.

Figure II-12. SENP2 interacts with ER, Golgi and inner nuclear membrane-associated proteins. SENP2^{WT} or SENP2^{I8D} fused to a promiscuous biotin ligase was stably expressed in 293T-REx Flp-In cells. Biotinylated proteins, comprising the pool of SENP2 interactors, were affinity purified using streptavidin and identified by mass spectrometry. (A) Schematic diagram showing SENP2^{WT} interactors. Black arrows indicate previously reported SENP2 interactions, and the green arrows indicate newly identified SENP2 interactions. Proteins were categorized into four broad categories: nuclear envelope (including karyopherins, nucleoporins, and inner nuclear membrane), ER membrane, ER/Golgi, and Golgi, indicated by pink, blue, green, and yellow circles, respectively. The complete list of BioID hits passing SAINT analysis (> 0.75) is provided in the supplemental materials of the following paper: Odeh *et al.*, 2018. (B) Volcano plot showing the log₂ fold change of protein hits identified to interact with SENP2^{WT} vs. those interacting with SENP2^{I8D}. Interactors were categorized into four different categories: membrane proteins, nuclear pore complex, nucleoplasm, and others/unknown, indicated by yellow, red, blue, and grey circles, respectively. The p-value was obtained from a t-test comparing a series of four runs between the two baits (SENP2^{WT} and SENP2^{I8D}). SENP2^{I8D} lost association with multiple membrane proteins, and gained new nucleoplasmic interactors. The complete list of protein hits is provided in the supplemental materials of the following paper: Odeh *et al.*, 2018.

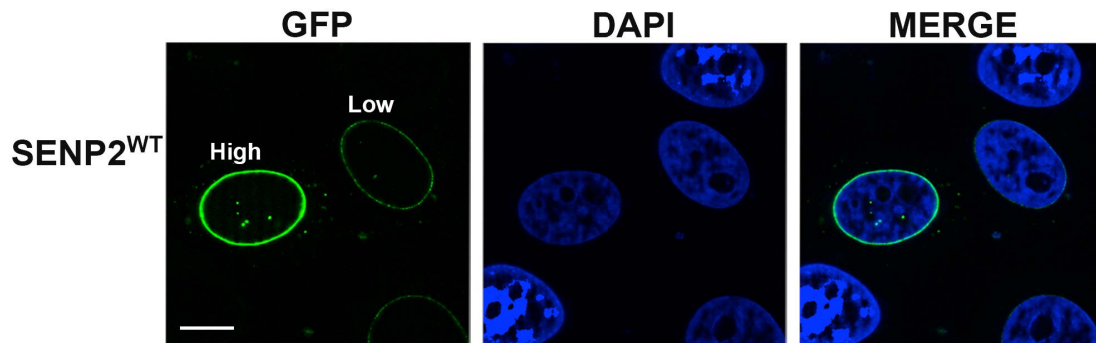
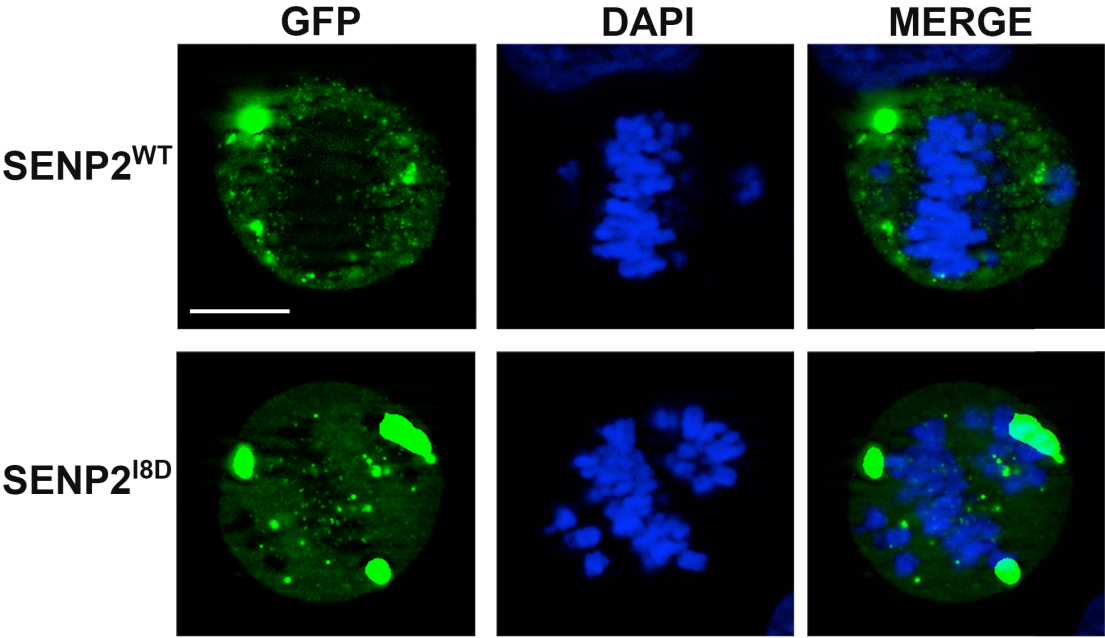


Figure II-13. Varying expression levels of GFP-SEN2 could explain the differences in SEN2 localization. HeLa cells were transiently transfected with full length GFP-SEN2 and analyzed by fluorescence microscopy. The punctate staining for GFP-SEN2 in low expressing cells resembled NPC staining. Whereas the continuous staining for GFP-SEN2 in moderate to high expressing cells showed localization to both the NPCs and the nuclear membrane. Scale bar = 5 μ m.

A.



B.

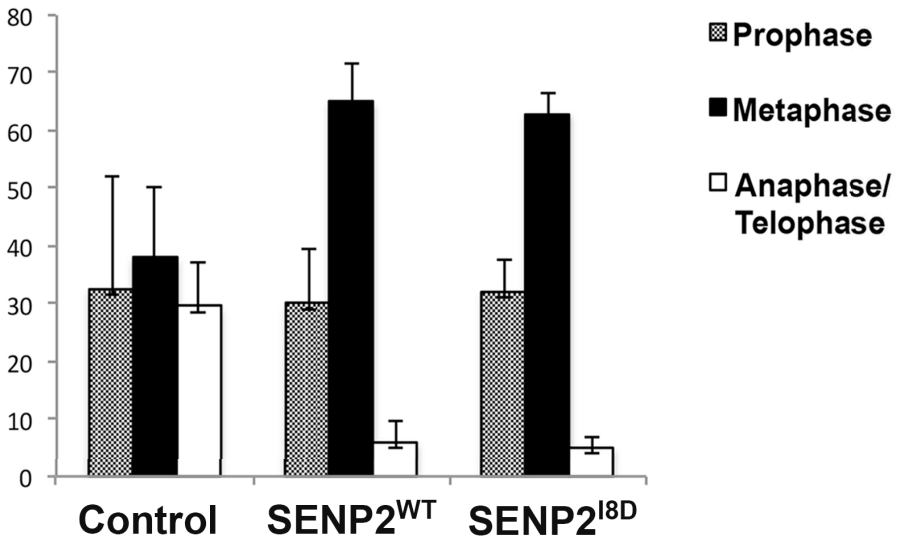


Figure II-14. The overexpression of either SENP2^{WT} or SENP2^{I8D} results in a similar mitotic phenotype. HeLa cells were transiently transfected with either GFP-SENP2^{WT} or GFP-SENP2^{I8D} mutant. Cells were harvested after 48 hours and analyzed by fluorescence microscopy. (A) Cells transfected with either SENP2 constructs experienced mitotic arrest, evident from the misalignment of chromosomes during metaphase. Scale bar = 10 μ m. (B) Quantitative analysis from two independent experiments showing the relative distribution of cells undergoing mitosis. Error bars indicate standard deviations. As reported previously, overexpression of SENP2 increases the percentage of cells arrested in metaphase (Zhang *et al.*, 2008). This phenotype is not attributed to the amphipathic α -helix of SENP2.

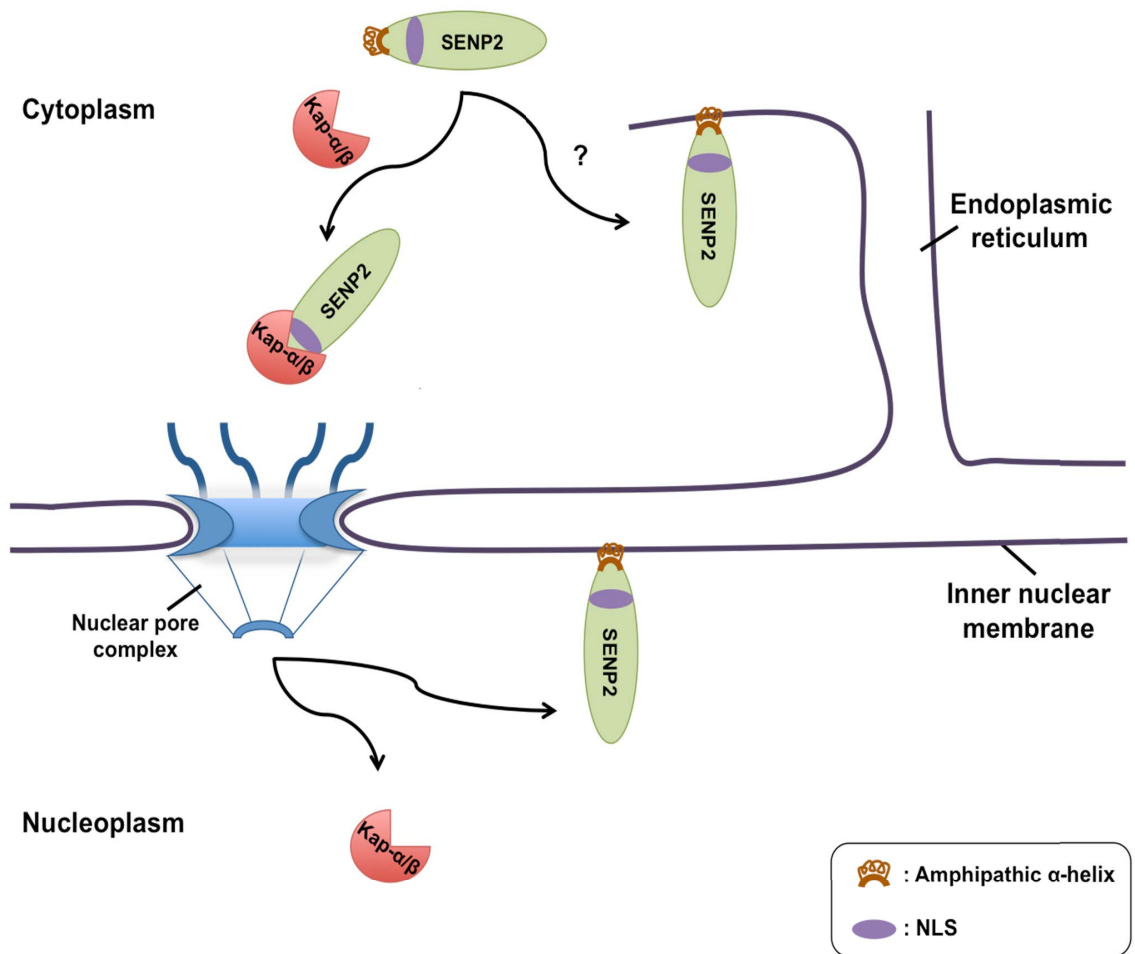


Figure II-5. Schematic illustrating SENP2 membrane association and regulation by Kap- α binding. The binding of Kap- α to SENP2 impedes interactions with membranes in the cytoplasm. Following protein complex translocation to the nucleus via the import machinery Kap- α/β , Kap- α is released from SENP2, allowing the amphipathic α -helix to associate with the inner nuclear membrane. The binding of Kap- α to SENP2 may also be inhibited through unknown mechanisms (?) permitting the amphipathic α -helix to interact with the ER or Golgi membranes.

CHAPTER III
THE SUMO CAPTURE

ABSTRACT

The SUMO-specific isopeptidase SENP2 associates with intracellular membranes where it interacts directly with membrane-associated proteins. BioID analysis revealed interactions between SENP2 and ER, Golgi, and inner nuclear membrane-associated proteins. However, whether those proteins are SUMO-modified and substrates of SENP2 remain uncertain. To assist in further identification of SENP2 substrates, in this study we developed a new method called “SUMO capture”, which is dependent on utilizing a SENP2 catalytically dead mutant, SENP2^{CS}, in which the catalytic site cysteine residue is mutated to serine. By forming a stable complex with sumoylated substrates, it is possible to use SENP2^{CS} to enrich for sumoylated proteins recognized and bound by SENP2. We performed proof-of-concept experiments to verify the efficiency of the SUMO capture technique. We also developed stable cell lines expressing SENP2^{CS}, and optimized co-immunopurification conditions necessary for subsequent identification of SENP2 substrates by either immunoblotting or mass spectrometry. Using our approach, we verify that LAP2 is a SUMO-modified substrate of SENP2. Collectively, our newly developed method can be used for the identification of unique substrates of SENP2 and other SUMO-specific proteases.

INTRODUCTION

To investigate the role of SUMO regulation at membranes, in Chapter II we focused on characterizing SENP2 and its ability to interact with and potentially regulate de-sumoylation at membranes. We discovered a new signal within the N-terminus of SENP2, a unique amphipathic α -helix that allows it to directly interact with intracellular membranes. We also found using BioID that SENP2 interacts with a subset of ER, Golgi and inner nuclear membrane-associated proteins. We showed that these interactions are dependent on SENP2 amphipathic α -helix and membrane binding. Taken together, we have established that SENP2 may be playing an important role in regulating the many functions associated with membrane proteins, however, further investigation is required to fully understand the functions of sumoylation and its regulation by SENP2 at membranes. To this end, we first need to more definitively identify SUMO-modified SENP2 substrates, which is the focus of this chapter.

Using BioID to identify SENP2 interacting binding partners has the advantage of effectively capturing dynamic, transient protein-protein interactions. The covalent biotin modification also allows for employing stringent purification methods, which can aid in identifying insoluble or membrane-associated proteins (Coyaud *et al.*, 2015). However, one caveat with BioID is that it is not possible to distinguish between SENP2 interacting proteins and bona-fide SUMO-substrates. Therefore, it is necessary to develop other complementary methods to specifically identify SENP2 substrates. In the SUMO field, the identification of substrates for a specific SUMO protease is a challenging task for a number of reasons. First, sumoylation is a highly dynamic process. The conjugation and

de-conjugation cycles are fast reactions, hence a SUMO protease is only transiently associated with its substrate for a relatively short period of time. Additionally, as mentioned in Chapter I, a very low percentage of any given substrate is present in its sumoylated form at steady state level, making it challenging to detect. Very little progress has been made to circumvent those challenges in the field, so with that in mind, our goal has been to develop a new method that would serve two main purposes: enrich for sumoylated proteins, and define SENP2 substrates.

Our approach to developing a new method takes into account a previously established concept: a mutation in the catalytic cysteine of SUMO proteases renders the protein inactive by interfering with its de-sumoylation activity (Bailey and O'Hare, 2004; Chow *et al.*, 2012). Several studies have suggested that the SENP1 catalytic site mutant (C603S) exhibits stable interactions with SUMO-modified proteins. Further evidence, by indirect immunofluorescence microscopy, showed that the catalytically dead SENP1^{CS} concentrates at foci where SUMO1 is present (Bailey and O'Hare, 2004). The same analysis was performed with the wild type protein and no obvious co-localization between SUMO1 and SENP1^{WT} was observed. This suggests that SENP1^{CS} stably binds and “captures” sumoylated substrates *in vivo*. Most importantly, SUMO1 conjugates can be co-purified with SENP1^{CS}, suggesting a potentially useful strategy for identifying targets of SUMO-specific proteases (Bailey and O'Hare, 2004). Although this evidence suggests that SENP1^{CS} can be used to identify SENP1-specific substrates, this method has not been developed or utilized, except in few cases mentioned below. Moreover, less is known about other SENP catalytically dead mutants and their potential to capture sumoylated proteins. SENP1^{CS} was used to identify Elk-1 (E twenty six-like 1) as a

substrate of SENP1. Elk-1 is a transcription factor that undergoes rapid de-sumoylation following growth factor stimulation, which results in its potent activity as a transcriptional activator. Therefore, sumoylation and its regulation by SENP1 play an important role in determining Elk-1-dependent transcriptional programs (Witty *et al.*, 2010). Besides Elk-1, SENP1^{CS} was also utilized to identify a slower migrating band of the nucleoporin Nup153 that was confirmed to be sumoylated and therefore regulated by SENP1 (Chow *et al.*, 2012). In contrast to SENP1^{CS} utilization, SENP2^{CS} (with a cysteine to a serine mutation at amino acid position 548) has only been studied to show that SENP2 can regulate the sumoylation of Nup153 (Chow *et al.*, 2012), however, mutant characterization and unique substrate identification is lacking.

In this study, we utilized SENP2^{CS} to capture SUMO at membranes. We also present evidence that this method can be used to purify sumoylated substrates for further identification. Consistent with our BioID data, and by using SUMO capture, we established that the lamin-associated polypeptide 2 (LAP2) is a true SENP2 substrate. Together, our findings reveal a new method for the identification of unique substrates of SUMO proteases.

MATERIALS AND METHODS

Antibodies

Mouse monoclonal SUMO2/3, and rabbit polyclonal SENP2 and LAP2 antibodies were all produced as previously described (Fischer *et al.*, 2001; Zhang *et al.*, 2008; Goeres *et al.*, 2011). Remaining antibodies were obtained from the following sources: anti-GFP (Clontech, Mountain View, CA); anti-tubulin (Sigma-Aldrich, St. Louis, MO); anti-calnexin (Enzo Life Sciences, Inc., Farmingdale, NY); anti-FLAG M2 (Sigma-Aldrich, St. Louis, MO); anti-ECS (DDDDK) agarose-immobilized (Bethyl Laboratories Inc., Montgomery, TX); anti-Myc (Sigma-Aldrich, St. Louis, MO).

Plasmid constructs

SENP2 cDNA was obtained as previously described (Zhang *et al.*, 2002). Full length SENP2 was PCR amplified and cloned into pEGFP-C1 as described (Goeres *et al.*, 2011), and cloned into pcDNA5 FRT/TO FLAG expression vector, using standard cloning procedures. SENP2 NLS mutation (mNLS: R29A/R49A) and/or catalytic cysteine mutation (C548S) were introduced using PCR based, site-directed mutagenesis. SUMO1 and SUMO2 were cloned into pcDNA3 c-Myc expression vector.

Cell culture, and transfection

HeLa, 293FT, and 293T-REx Flp-In cells were all maintained and transfected as described in the Materials and Methods section of Chapter II.

Stable cell lines

Stable cell lines were established essentially as previously described (Gupta *et al.*, 2015). In brief, using the Flp-In system (Invitrogen, Carlsbad, CA), 293T-REx Flp-In cells stably expressing FLAG alone, FLAG-SENP2^{WT}, FLAG-SENP2^{mNLS}, FLAG-SENP2^{CS}, or FLAG-SENP2^{mNLS/CS} were generated. Cells were grown to sub-confluency (60%) and were incubated for 24 hours in complete media supplemented with 1µg/ml tetracycline (Sigma-Aldrich, St. Louis, MO). Cells were collected, pelleted (200 x g, for 3 minutes) and snap frozen, or immediately resuspended in lysis buffer for further analysis.

Immunoblotting, and immunofluorescence microscopy

Immunoblot and immunofluorescence microscopy analyses were performed as described in the Materials and Methods section of Chapter II.

Subcellular fractionation

Isolation of ER membranes was performed as previously described (Bozidis *et al.*, 2007), and in the Materials and Methods section of Chapter II.

Co-immunopurification

For co-immunopurification of FLAG fusion proteins, 293T-REx stable cell lines were incubated with tetracycline as described above. Cells were washed with 1X PBS, harvested and flash frozen at -80°C or lysed immediately with lysis buffer, recipe 1 (50mM Tris pH 8.5, 150mM NaCl, 1mM EDTA, 1% Triton X-100) or recipe 2 (50mM

HEPES pH 7.4, 100mM KCl, 2mM EDTA, 0.1% NP-40, 10% Glycerol, 1mM DTT). Protease inhibitors and 10mM NEM were freshly added. Cells were lysed for 15 minutes on ice with gentle shaking then centrifuged at 12,000 x g for 5 minutes. Cleared lysates were incubated with anti-FLAG (anti-ECS; DDDDK) agarose-immobilized antibody for 30 minutes up to 3 hours at 4°C, with gentle end-to-end rotation. An input fraction was saved before the incubation with the beads. After incubation, beads were pelleted at 8,200 x g for 30 seconds and washed at least three times with lysis buffer. Samples were eluted with 20µl 2X-sample buffer (125mM Tris HCl pH6.8, 4% SDS, 20% (v/v) glycerol, and 0.004% bromophenol blue), and then boiled for 3 minutes. Input and IP samples were analyzed by SDS-PAGE and immunoblotting.

RESULTS

Catalytically dead SENP2 captures sumoylated proteins

It has been previously shown that mutating the catalytic cysteine to a serine in SUMO proteases would render the protease catalytically inactive (Bailey and O'Hare, 2004; Chow *et al.*, 2012). To show that this mutation can be utilized to specifically capture sumoylated proteins recognized by SENP2, we generated a mutant GFP-SENP2 expression construct with cysteine 548 mutated to serine (CS: C548S). We transiently co-expressed GFP-tagged wild type SENP2 (SENP2^{WT}) or catalytically dead SENP2 (SENP2^{CS}) together with Myc-tagged SUMO1 or SUMO2 in HeLa cells (Figure III-1). As expected, cells expressing SENP2^{WT} had reduced levels of detectable SUMO conjugates, indicating that SUMO was de-conjugated from proteins by SENP2 activity. In contrast, cells expressing the catalytically dead mutant SENP2^{CS} had a significant increase of sumoylated proteins indicated by a large high molecular weight smear (Figure III-1A). Expression of GFP alone was used to indicate the baseline level of global sumoylation at steady state. This result suggests that sumoylated proteins are recognized and stabilized by SENP2^{CS}, where the protease binds to its substrate but is incapable of de-conjugating SUMO. To further validate this model, we looked at the co-localization of GFP-SENP2^{WT} or GFP-SENP2^{CS} with Myc-SUMO by indirect immunofluorescence microscopy (Figure III-1B). Consistent with our model, SENP2^{CS} but not SENP^{WT} co-localized with Myc-SUMO2 at foci around the nuclear periphery and in the nucleoplasm, indicating that the catalytically dead mutant is capturing sumoylated proteins. Collectively, our results support the idea of utilizing SENP2^{CS} as a tool to capture

SUMO-modified substrates. Next, we wanted to investigate the use of SENP2^{CS} to specifically enrich for sumoylated proteins at intracellular membranes.

Catalytically dead SENP2 captures SUMO at membranes

We have previously established that SENP2 has a predicted amphipathic α -helix at its extreme N-terminus that allows it to interact with intracellular membranes and with membrane-associated proteins at the ER and Golgi (refer to Chapter II). However, our initial studies did not address whether SENP2 interacting proteins represent SUMO-modified substrates. To test whether we can utilize SENP2^{CS} as a tool to enrich for SUMO-modified substrates at membranes in the cytoplasm, we first generated a mutant of GFP-SENP2^{CS} in which the NLS had been mutated at two residues (mNLS: R29A/R49A), thereby allowing SENP2 to associate with membranes in the cytoplasm (SENP2^{mNLS/CS}). We then transiently co-expressed either GFP-SENP2^{mNLS} or GFP-SENP2^{mNLS/CS} with Myc-SUMO in HeLa cells and analyzed them by immunofluorescence microscopy. Consistent with results in SENP2^{CS}-expressing cells, SENP2^{mNLS/CS} co-localized with SUMO at foci in the cytoplasm, suggesting an ability to capture membrane-associated SUMO substrates (Figure III-2A). To further verify the capture of SUMO substrates at membranes, we isolated a fraction enriched with ER membranes by sucrose gradient sedimentation and performed immunoblot analysis. Consistent with SUMO capture, SUMO conjugates were specifically detected in the membrane fraction isolated from cells expressing SENP2^{mNLS/CS} but not SENP2^{mNLS} or GFP alone (Figure III-2B). Together, our findings suggest that the catalytically dead

mutant of SENP2 can be used to stabilize and capture SUMO-modified proteins in the nucleus and at intracellular membranes.

Stable cell lines development and validation

Our results thus far provide evidence that SENP2^{CS} can be utilized to enrich for sumoylated proteins recognized by SENP2. In order to further develop this as a tool to purify and identify substrates, we next generated FLAG-tagged constructs of SENP2 and tested their transient expression levels and localization in HeLa cells (Figure III-3). FLAG-SENP2^{WT} and FLAG-SENP2^{CS} localized to the nuclear periphery, and more specifically at the inner nuclear membrane. In contrast, FLAG-SENP2^{mNLS} and FLAG-SENP2^{mNLS/CS} were concentrated in the cytoplasm as predicted (Figure III-3A). The expression levels for each SENP2 protein variant was detected by immunoblotting with anti-FLAG antibody (Figure III-3B). Besides HeLa cells, we also tested the transient expression of FLAG-SENP2 in other cell lines, including 293FT and 293T-REx Flp-In cells, and found that the level of expression of FLAG-SENP2^{WT} and FLAG-SENP2^{CS} was comparable to that in HeLa (Figure III-3C). Collectively, our results validate the use of these constructs for the development of stable cell lines using 293T-REx Flp-In cells. Stable cell lines for inducible expression of full-length wild type SENP2, SENP2^{CS}, SENP2^{mNLS}, and SENP2^{mNLS/CS} fused to FLAG were generated and the localization and expression levels of SENP2 were validated by indirect immunofluorescence microscopy and immunoblotting, respectively (Figure III-4, A and B). Notably, a higher molecular weight band, potentially corresponding to a sumoylated form of SENP2, was detected with the stably expressing FLAG-SENP2^{CS} cell line (Figure III-4B, upper panel). This

suggests that SENP2^{CS} is capable of capturing sumoylated proteins, possibly including its own sumoylated form. This result is consistent with previously described observations where higher molecular weight bands were detected with SENP1^{CS} and SENP2^{CS} overexpression, which were then confirmed to correspond to their sumoylated forms (Bailey and O'Hare, 2004; Chow *et al.*, 2012).

The SUMO capture: method development and optimization

A crucial step in developing the SUMO capture technique is to find the most optimal co-immunopurification (Co-IP) conditions that would yield a highly enriched fraction of sumoylated proteins. Four different variables were considered for optimization: the overexpression of SUMO, lysis buffer and lysis conditions, and duration of binding to FLAG beads (Figure III-5). We first evaluated effects of increasing overall levels of SUMO-modified proteins on SENP2 pull-downs by transient overexpression of SUMO in the stable cell lines (Figure III-5A). We found that there was no difference in the levels of sumoylated products captured by SENP2^{CS} with or without the overexpression of Myc-SUMO2 (Figure III-6, B, D and E). Therefore, increasing the SUMO pool does not necessarily increase the amount of sumoylated products captured by SENP2. Additionally, different lysis buffers were tested with or without the addition of 10mM N-Ethylmaleimide (NEM), a cysteine protease inhibitor (Figure III-5B). The addition of NEM was favorable in our conditions and resulted in a more efficient capture of conjugated SUMO, evident from the increase in high molecular weight smear (Figure III-5E). This is likely due to the fact that the active endogenous SENPs can still compete with the stably expressed SENP2^{CS} on binding to sumoylated proteins, particularly

following lysis and incubation with antibody beads. We also tested three different lysis conditions: sonication, gentle shaking at 4°C, or introducing one freeze/thaw cycle and found that shaking the samples at 4°C is the most optimal lysis method (Figure III-5C, and data not shown). Finally, we tested different incubation times with FLAG beads and found that a 30-minute incubation with end-to-end rotation worked better than longer durations (Figure III-5, D and E). In summary, different conditions were tested and optimized for the Co-IP of sumoylated SENP2 substrates. Next, after Co-IP, we probed for potential substrates of SENP2.

We successfully pulled down SENP2^{WT} and SENP2^{CS} using anti-FLAG beads (Figure III-6A), and with our optimized Co-IP conditions, SUMO2/3 co-immunopurified with SENP2^{CS} (Figure III-6B). We next wanted to probe for a candidate substrate. We chose to probe for LAP2 since it was one of the prominent hits in our BioID analysis. We predicted that if LAP2 is sumoylated, it would co-immunopurify with SENP2^{CS}-SUMO complex but not with SENP2^{WT}. Consistent with our prediction, and our BioID analysis, we identified a higher molecular weight band with SENP2^{CS} expressing cells and using anti-LAP2 antibody (Figure III-6C). Given its absence in the FLAG alone and SENP2^{WT} cell lines, the higher molecular weight band most likely corresponds to the sumoylated form of LAP2. This result provides evidence that our method successfully captured sumoylated LAP2 and identified LAP2 as a substrate of SENP2.

DISCUSSION

In our previous study, we showed that SENP2 uniquely and directly associates with intracellular membranes. By using BioID, we identified SENP2 interacting binding partners. However, to fully understand the significance of SENP2 at membranes, it is important to identify which of those interacting proteins are SENP2-specific substrates. In this study, we have developed and tested a new method called “SUMO capture”, which utilizes the catalytically dead mutant of SENP2 (SENP2^{CS}). With SUMO capture, we showed that we could enrich and identify sumoylated proteins recognized and bound by SENP2. SUMO capture is a newly developed tool that can be used to identify unique substrates of SUMO proteases.

The SUMO capture: biased and non-biased approaches

We developed a Tetracycline-inducible (TET-inducible) cell line stably expressing FLAG-SENP2^{CS}, and provided evidence that we can pull-down, or capture, sumoylated proteins by FLAG Co-IP. Following FLAG Co-IP, we identified LAP2 as a substrate of SENP2 by immunoblotting using anti-LAP2 antibody. This targeted, or biased, approach was made possible by our previously published BioID data (Odeh *et al.*, 2018). LAP2 was previously identified as a SENP2 interacting partner and using our new SUMO capture technique followed by immunoblotting, we confirmed LAP2 as a SENP2 substrate. We are also interested in identifying other SENP2 substrates by taking a non-biased approach, as this will provide us with a comprehensive catalog of unique

substrates. The non-biased approach would entail identification of co-purifying proteins by mass spectrometry, which is currently underway.

LAP2 as a substrate of SENP2

Using SUMO capture, we identified LAP2 as a substrate of SENP2. The LAP2 gene (also known as thymopoietin, or TMPO) encodes six spliced isoforms. Of those, we can at least detect three isoforms by western blotting: α , β , and γ . With the exception of LAP2 α , all isoforms share a similar C-terminal transmembrane domain that allows for direct interaction with the inner nuclear membrane. All of LAP2 proteins play a role in lamina organization, and maintenance of nuclear growth and integrity (Gant *et al.*, 1999). From previous mass spectrometry-based analyses, LAP2 was identified as a SUMO substrate (Tammsalu *et al.*, 2014; Hendriks *et al.*, 2015). However, those findings were not further validated. Given the predicted size of LAP2 β , and consistent with the fact that SENP2 also interacts with the inner nuclear membrane, the higher molecular weight band that was observed in our SUMO capture likely corresponds to LAP2 β protein. How sumoylation and SENP2 regulation affects LAP2 β function is still a question that needs to be further investigated, however, we speculate that the sumoylation of LAP2 β regulates its localization and function at the inner nuclear membrane.

The SUMO capture: pros & cons

We developed SUMO capture to address major challenges in the SUMO field: the transient nature of sumoylation, and the resulting low, steady state abundance of sumoylated proteins. While we were successfully able to tackle both issues with SUMO

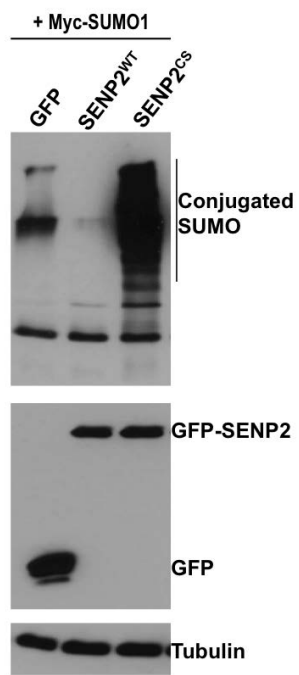
capture, our pull-downs were not efficient. The input and IP samples showed comparable amounts of FLAG-SEN2 (refer to Figure III-6A), meaning that the 10% of IP sample loaded is only about 20ug of FLAG-SEN2 protein. Since our total input in each IP was about 4-5mg, it appears that only a small fraction of total protein is being pulled down. This inefficiency could be attributed to multiple issues. The FLAG-SEN2 plasmid constructs used for generating the stable cell lines were designed with a single FLAG, and the detection of FLAG-SEN2 with anti-FLAG antibody was very inefficient (refer to Figure III-4B). This could be due to epitope masking, which could also explain the low level of binding of FLAG-SEN2 to agarose-immobilized anti-FLAG antibody during immunopurification. Based on evidence from the current literature, one way to circumvent this issue would be to add tandem FLAG tags (at least 3X FLAG) to the construct, or to use a different tag. It has also been suggested that the FLAG tag itself can be modified when expressed in certain cell lines, including 293T cells, contributing to epitope masking (Schmidt *et al.*, 2012). Therefore, changing the cell line could be taken into consideration. Another reason that could add to the pull-down inefficiency is the on and off rate of SEN2^{CS}-bound substrates. The SEN2^{CS}-SUMO complex might be dissociating during lysis, binding, or Co-IP steps, making the conjugated SUMO available for active endogenous SENPs. NEM was added to the lysis buffer to inhibit the activity of endogenous SENPs, however, developing the stable cell line in a SEN2 knockdown background, or alternatively, light crosslinking between SEN2^{CS} and its sumoylated substrate might be helpful. Finally, we have observed a higher molecular weight band co-immunopurifying with SEN2^{CS}, most likely corresponding to the sumoylated form of SEN2, as described previously (Bailey and O'Hare, 2004; Chow *et*

al., 2012). One could predict that since the catalytic cysteine is mutated to a serine, when cysteine and serine proteases have similar mechanism of action, an intermediate is forming between SUMO and the catalytic mutant that would account for the shift in weight (Bailey and O'Hare, 2004). However, the same higher molecular weight band is observed when the catalytic cysteine is mutated to an alanine, ruling out the possibility of an intermediate and reinforcing that the shifted band corresponds to a modified form of the inactive enzyme (Bailey and O'Hare, 2004). Collectively, this raises the concern that SENP2^{CS} might favor capturing its own sumoylated form rather than other sumoylated substrates. To better capture sumoylated proteins, the identification and mutation of the sumoylated SENP2 residue might be important.

Although we discuss here a few challenges with SUMO capture efficiency, we are confident that this method can be further optimized for the successful identification of SENP2-specific substrates by targeted immunoblotting and unbiased mass spectrometry approaches.

FIGURES AND FIGURE LEGENDS

A.



B.

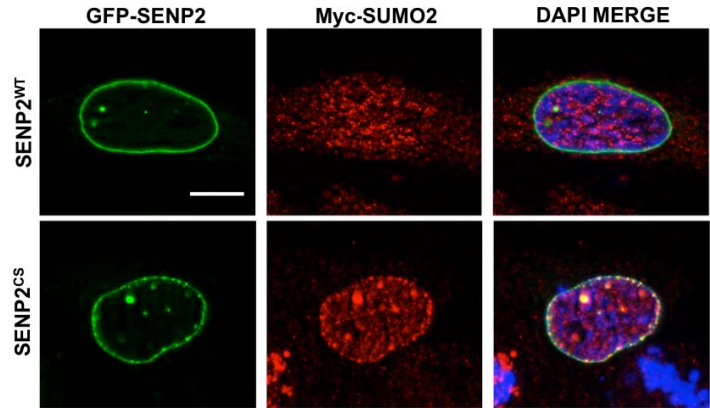
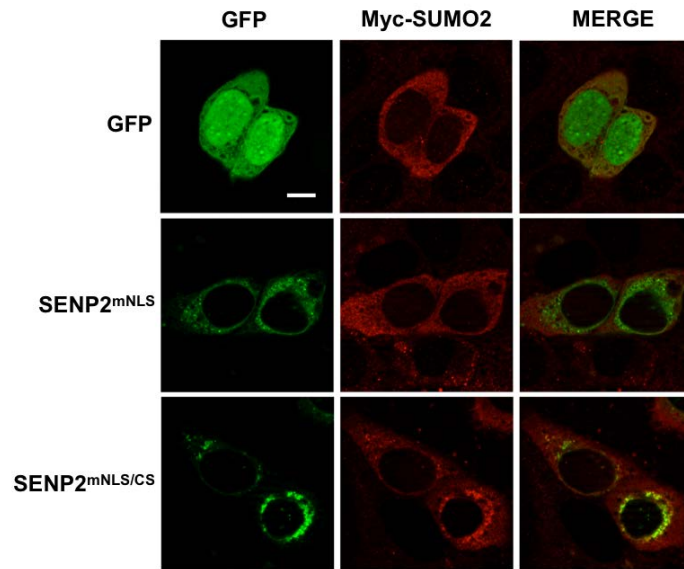


Figure III-1. The SUMO capture: proof-of-concept. HeLa cells were transiently co-transfected with Myc-SUMO and either GFP alone, GFP-SEN2^{WT}, or GFP-SEN2^{CS} for 24 hours. Cells were then harvested and analyzed by immunoblotting and indirect immunofluorescence microscopy. (A) Immunoblotting using anti-Myc showed that GFP-SEN2^{CS} can enrich for the conjugated SUMO pool, compared to GFP alone or SEN2^{WT}. Anti-GFP antibody was used to detect the expression levels of each GFP-tagged construct, and anti-tubulin was used as a loading control. (B) Cells were stained with anti-Myc antibody and analyzed by indirect immunofluorescence microscopy. Consistent with the immunoblotting results, Myc-SUMO showed clear co-localization with GFP-SEN2^{CS} at foci within the nucleus and the nuclear periphery. No clear co-localization was detected with GFP-SEN2^{WT}, suggesting that SUMO is being trapped at locations where the catalytically dead SEN2 is present but not the WT protein. Scale bar = 5 μ m.

A.



B.

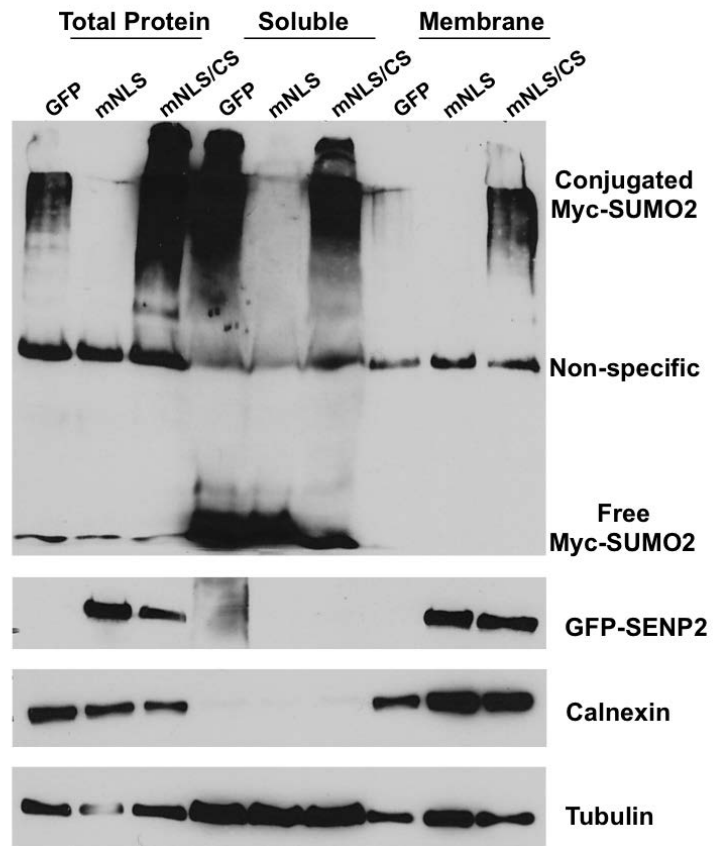


Figure III-2. Catalytically dead SENP2 captures SUMO at membranes in the cytoplasm. HeLa cells were transiently co-transfected with Myc-SUMO2 and either GFP, GFP-SENP2^{mNLS}, or GFP-SENP2^{mNLS/CS} for 24 hours. (A) Cells were harvested, permeabilized with digitonin, and stained with anti-Myc antibody and analyzed by indirect immunofluorescence microscopy. SUMO only co-localized with GFP-SENP2^{mNLS/CS} in foci at cytoplasmic membranes. No apparent co-localization was observed with SUMO and SENP2^{mNLS}. Scale bar = 5 μ m. (B) HeLa cells were harvested 24 hours post-transfection and fractions enriched in ER membranes were isolated using sucrose gradient sedimentation. Soluble and membrane fractions were analyzed by immunoblotting. Tubulin and calnexin were detected as markers for soluble and membrane fractions, respectively. A fraction of tubulin protein was present in the membrane fraction, indicating an impure fraction, however, the trends of capturing SUMO at membranes still hold true. Both GFP-SENP2 constructs were concentrated in the membrane fraction, whereas GFP alone, used as a control, was soluble (not shown). SUMO2 was enriched with GFP-SENP2^{mNLS/CS} in the membrane fraction when compared to control cells transfected with GFP alone. Given that GFP-SENP2 constructs were not found in the soluble fraction, no differences were observed in SUMO2 enrichment between GFP and GFP-SENP2^{mNLS/CS} in the soluble fraction.

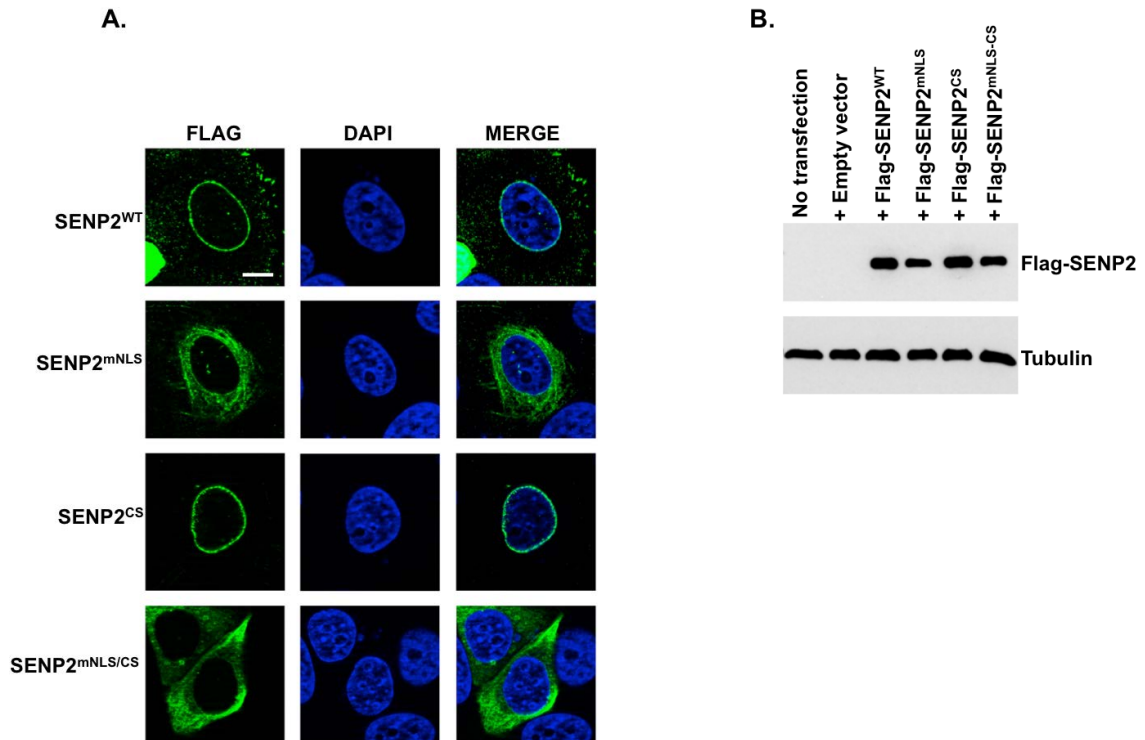


Figure III-3. Validation of newly generated FLAG-SENP2 constructs. Cells were transiently transfected with FLAG-SENP2 to validate the protein expression and localization of each SENP2 variant (WT, mNLS, CS, and mNLS/CS). Cells were harvested after 24 hours and analyzed by indirect immunofluorescence microscopy and immunoblotting. (A) HeLa cells were fixed and stained with anti-FLAG antibody. SENP2^{WT} and SENP2^{CS} are localized at the nuclear rim, more specifically at the inner nuclear membrane. SENP2^{mNLS} and SENP2^{mNLS/CS} are in the cytoplasm, mostly at intracellular membranes (ER and Golgi), as expected. Scale bar = 5 μ m. (B) Validation of the expression levels of each overexpressed SENP2 variant in HeLa cells by immunoblotting. Anti-FLAG antibody was used to detect FLAG-SENP2. Tubulin was used as a loading control.

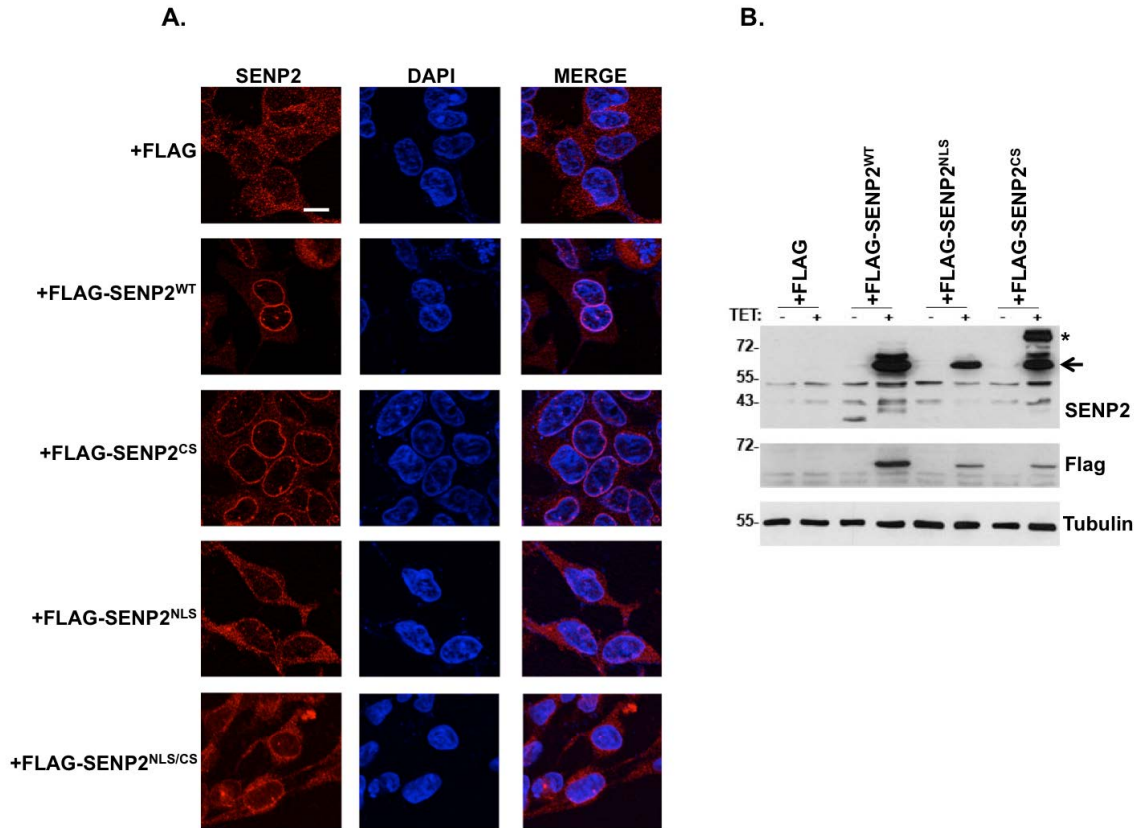
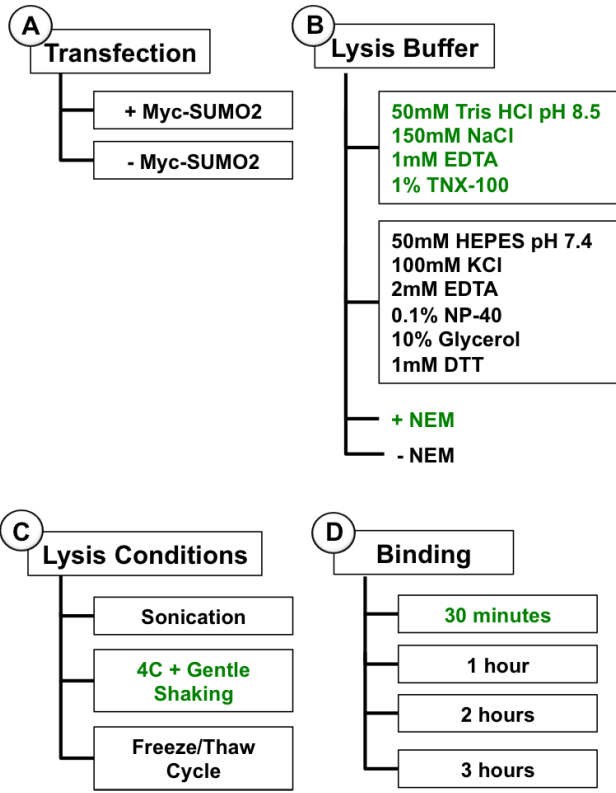


Figure III-4. FLAG alone or FLAG-SEN2 expression in 293T-REx Flp-In cells. Cells were incubated for 24 hours with complete media supplemented with 1 μ g/ml TET, or with no TET as a control. (A) Cells supplemented with TET were harvested and stained with anti-SEN2 antibody and analyzed by indirect immunofluorescence microscopy. Scale bar = 10 μ m. (B) Cells were harvested and analyzed by immunoblotting. Anti-SEN2 was used to detect the expression levels of FLAG-SEN2, indicated by an arrow. Lower molecular weight bands represent endogenous SEN2. A potentially sumoylated form of SEN2 is detected with FLAG-SEN2^{CS}, indicated by an asterisk (*). FLAG-SEN2 can be detected using anti-FLAG antibody, however, the signal is weak. Tubulin was used as a loading control.



E.

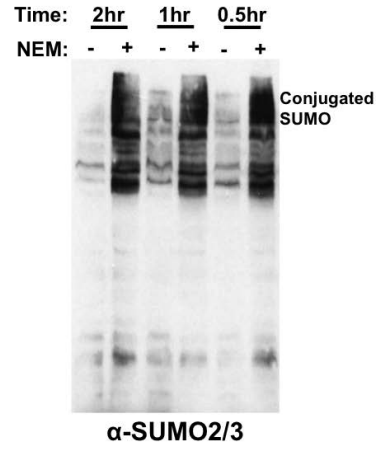


Figure III-5. FLAG Co-IP conditions: method development and optimization. Schematic diagram illustrating the different conditions that were tested to find the most optimal conditions to enrich for sumoylated, SENP2-dependent substrates. (A) 293T-REx cells stably expressing FLAG-SENP2 upon TET induction were transiently transfected with Myc-SUMO2 for 24 hours or kept non-transfected. (B) Cells were harvested in either buffer recipes indicated, with or without the presence of 10mM NEM (cysteine protease inhibitor). (C) Cell lysis was carried out either by sonication, 15 minute gentle shaking at 4C, or by one freeze/thaw cycle. (D) Cell lysates were incubated with agarose immobilized anti-FLAG (anti-ECS, DDDDK) antibody for the time indicated, at 4C with gentle end-to-end rotation. The most optimal conditions tested are highlighted in green. (E) Immunoblot showing the optimization results. The addition of 10mM NEM to the lysis buffer stabilizes the conjugated form of SUMO. Cell lysates were incubated with antibody beads for the indicated amount of time (2 hours, 1 hour, or 30 minutes). A 30-minute incubation maintained a higher amount of conjugated SUMO.

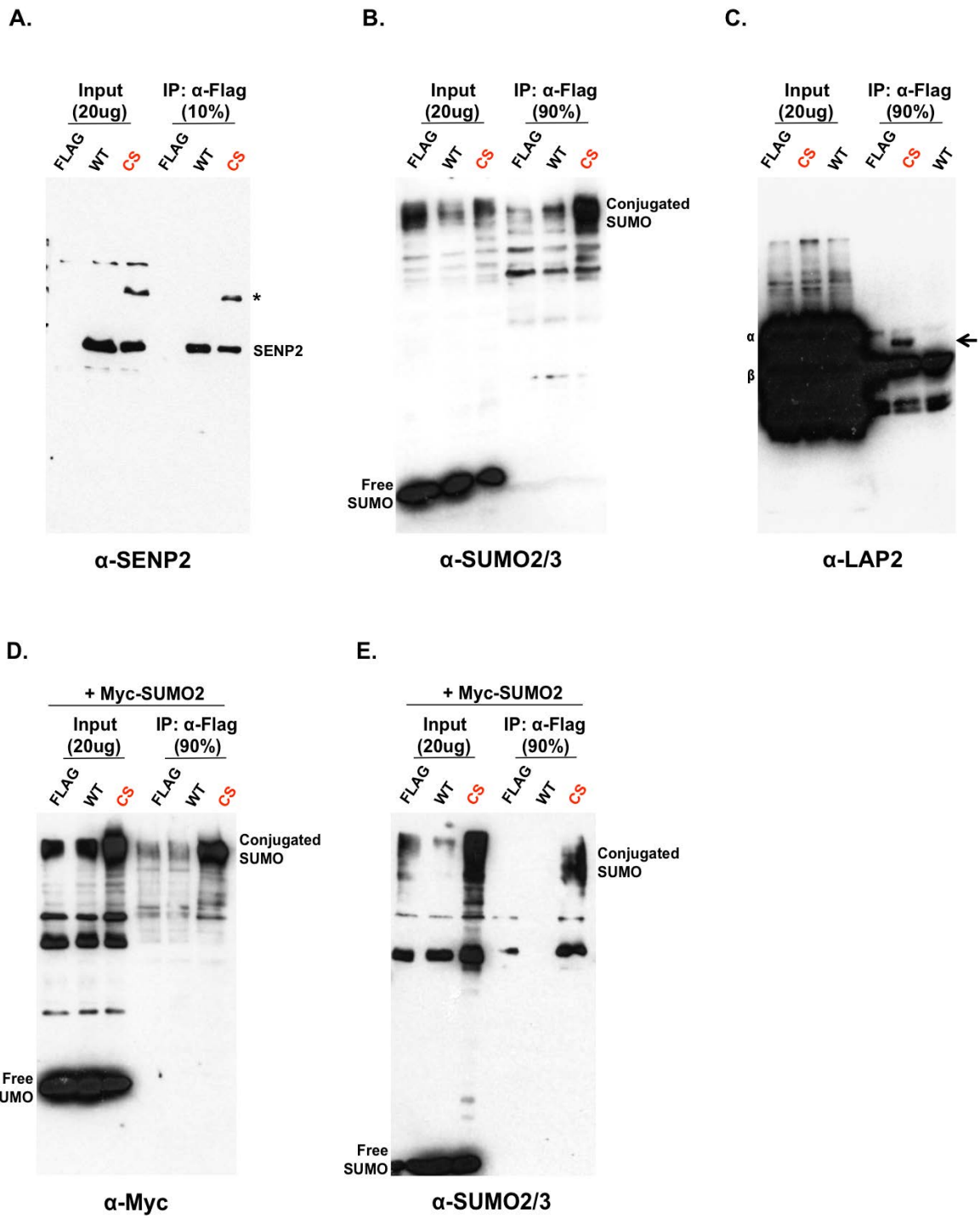


Figure III-6. Co-IP of FLAG-SEN2 and potential sumoylated substrates. (A-C) Stable cell lines expressing FLAG alone, FLAG-SEN2^{WT}, or FLAG-SEN2^{CS} were harvested after TET induction for 24 hours. Cells were lysed and incubated with agarose immobilized anti-FLAG antibody for 1 hour, and FLAG-SEN2 and associated proteins were eluted and analyzed by immunoblotting. (A) anti-SEN2 antibody was used to detect FLAG-SEN2 in the input and IP samples. A potentially sumoylated form of SEN2 is indicated by an asterisk (*). (B) anti-SUMO2/3 antibody was used to detect the amount of sumoylated proteins that are pulled down with FLAG-SEN2. (C) Multiple LAP2 isoforms are recognized by LAP2 antibody. Indicated by an arrow is a potentially sumoylated form of LAP2 β , and is exclusively pulled down with the catalytically dead mutant SEN2^{CS} suggesting that LAP2 β is a confirmed substrate of SEN2. (D-F) Stable cell lines were transiently transfected with Myc-SUMO2 to increase the sumoylated pool of proteins and then were harvested and analyzed as described above. (D) and (E) anti-Myc and anti-SUMO2/3 antibodies were used to detect Myc-SUMO2 in the input and FLAG IP samples. There is an increase in the pool of sumoylated proteins, however, the amount of sumoylated proteins pulled down after IP are not significantly higher relative to the amount pulled down without Myc-SUMO2 overexpression (compare with panel B).

APPENDIX I

TRIALS AND TRIBULATIONS: IN SEARCH FOR SENP2 FUNCTION

INTRODUCTION

We have established that SENP2 directly interacts with intracellular membranes via a unique amphipathic α -helix (refer to Chapter II). We also showed that SENP2 associates with a subset of membrane-associated proteins at the ER, Golgi, and inner nuclear membranes, and have developed methods to identify unique SENP2 substrates (refer to Chapter II and III). Though the questions still remain: Why is SENP2 at membranes? What is the functional significance of SENP2 regulation through targeted localization? In this appendix, we present several approaches to address these questions.

Our BioID analysis revealed that SENP2 interacts with proteins involved in ER-to-Golgi trafficking, ER biogenesis, and protein quality control. SENP2 interactors at the inner nuclear membrane are also involved in chromatin regulation, and maintaining nuclear shape and integrity. SUMO is implicated in some of these essential functions, however, how sumoylation is regulated remains unknown. We hypothesize that SENP2 plays a role in regulating membrane-associated functions by controlling the sumoylation of identified interacting proteins.

At the inner nuclear membrane, SENP2 interacts with lamins and lamin-associated proteins. We identified LAP2 as a substrate of SENP2, however, we have yet to investigate how LAP2 sumoylation and SENP2 regulation is functionally significant. Sumoylation is also implicated in the regulation of chromatin organization, for example, regulating the interactions between lamins and chromatin (Neyret-Kahn *et al.*, 2013). SUMO plays an important role in orchestrating the “on” and “off” states of chromatin, yet again, very little is known about the regulation of this process. Finally, sumoylation is

also involved in regulating several ion channels, including CFTR. A defective CFTR, most commonly CFTR^{ΔF508}, leads to cystic fibrosis, a disease in which patients suffer from a build up of viscous secretions and infections by pathogenic bacteria. Both wild type and mutant CFTR proteins are regulated by sumoylation (Gong *et al.*, 2016; Meng *et al.*, 2017); however, the exact molecular mechanisms are not yet elucidated.

In this appendix, we present three different attempts for studying SENP2 and possible membrane-associated functions. We investigated the role of SENP2 regulation at the inner nuclear membrane, more specifically, regulation of LAP2. Secondly, we closely examined the role of SENP2 regulation in chromatin organization. Finally, we investigated SENP2 function at the ER membrane and its role in regulating CFTR degradation or stability. Overall, the data presented here reveals promising avenues of research that could be further explored.

MATERIALS AND METHODS

Antibodies

Rabbit polyclonal SENP2, LAP2, and lamin B antibodies were produced as previously described (Chaudhary and Courvalin, 1993; Fischer *et al.*, 2001; Goeres *et al.*, 2011). Remaining antibodies were obtained from the following sources: anti-GFP (Clontech, Mountain View, CA); anti-tubulin (Sigma-Aldrich, St. Louis, MO); and anti-CFTR (Millipore Sigma, Burlington, MA).

Plasmid constructs

SENP2 cDNA was obtained as previously described (Zhang *et al.*, 2002). Full length SENP2 was PCR amplified and cloned into pEGFP-C1 as described (Goeres *et al.*, 2011), and cloned into pmCherry-C1 expression vector, using standard cloning procedures. SENP2 NLS mutation (mNLS: R29A/R49A) was introduced using PCR based, site-directed mutagenesis. CFTR^{WT} and CFTR^{ΔF508} were cloned into pcDNA expression vector. Both CFTR plasmids were a generous gift from the Zeitlin lab (Johns Hopkins University, Baltimore, MD).

Cell culture

HeLa cells were maintained in DMEM supplemented with 10% fetal bovine serum. IB3-1 cells were maintained in LHC-8 without gentamicin, supplemented with 10% fetal bovine serum. TCIS system cell lines (EGFP-LacI, I/D6+EGFP-LacI, and YY1-EGFP-LacI) were maintained in DMEM with high glucose, supplemented with

1mM sodium pyruvate, 10% fetal bovine serum, 100 U/ml penicillin-streptomycin, 2mM L-Glutamine, 1µg/mL puromycin, and 1mM IPTG. EGFP-LacI and YY1-EGFP-LacI were also supplemented with 500µg/mL hygromycin. To allow binding of EGFP-LacI to LacO, IPTG was removed 24-36 hours prior to visualization. All cell lines were incubated at 37°C and 5% CO₂.

Transient transfection, and RNA interference

Cells were grown at a confluency of 50-60% for transfection with the indicated plasmids using Lipofectamine 2000 according to manufacturer's protocol (Invitrogen, Carlsbad, CA). For RNA interference, cells were grown to 40-50% confluency and then transfected using RNAiMAX (Invitrogen, Carlsbad, CA). siRNA oligos were used at a final concentration of 25nM. siRNA oligos included the following: scramble control, 5'-CUUCCUCUCUUUCUCUCCCUUGUGA-3'; and SENP2 oligo, 5'-GAAAGAGAGAAGUACCGAA-3'. Cells were harvested either at 24 or 48 hours post-transfection, as indicated, for immunoblotting, or immunofluorescence microscopy.

Viral transduction

shSENP2 cloned into pLKO.1 was purchased from The RNA Consortium (TRC) Broad Institute (http://hitcores.bs.jhmi.edu/search_rna.php), clone ID: NM_029457.2-1809s1c1. Control shRNA directed against firefly luciferase (5'-CGCTGAGTACTTCGAAATGTC-3') was obtained from the Reddy lab (Johns Hopkins University, Baltimore, MD). Lentivirus was produced by co-transfecting the shRNA- or mCherry-SENP2 plasmid, with psPAX2 (packaging plasmid) and pMD2.G (envelope

plasmid) into HEK 293FT cells. Virus was harvested after 48 hours, filtered, and added to 30-40% confluent TCIS cells and removed after 24 hours. Cells were harvested after 3-4 days post-infection for analysis by RT-PCR and immunofluorescence microscopy. RT-PCR was used to verify SENP2 knockdown efficiency. Reverse transcription was carried out using SuperScript III Reverse Transcriptase according to manufacturer's protocol (Invitrogen, Carlsbad, CA).

Immunoblotting, and immunofluorescence microscopy

Immunoblot and immunofluorescence microscopy analyses were performed as described in the Materials and Methods section of Chapter II.

RESULTS AND DISCUSSION

SENP2 and LAP2

We have identified LAP2 as a substrate of SENP2 by two complementary approaches, BioID and SUMO capture (refer to chapter II and III). However, how SENP2 and sumoylation are involved in regulating LAP2 functions are not known. Based on known functions of sumoylation, we hypothesized that SENP2 plays a role in regulating LAP2 localization at the inner nuclear membrane. To test this, we reduced the levels of SENP2 in HeLa cells by siRNA-mediated knockdown, and analyzed LAP2 localization and expression levels (Figure A-1). In control cells, LAP2 localized to the nuclear periphery and the nucleoplasm. With SENP2 knockdown, we observed a significant decrease in LAP2 nucleoplasmic signal, and an increased signal at the nuclear periphery (Figure A-1A and B). However, when we looked at LAP2 isoforms by immunoblotting, there was no difference in LAP2 expression levels between SENP2 knockdown and control cells (Figure A-1C). Therefore, the loss of signal observed by immunofluorescence microscopy cannot be explained by a decrease in LAP2 protein expression. Whether this apparent shift in LAP2 localization from the nucleoplasm to the nuclear membrane is directly linked to LAP2 sumoylation remains to be tested. One could hypothesize however, that SENP2 knockdown results in increased LAP2 sumoylation and enhanced interactions with proteins at the inner nuclear membrane. We have repeated the same experiment with an overexpression of SENP2^{WT}, however, there were no differences observed in LAP2 localization compared to the control (data not shown).

Thus far, there are three known LAP2 isoforms (α , β , and γ). LAP2 α lacks a transmembrane domain and is therefore soluble, while the other two isoforms are anchored to the inner nuclear membrane by a single transmembrane span near the C-terminus (Gant *et al.*, 1999). In this experiment, we were not able to determine which specific LAP2 isoform is being affected by SENP2 knockdown. It is reasonable to suggest that membrane-associated LAP2 β and LAP2 γ are more likely to be regulated by SENP2, however, given the change in LAP2 localization from nucleoplasmic to nuclear membrane, we cannot rule out that SENP2 might also indirectly regulate LAP2 α . One could hypothesize that the sumoylation of LAP2 β results in the recruitment and stable association of LAP2 α with the membrane. Our SUMO capture data implied that LAP2 β is the specific isoform regulated by SENP2, based on the size of LAP2 β and the higher molecular weight band observed with SENP2^{CS} pull-down (refer to Chapter III, Figure III-6C). The anti-LAP2 antibody used in this experiment detected all three isoforms, and although there was no change in LAP2 expression levels, the disappearance of the nucleoplasmic signal and change in LAP2 localization was intriguing. Therefore, as a future direction, it would be interesting to decipher which particular isoform is being affected by SENP2 knockdown by using isoform-specific antibodies.

In addition to investigating each LAP2 isoform, another future direction would be to test SENP2 effect on LAP2-specific functions. LAP2 plays a role in mediating chromatin-membrane attachment, and nuclear lamina assembly, but whether sumoylation regulates those functions is unknown (Gant *et al.*, 1999). In summary, our preliminary findings support a role for SENP2 and sumoylation in regulating LAP2 localization at the

inner nuclear membrane. Understanding the molecular mechanisms and functional significance of this regulation will require further investigation.

SENP2 and chromatin organization

SENP2 uniquely interacts with the inner nuclear membrane, where it directly associates with the nuclear lamina and lamin-associated proteins. Lamin A and lamin B were among our significant BioID hits, and both are known to be sumoylated. Defects in their sumoylation are implicated in lamin-associated diseases (laminopathies) (Sarge and Park-Sarge, 2011; Simon *et al.*, 2013). What regulates the sumoylation of lamins, however, has not been investigated. Given our data on SENP2 localization and interactions with lamins, we hypothesize that SENP2 plays a role in the regulation of their sumoylation and associated functions, a major one being chromatin organization. Sumoylation is also strongly tied with transcriptional repression, but the mechanisms still await full characterization (Neyret-Kahn *et al.*, 2013). We hypothesize that SENP2, through effects on sumoylation of specific proteins at the inner nuclear membrane, can coordinate the association of chromatin with the nuclear lamina, and therefore indirectly regulate gene expression. To test the role of SENP2 in regulating chromatin organization at the inner nuclear membrane and lamina, we turned to the tagged chromosomal insertion site (TCIS) system (Figure A-2) (Harr *et al.*, 2015). The TCIS system utilizes three cell lines to quantitatively monitor the localization and association of a specific, EGFP-tagged, lamin-associated sequence (LAS) of chromatin to the nuclear lamina/periphery (detailed description of the TCIS system is provided in the figure legend of Figure A-2). In control cells (EGFP-LacI), the EGFP-tagged chromatin is not

associated with the nuclear lamina and therefore is scored as “central” by fluorescence microscopy (Figure A-2, A and D). In contrast, in I/D6+EGFP-LacI cells, EGFP-tagged chromatin associates with the nuclear lamina due to the presence of D6 – a known LAS – therefore, the signal of D6 overlapping with the nuclear periphery is scored as “peripheral” by fluorescence microscopy (Figure A-2, B and D). Similarly, EGFP-tagged chromatin associates with the nuclear periphery in YY1-EGFP-LacI cell line harboring the Ying-Yang 1 (YY1) protein, which also directs chromatin association with the nuclear lamina (Figure A-2C). We used the three TCIS system cell lines to overexpress or knockdown SENP2 and then monitor the localization of EGFP-tagged chromatin by fluorescence microscopy. We hypothesized that changes in SENP2 expression levels would affect the recruitment of chromatin domains to the nuclear periphery (Figure A-2, B and C).

We first used RNAi to knockdown SENP2 expression and assessed effects on chromatin localization in the three TCIS cell lines. Knockdown efficiency was verified using RT-PCR (data not shown). In EGFP-LacI control cells, the tagged chromatin was centrally located in 80% of cells, and this was unaffected by SENP2 depletion (Figure A-3). I/D6+EGFP-LacI and YY1-EGFP-LacI cell lines exhibited 80% peripheral signal, and this localization was also not significantly different between control and SENP2 knockdown conditions (Figure A-3). We next overexpressed mCherry-SENP2 and only scored cells with a mCherry signal. Again, we observed no significant difference in chromatin localization in EGFP-LacI control cells (Figure A-4). In contrast, SENP2 overexpression caused an ~15% decrease in peripherally associated chromatin in I/D6+EGFP-LacI expressing cells (Figure A-4). This result suggests that SENP2 may

play an active role in limiting SUMO-dependent chromatin recruitment and repression at the inner nuclear membrane, and is consistent with known roles for sumoylation in chromatin repression. One might argue that a 15% decrease in chromatin association with the nuclear periphery is not significant, however, earlier studies have shown that a slight 15-20% change in chromatin organization is sufficient to have measurable effects on gene activation or repression (Harr *et al.*, 2015). Overall, our overexpression results provide evidence for a role for SENP2 in regulating chromatin localization and organization at the inner nuclear membrane. Further studies are needed to fully explore this finding and implications for control of gene expression.

Using our experimental design, it was challenging to study whether SENP2 positively affects chromatin association with the nuclear periphery since the cell lines used were harboring LASs that would target chromatin to the nuclear periphery, and therefore, more than 80-90% of the chromatin was already associated with the lamina. Electron microscopy to look at chromatin organization, or looking at the levels of specific heterochromatin and euchromatin markers might present alternative methods to further investigate SENP2 regulation.

SENP2 and CFTR

In another attempt to investigate the role of SENP2 at intracellular membranes, we have focused on CFTR as a promising candidate substrate. CFTR functions as a chloride ion channel at the plasma membrane. The folding, packaging and export of CFTR from the ER to the plasma membrane is highly regulated by many posttranslational modifications, one of which is sumoylation (Gong *et al.*, 2016). Since

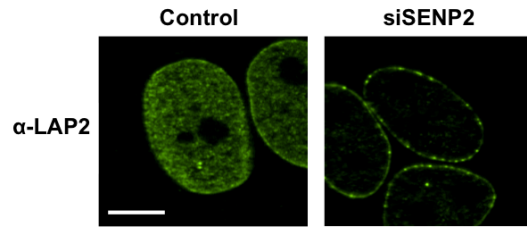
SEN2 is associated with intracellular membranes, we hypothesized that SEN2 might play a role in regulating CFTR sumoylation. Both mature and immature forms of CFTR are regulated by SUMO. Evidence suggests that the sumoylation of CFTR^{ΔF508}, the most common CFTR mutation associated with cystic fibrosis, blocks its export to the plasma membrane by targeting it for degradation (Ahner *et al.*, 2013). Here, we hypothesize that the overexpression of SEN2 and the subsequent de-conjugation of SUMO would delay the degradation of the mutant protein, giving it time for proper folding and subsequent export from the ER to the plasma membrane (Figure A-5A). To test this, we used IB3-1 cells derived from patients with cystic fibrosis carrying the CFTR^{ΔF508} mutation, and we transiently overexpressed GFP-SEN2. To assess whether the mutant protein was rescued, we looked at the abundance of the three different molecular weight forms of CFTR protein: 127kDa (A band), 131kDa (B band), and 160kDa (C band). Bands A, B, and C represent different glycoforms of CFTR: the non-glycosylated, the core glycosylated, and the mature CFTR with complex glycosylation, respectively (O'Riordan *et al.*, 2000). The overexpression of CFTR^{WT} served as a positive control. The most abundant form of CFTR^{WT} is the mature, C band (Figure A-5B, first lane). In contrast, CFTR^{ΔF508} is predominantly synthesized as A and B bands (Figure A-5B, second lane). In cells expressing CFTR^{ΔF508}, with or without SEN2^{WT}, A and B bands were observed, but no C band (Figure A-5B). This indicates that SEN2^{WT} had no effect on the maturity of the mutant protein. We also expressed SEN2^{mNLS} to enrich for SEN2 at the ER membrane, but again, there was no effect on CFTR maturation (Figure A-5B). This indicates that simply overexpressing SEN2 does not rescue the mutant CFTR^{ΔF508} from degradation, and perhaps the role of sumoylation and potentially SEN2 is more complex

and requires further investigation. It is reasonable to suggest that SENP2 might not recognize sumoylated CFTR, and that SENP2 substrate specificity extends beyond its association with membranes.

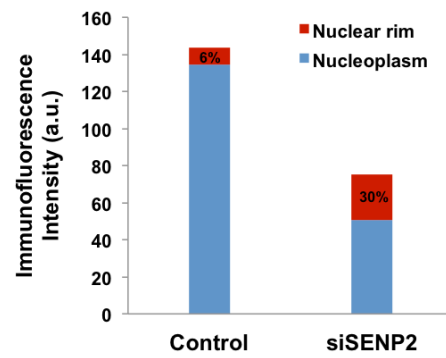
CFTR has a complex folding pattern that involves a variety of post-translational modifications including sumoylation, ubiquitination, phosphorylation and glycosylation. It is the crosstalk between these different modifications that could determine the fate of the protein (Ahner *et al.*, 2013). Multiple lysine residues in both wild type and mutant CFTR are sumoylated and ubiquitinated at different subcellular locations, including the ER, Golgi and plasma membrane (Ahner *et al.*, 2013; Lee *et al.*, 2014). Overall, the complexity of CFTR regulation makes it challenging to determine the specific roles of SENP2 without considering the crosstalk between those various modifications. More specifically, SUMO and ubiquitin modifications can result in unique “codes” that determine whether the protein is targeted to degradation or is stabilized at the plasma membrane (Figure A-6). Therefore, more detailed analyses are required to untangle SUMO-specific regulatory functions.

FIGURES AND FIGURE LEGENDS

A.



B.



C.

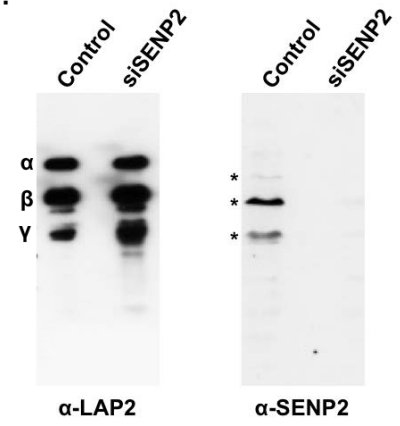
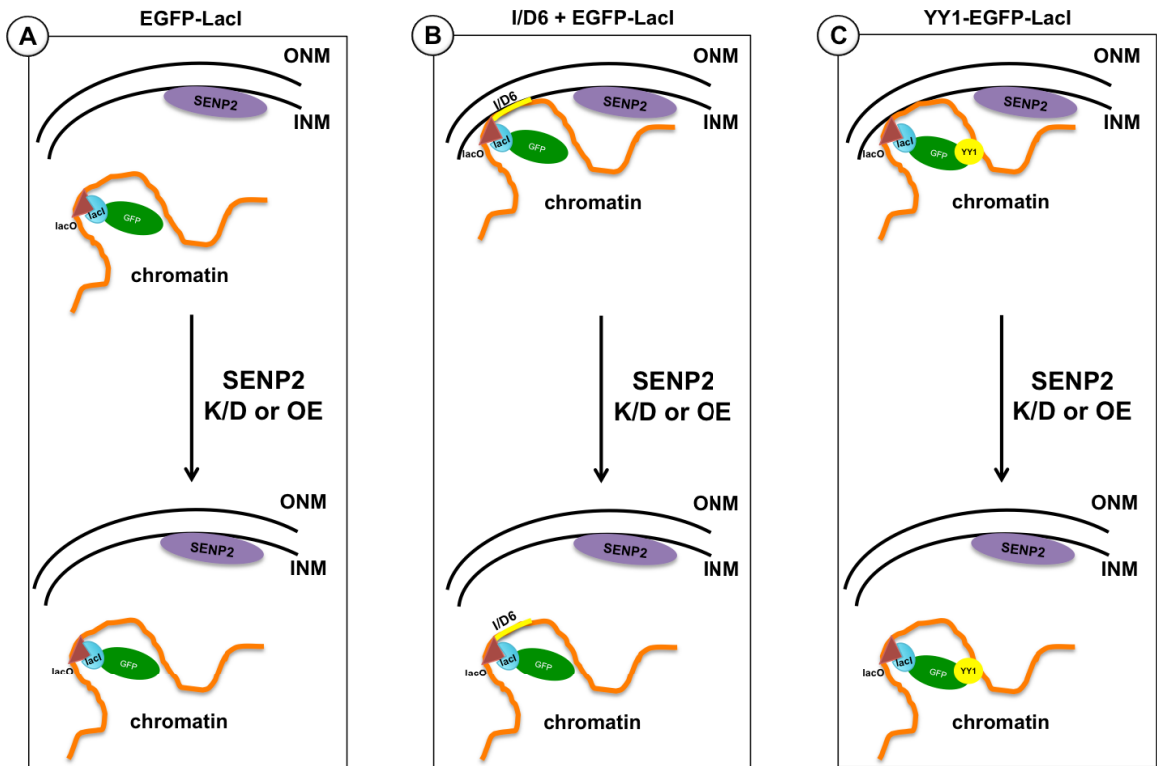


Figure A-1. Effect of SENP2 knockdown on LAP2 localization and expression levels. HeLa cells were transfected with scramble (control) or SENP2-specific siRNA oligos then harvested after 48 hours. (A) Cells were stained with anti-LAP2 antibody and analyzed by indirect immunofluorescence microscopy. Control cells show the typical localization of LAP2, around the nuclear rim and in the nucleoplasm. SENP2 knockdown caused a general loss of LAP2 signal with a concentrated signal around the nuclear periphery. Scale bar = 5 μ m. (B) Quantification of LAP2 nucleoplasmic signal and nuclear rim signal, based on immunofluorescence intensity. As observed in part A, there is a decrease in overall signal but an increase in nuclear rim staining from 6% to 30%. (C) Immunoblot analysis using anti-LAP2 and anti-SENP2 antibodies. Anti-LAP2 antibody recognizes at least three LAP2 isoforms: α , β , and γ . No difference was observed in the expression levels of LAP2 between control and SENP2 knockdown cells. Anti-SENP2 was used to detect SENP2 knockdown efficiency. Asterisks (*) indicate different SENP2 isoforms.

TCIS SYSTEM



D.

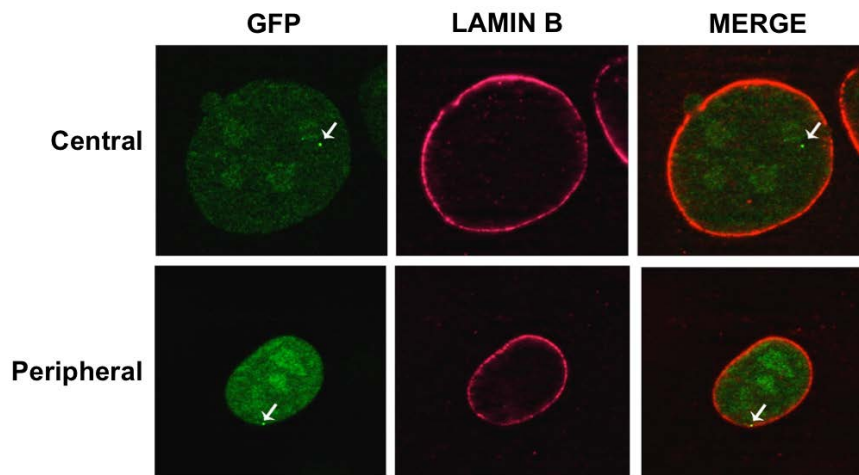
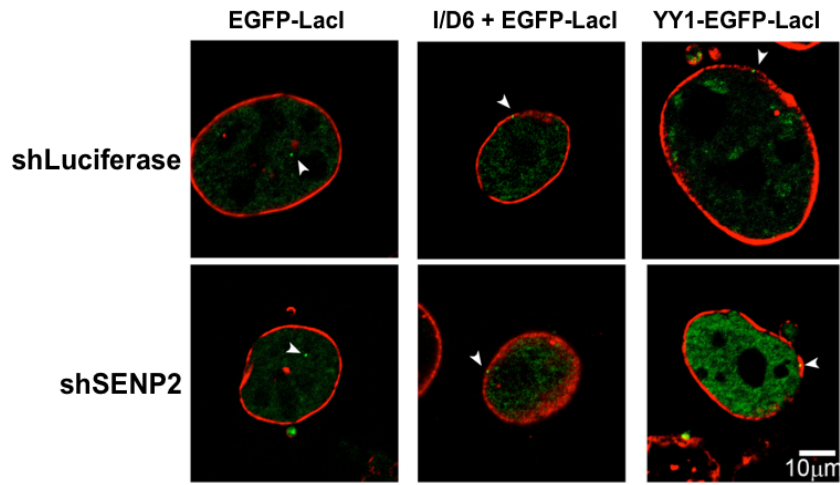


Figure A-2. Schematic diagram of the three TCIS system cell lines. 3T3 derived C57BL/6 fibroblast cell lines stably expressing EGFP-LacI or YY1-EGFP-LacI with randomly co-integrated bacterial artificial chromosomes (BACs) and hygromycin-selectable LacO arrays were used to study the effect of SENP2 knockdown or overexpression on chromatin organization. LacO arrays serve as docking sites for EGFP-LacI enabling quick identification by fluorescence microscopy. (A) Control cell line stably expressing EGFP-LacI (designated in green and blue) and integrated BACs with LacO (designated in orange). LacI binds to LacO, and GFP provides the localization of that specific chromatin region. In control, the signal is mostly concentrated in the nucleoplasm and therefore scored as “central”. Upon SENP2 overexpression or knockdown, we expect no change in the localization. (B) I/D6+EGFP-LacI cell line contains a BAC carrying a lamin-associated sequence (LAS) containing the gene Ikaros (designated in yellow and labeled “I/D6”). I/D6 sequence targets DNA to the periphery of the nucleus, to associate with the nuclear lamina, and hence the signal is scored as “peripheral” by fluorescence microscopy. Again, stably expressed EGFP-LacI assists in visualization. We hypothesize that SENP2 might directly affect chromatin organization by altering the signal from “peripheral” to “central”. (C) YY1-EGFP-LacI cell line stably expressing YY1 fused to EGFP-LacI (designated with a yellow circle). YY1 interacts with chromatin and indirectly targets DNA to the nuclear periphery, hence signal is scored “peripheral”. In this case, we hypothesize that SENP2 may indirectly affect chromatin organization and result in changing the localization from peripheral to central. Abbreviations used: INM = inner nuclear membrane; ONM = outer nuclear membrane; K/D = knockdown; OE = overexpression. (D) Representative images for all 3 cell lines

showing the difference between a central and peripheral signal for scoring purposes. Arrows indicate GFP signal scored. An overlap between EGFP-LacI/LacO focus and Lamin B signal is scored as peripheral.

A.



B.

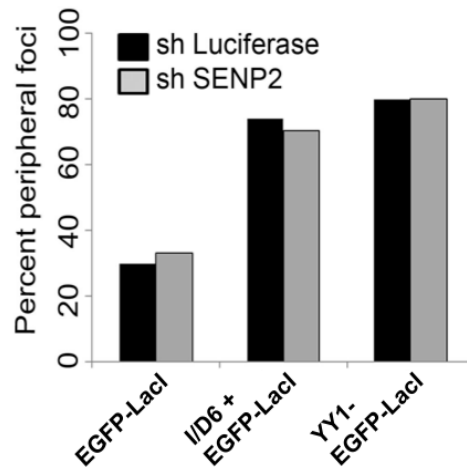
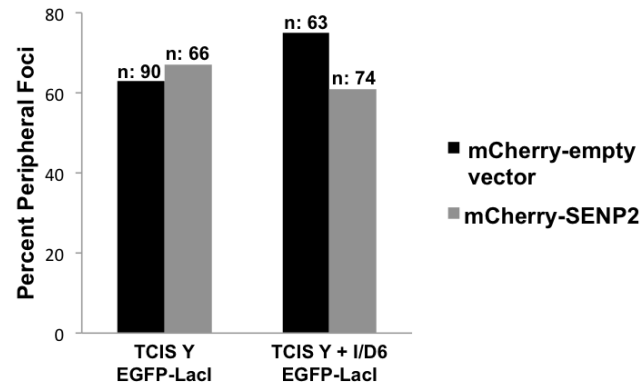


Figure A-3. Effect of SENP2 knockdown on chromatin organization. Cells were treated with lentivirus containing SENP2 shRNA or luciferase shRNA (control) for 3 days then harvested and analyzed by indirect immunofluorescence microscopy. SENP2 knockdown efficiency was verified at the mRNA level by PCR. (A) Cells were stained with anti-Lamin B antibody to stain the periphery of the nucleus. The GFP signal (indicated with white arrows) represents the EGFP-LacI/LacO focus. Signal for EGFP-LacI cells was peripheral as expected and no changes were observed with SENP2 knockdown. I/D6+EGFP-LacI and YY1-EGFP-LacI cell lines exhibited an 80% peripheral signal, with no difference observed between control cells and SENP2 knockdown cells, indicating that SENP2 knockdown has no effect on chromatin organization. (B) Quantification of peripheral foci observed for each cell line. n=20-50 cells per condition.

A.

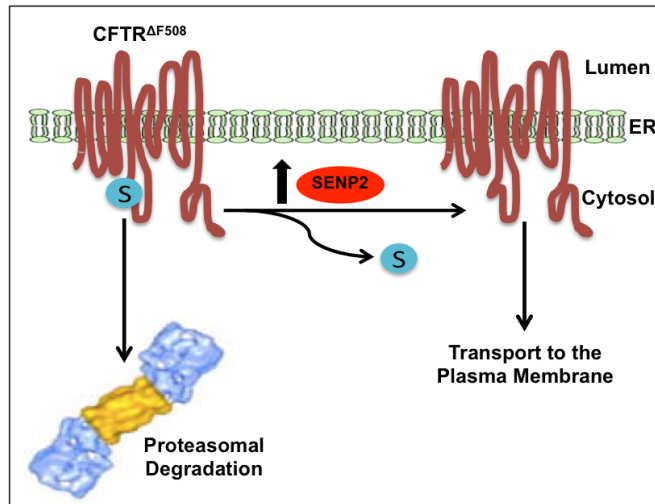


B.

	mCherry-empty vector	mCherry-SEN2
EGFP-Lacl	63%	67%
I/D6+EGFP-Lacl	75%	61%

Figure A-4. Effect of SENP2 overexpression on chromatin organization. Cells were transiently transfected with mCherry alone or mCherry-SENP2 for 24 hours. Cells were then harvested and analyzed by indirect immunofluorescence microscopy. To stain the nuclear periphery, cells were stained with anti-Lamin B antibody. (A) Quantification of peripheral foci from the two transfected cell lines: EGFP-LacI (control) and I/D6+EGFP-LacI. No differences were observed between the empty vector and SENP2 overexpression in the control cell line. However, a higher number of peripheral foci was observed in the control cell line for both conditions, which could be an artifact due to transfection. SENP2 knockdown in the I/D6+EGFP-LacI cell line exhibited a 15% decrease in the number of peripheral foci compared to control, indicating that SENP2 knockdown has an effect on chromatin association with the nuclear lamina. Even though the control cell line exhibited a higher number of peripheral foci, the trends still hold true. “n” indicates the number of cells counted in each condition. (B) Percentages of peripheral foci counted for each cell line from part A.

A.



B.

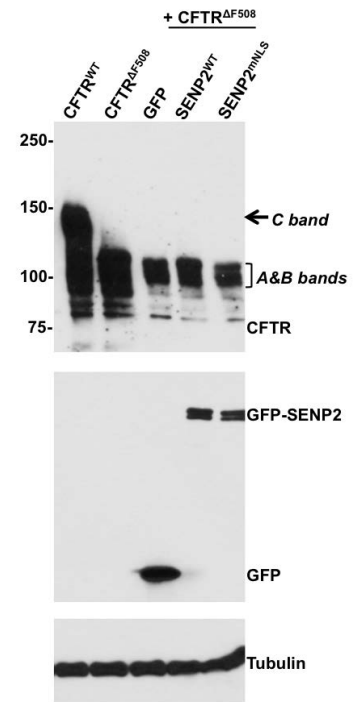


Figure A-5. Effect of SENP2 overexpression on CFTR^{ΔF508} stability. (A) Schematic diagram representing our model for the effect of SENP2 overexpression. The sumoylation of CFTR^{ΔF508} targets the protein for proteasomal degradation. We hypothesize that SENP2 overexpression and the subsequent de-conjugation of SUMO from CFTR^{ΔF508} can rescue the protein from degradation and target it to the plasma membrane. (B) IB3-1 cells were transiently transfected with CFTR^{WT} or CFTR^{ΔF508}, with or without co-transfection with GFP-SENP2^{WT} or GFP-SENP2^{mNLS}. Cells were harvested 48 hours post-transfection and analyzed by immunoblotting. Expression of CFTR^{WT} or CFTR^{ΔF508} alone was used as positive and negative controls, respectively. With wild type, the C band is the major form present at the plasma membrane, which represents the mature form of the channel with complex glycosylation. In contrast, CFTR^{ΔF508} is synthesized predominantly as bands A and B, representing immature, non-glycosylated or core glycosylated forms, respectively. Co-expression of SENP2^{WT} or SENP2^{mNLS} had no effect on CFTR^{ΔF508} maturation or stability, since no C band was observed. Anti-GFP antibody was used to detect the expression levels of GFP-SENP2 constructs. Tubulin was used as a loading control.

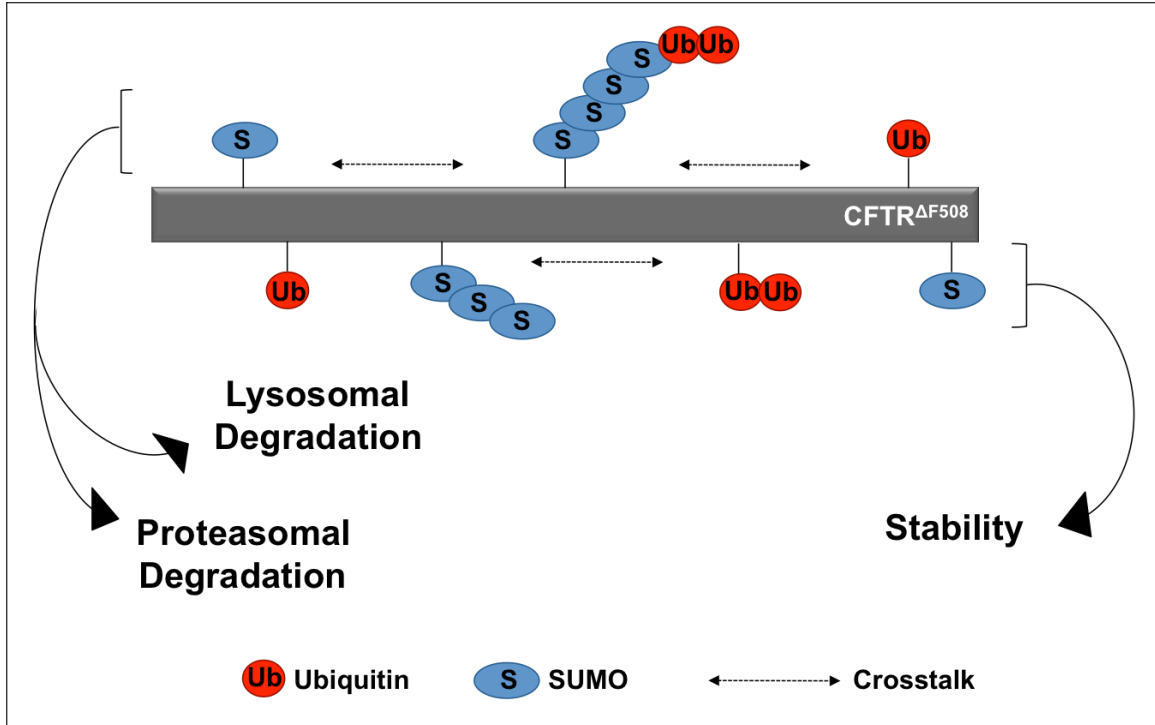


Figure A-6. Schematic model showing the crosstalk between CFTR^{ΔF508} sumoylation and ubiquitination. Modification of different lysine residues results in a unique “code” that determines the fate of CFTR^{ΔF508}. Depending on this crosstalk between sumoylation and ubiquitination, mutant CFTR may be targeted to degradation, via the proteasomal or the lysosomal pathway, or may be stabilized at the cell surface.

OVERVIEW AND FUTURE DIRECTIONS

OVERVIEW

There is growing evidence for the role of sumoylation outside the nucleus. From glucose transport and ion channel regulation at the plasma membrane, to mitochondrial fission and fusion, SUMO touches multiple cellular functions in the cytoplasm and at intracellular membranes. How sumoylation is regulated within these different subcellular domains however, remains a question in the field. This thesis focused on understanding how sumoylation is regulated at intracellular membranes, a relatively new domain being explored. We found that the SUMO protease SENP2 interacts with intracellular membranes via a unique N-terminal targeting signal, an amphipathic α -helix. We showed that SENP2-membrane interaction is regulated by the nuclear import machinery, more specifically, Kap- α . Furthermore, we identified SENP2 interacting binding partners by BioID, and found that SENP2 interacts with a specific subset of membrane-associated proteins at the ER, Golgi, and inner nuclear membranes. We also developed a new method, called “SUMO capture”, to identify SENP2 substrates. Combining BioID and SUMO capture data, we identified LAP2 as a SUMO-modified SENP2 substrate. Finally, we initiated studies to investigate functional roles for SENP2 at membranes, and in particular its effects on LAP2 and chromatin association with the inner nuclear membrane, and ion channel maturation in the ER. Overall, we have elucidated a novel mechanism for regulating SENP2 via a unique N-terminal membrane-targeting signal, and provided insights on potential new roles for sumoylation at membranes.

SENP2-MEMBRANE INTERACTION

In Chapter II, we provided *in vivo* and *in vitro* evidence for SENP2-membrane interaction. We found that Kap- α binding regulates this interaction, where it impedes SENP2 amphipathic α -helix from associating with membranes in the cytoplasm. This intriguing finding begs us to ask the question: Do mechanisms exist to regulate SENP2 interactions with Kap- α , thereby modulating cytosolic membrane binding? Given our evidence that SENP2 interacts with ER and Golgi, there must be other mechanisms by which the amphipathic α -helix is still capable of interacting with membranes in the cytoplasm, even with the presence of Kap- α . To study this, it would be important to first pursue structural analyses of SENP2 in complex with Kap- α , in order to understand the molecular basis of Kap- α interaction. Secondly, there are predicted SENP2 isoforms lacking the amphipathic α -helix or the nuclear localization signal that remain uncharacterized (Nishida *et al.*, 2001). These isoforms are expected to be differentially targeted to membranes, and therefore it will be important to identify and characterize these and other isoforms more carefully. It is also possible that different cell types may express different SENP2 isoforms based on specific cellular functions. Finally, other post-translational modifications of SENP2 might play a role in its regulation. SENP2 is phosphorylated and sumoylated (Bailey and O'Hare, 2004), however, it is not yet known how these modifications affect SENP2 localization or function, and they should also be further investigated.

SEN2 SUBSTRATES AND FUNCTIONAL SIGNIFICANCE

We developed a method to capture and identify sumoylated SEN2 substrates as outlined in Chapter III. It is anticipated that utilizing the SUMO capture approach in combination with mass spectrometry will provide comprehensive catalogs of SEN2 substrates and related functions. In the appendix, we described efforts to explore the functional significance for SEN2 at membranes. We provided insights on SEN2 function in relation to LAP2 regulation, chromatin organization, as well as CFTR regulation. We found that the signal of LAP2 localization changes from nucleoplasmic to peripheral upon SEN2 knockdown. One of the immediate future directions is to study SEN2 effects on specific LAP2 isoforms by using isoform-specific antibodies. Once we determine which LAP2 isoform is regulated by SEN2, we can investigate downstream functional consequences of SEN2 regulation, including changes in localization, protein expression, and utilizing RT-qPCR (real time-quantitative PCR) for studying changes in gene expression of LAP2-specific transcription factors. Besides the effect on LAP2 localization, changes in SEN2 levels also changed the localization of chromatin from the periphery to the nucleoplasm. In the future, we hope to look more closely at the effect of SEN2 on chromatin organization by utilizing electron microscopy techniques. Finally, although we did not find a direct link between SEN2 regulation and CFTR in our experiments, we are eager to decipher the molecular mechanism behind the regulation of CFTR sumoylation and its implication in cystic fibrosis. A global approach to study CFTR sumoylation in the context of disease is to turn to animal models. There are mice models of cystic fibrosis that are widely used for experimental therapies (Wilke

et al., 2011). It would be interesting to knock-in SENP2^{I8D} in this mouse background to determine the role of SENP2-membrane interaction on disease development.

Given that SENP2 shares the common feature of having an amphipathic α -helix with many nucleoporins, and localizes to NPCs, it would be interesting to investigate whether SENP2 plays an important role in NPC assembly, especially after nuclear envelope breakdown (NEBD). During NEBD, specific nucleoporins are thought to induce the formation of membranous vesicles that carry and stabilize some membrane-associated proteins until cell division is complete (Prunuske *et al.*, 2006; Alber *et al.*, 2007; Doucet and Hetzer, 2010; Doucet *et al.*, 2010; Drin and Antonny, 2010; Meszaros *et al.*, 2015; Souquet and Doye, 2015). Those nucleoporins are also sumoylated, and it is possible that SENP2, with its ability to associate with membranes, maintains the regulation of nucleoporins associated with membranous vesicles and assists in nuclear envelope and NPC re-assembly (Chow *et al.*, 2012; Chow *et al.*, 2014). To study this, we could turn to live-cell imaging. Monitoring the events of pre- and post-NEBD under SENP2 knockdown and overexpression conditions, and tracking specific nucleoporins involved in NPC and nuclear envelope re-assembly will provide insight on the role of SENP2 in regulating this process.

Besides inner nuclear membrane-associated proteins, BioID analysis revealed that SENP2 uniquely interacts with ER and Golgi proteins. When clustered into functional groups, the majority of these proteins are associated with ER-to-Golgi trafficking, implying that SENP2 might have a role in regulating vesicular transport. Furthermore, it was intriguing to find that SENP2 interacts with 8 out of 10 subunits of the EMC complex (refer to Chapter II). The EMC complex is involved in cellular response to ER

stress, ERAD, and lipid homeostasis (Jonikas *et al.*, 2009; Christianson *et al.*, 2011; Richard *et al.*, 2013; Lahiri *et al.*, 2014; Satoh *et al.*, 2015; Wideman, 2015). We are interested in investigating whether SENP2 is involved in regulating EMC complex assembly, and its associated functions. Future studies will focus on determining the localization and expression of each EMC subunit in the context of SENP2 knockdown and overexpression. Later on, we would like to decipher the effect of EMC complex sumoylation on the ER stress response by treating cells with different ER stress inducers and determining the effects on overall sumoylation of the EMC complex, and its subsequent functions. Interestingly, the EMC complex also facilitates efficient insertion of tail-anchored proteins into ER membranes (Guna *et al.*, 2018). Whether the EMC complex itself facilitates SENP2 binding to the ER membrane is worth pursuing. This could be further studied by knocking down EMC subunits and looking at the localization of SENP2. As mentioned earlier, a SENP2^{18D} knock-in mouse model would also be helpful to look at the physiological relevance of SENP2-membrane association in relation to EMC-associated functions.

IS MEMBRANE ASSOCIATION REGULATORY?

In this thesis, we have described SENP2-membrane targeting as a way to regulate sumoylation at intracellular membranes, subsequently regulating the many membrane-associated functions. Together with other published findings, there is a plethora of evidence demonstrating SUMO-mediated regulation at membranes and leading us to propose that SENP2 serves as the master regulator within that particular domain. However, it is also important to consider the possibility that SENP2 evolved to contain a

membrane-targeting signal as a way to restrict its activity and the de-conjugation of soluble nucleoplasmic and cytoplasmic proteins. In other words, membrane targeting could function to both restrict and promote specific SENP2-substrate interactions. In fact, there is evidence showing that NPC-association of the SUMO isopeptidase Ulp1 in yeast has an essential role in preventing de-conjugation of soluble sumoylated proteins (Li and Hochstrasser, 2003). It would be interesting to fully investigate whether such mechanism of regulation also exists in mammalian cells. Again, a SENP2^{I8D} knock-in mouse model can be utilized to determine the physiological effects of losing SENP2-membrane association. Overall, the significance of SENP2-membrane interaction and how it relates to the overall physiological needs of the cell is worth pursuing.

BIBLIOGRAPHY

- Ahner, A., Gong, X., and Frizzell, R.A. (2013). Cystic fibrosis transmembrane conductance regulator degradation: cross-talk between the ubiquitylation and SUMOylation pathways. *FEBS J* 280, 4430-4438.
- Alber, F., Dokudovskaya, S., Veenhoff, L.M., Zhang, W., Kipper, J., Devos, D., Suprpto, A., Karni-Schmidt, O., Williams, R., Chait, B.T., Sali, A., and Rout, M.P. (2007). The molecular architecture of the nuclear pore complex. *Nature* 450, 695-701.
- Anderson, C.A., and Blackstone, C. (2013). SUMO wrestling with Drp1 at mitochondria. *The EMBO journal* 32, 1496-1498.
- Baba, D., Maita, N., Jee, J.G., Uchimura, Y., Saitoh, H., Sugasawa, K., Hanaoka, F., Tochio, H., Hiroaki, H., and Shirakawa, M. (2005). Crystal structure of thymine DNA glycosylase conjugated to SUMO-1. *Nature* 435, 979-982.
- Bailey, D., and O'Hare, P. (2004). Characterization of the localization and proteolytic activity of the SUMO-specific protease, SENP1. *The Journal of biological chemistry* 279, 692-703.
- Bastos, R., Lin, A., Enarson, M., and Burke, B. (1996). Targeting and function in mRNA export of nuclear pore complex protein Nup153. *J Cell Biol* 134, 1141-1156.
- Benson, M., Iniguez-Lluhi, J.A., and Martens, J. (2017). Sumo Modification of Ion Channels. *Adv Exp Med Biol* 963, 127-141.
- Bernier-Villamor, V., Sampson, D.A., Matunis, M.J., and Lima, C.D. (2002). Structural basis for E2-mediated SUMO conjugation revealed by a complex between ubiquitin-conjugating enzyme Ubc9 and RanGAP1. *Cell* 108, 345-356.
- Bozidis, P., Williamson, C.D., and Colberg-Poley, A.M. (2007). Isolation of endoplasmic reticulum, mitochondria, and mitochondria-associated membrane fractions from transfected cells and from human cytomegalovirus-infected primary fibroblasts. *Curr Protoc Cell Biol Chapter 3*, Unit 3 27.
- Braschi, E., Zunino, R., and McBride, H.M. (2009). MAPL is a new mitochondrial SUMO E3 ligase that regulates mitochondrial fission. *EMBO Rep* 10, 748-754.
- Cappadocia, L., and Lima, C.D. (2017). Ubiquitin-like Protein Conjugation: Structures, Chemistry, and Mechanism. *Chem Rev*.
- CDC. (2017). Health, United States, 2016: With Chartbook on Long-term Trends in Health. National Center for Health Statistics.

Chaudhary, N., and Courvalin, J.C. (1993). Stepwise reassembly of the nuclear envelope at the end of mitosis. *J Cell Biol* *122*, 295-306.

Choi, H., Liu, G., Mellacheruvu, D., Tyers, M., Gingras, A.C., and Nesvizhskii, A.I. (2012). Analyzing protein-protein interactions from affinity purification-mass spectrometry data with SAINT. *Curr Protoc Bioinformatics Chapter 8*, Unit8 15.

Chow, K.H., Elgort, S., Dasso, M., Powers, M.A., and Ullman, K.S. (2014). The SUMO proteases SENP1 and SENP2 play a critical role in nucleoporin homeostasis and nuclear pore complex function. *Molecular biology of the cell* *25*, 160-168.

Chow, K.H., Elgort, S., Dasso, M., and Ullman, K.S. (2012). Two distinct sites in Nup153 mediate interaction with the SUMO proteases SENP1 and SENP2. *Nucleus* *3*, 349-358.

Christianson, J.C., Olzmann, J.A., Shaler, T.A., Sowa, M.E., Bennett, E.J., Richter, C.M., Tyler, R.E., Greenblatt, E.J., Harper, J.W., and Kopito, R.R. (2011). Defining human ERAD networks through an integrative mapping strategy. *Nature cell biology* *14*, 93-105.

Citro, S., and Chiocca, S. (2013). Sumo paralogs: redundancy and divergencies. *Frontiers in bioscience* *5*, 544-553.

Coyaud, E., Mis, M., Laurent, E.M., Dunham, W.H., Couzens, A.L., Robitaille, M., Gingras, A.C., Angers, S., and Raught, B. (2015). BioID-based Identification of Skp Cullin F-box (SCF) β -TrCP1/2 E3 Ligase Substrates. *Mol Cell Proteomics* *14*, 1781-1795.

Craig, R., and Beavis, R.C. (2004). TANDEM: matching proteins with tandem mass spectra. *Bioinformatics* *20*, 1466-1467.

Cubenas-Potts, C., Goeres, J.D., and Matunis, M.J. (2013). SENP1 and SENP2 Affect Spatial and Temporal Control of Sumoylation in Mitosis. *Molecular biology of the cell*.

Da Silva-Ferrada, E., Ribeiro-Rodrigues, T.M., Rodriguez, M.S., and Girao, H. (2016). Proteostasis and SUMO in the heart. *Int J Biochem Cell Biol* *79*, 443-450.

Desterro, J.M., Thomson, J., and Hay, R.T. (1997). Ubch9 conjugates SUMO but not ubiquitin. *FEBS Lett* *417*, 297-300.

Deutsch, E.W., Mendoza, L., Shteynberg, D., Farrah, T., Lam, H., Tasman, N., Sun, Z., Nilsson, E., Pratt, B., Prazen, B., Eng, J.K., Martin, D.B., Nesvizhskii, A.I., and Aebersold, R. (2010). A guided tour of the Trans-Proteomic Pipeline. *Proteomics* *10*, 1150-1159.

- Dorval, V., and Fraser, P.E. (2006). Small ubiquitin-like modifier (SUMO) modification of natively unfolded proteins tau and alpha-synuclein. *The Journal of biological chemistry* *281*, 9919-9924.
- Doucet, C.M., and Hetzer, M.W. (2010). Nuclear pore biogenesis into an intact nuclear envelope. *Chromosoma* *119*, 469-477.
- Doucet, C.M., Talamas, J.A., and Hetzer, M.W. (2010). Cell cycle-dependent differences in nuclear pore complex assembly in metazoa. *Cell* *141*, 1030-1041.
- Drag, M., and Salvesen, G.S. (2008). DeSUMOylating enzymes--SENPs. *IUBMB Life* *60*, 734-742.
- Drin, G., and Antony, B. (2010). Amphipathic helices and membrane curvature. *FEBS Lett* *584*, 1840-1847.
- Drin, G., Casella, J.F., Gautier, R., Boehmer, T., Schwartz, T.U., and Antony, B. (2007). A general amphipathic alpha-helical motif for sensing membrane curvature. *Nat Struct Mol Biol* *14*, 138-146.
- Enserink, J.M. (2015). Sumo and the cellular stress response. *Cell Div* *10*, 4.
- Fischer, A.H., Taysavang, P., Weber, C.J., and Wilson, K.L. (2001). Nuclear envelope organization in papillary thyroid carcinoma. *Histol Histopathol* *16*, 1-14.
- Floch, A.G., Taresté, D., Fuchs, P.F., Chadrin, A., Naciri, I., Leger, T., Schlenstedt, G., Palancade, B., and Doye, V. (2015). Nuclear pore targeting of the yeast Pom33 nucleoporin depends on karyopherin and lipid binding. *J Cell Sci* *128*, 305-316.
- Fu, J., Yu, H.M., Chiu, S.Y., Mirando, A.J., Maruyama, E.O., Cheng, J.G., and Hsu, W. (2014). Disruption of SUMO-specific protease 2 induces mitochondria mediated neurodegeneration. *PLoS genetics* *10*, e1004579.
- Gant, T.M., Harris, C.A., and Wilson, K.L. (1999). Roles of LAP2 proteins in nuclear assembly and DNA replication: truncated LAP2beta proteins alter lamina assembly, envelope formation, nuclear size, and DNA replication efficiency in *Xenopus laevis* extracts. *J Cell Biol* *144*, 1083-1096.
- Giorgino, F., de Robertis, O., Laviola, L., Montrone, C., Perrini, S., McCowen, K.C., and Smith, R.J. (2000). The sentrin-conjugating enzyme mUbc9 interacts with GLUT4 and GLUT1 glucose transporters and regulates transporter levels in skeletal muscle cells. *Proceedings of the National Academy of Sciences of the United States of America* *97*, 1125-1130.

- Goeres, J., Chan, P.K., Mukhopadhyay, D., Zhang, H., Raught, B., and Matunis, M.J. (2011). The SUMO-specific isopeptidase SENP2 associates dynamically with nuclear pore complexes through interactions with karyopherins and the Nup107-160 nucleoporin subcomplex. *Molecular biology of the cell* 22, 4868-4882.
- Gong, L., and Yeh, E.T. (2006). Characterization of a family of nucleolar SUMO-specific proteases with preference for SUMO-2 or SUMO-3. *The Journal of biological chemistry* 281, 15869-15877.
- Gong, X., Ahner, A., Roldan, A., Lukacs, G.L., Thibodeau, P.H., and Frizzell, R.A. (2016). Non-native Conformers of Cystic Fibrosis Transmembrane Conductance Regulator NBD1 Are Recognized by Hsp27 and Conjugated to SUMO-2 for Degradation. *The Journal of biological chemistry* 291, 2004-2017.
- Guerra de Souza, A.C., Prediger, R.D., and Cimarosti, H. (2016). SUMO-regulated mitochondrial function in Parkinson's disease. *J Neurochem* 137, 673-686.
- Guna, A., Volkmar, N., Christianson, J.C., and Hegde, R.S. (2018). The ER membrane protein complex is a transmembrane domain insertase. *Science (New York, N.Y.)* 359, 470-473.
- Gupta, G.D., Coyaud, E., Goncalves, J., Mojarad, B.A., Liu, Y., Wu, Q., Gheiratmand, L., Comartin, D., Tkach, J.M., Cheung, S.W., Bashkurov, M., Hasegan, M., Knight, J.D., Lin, Z.Y., Schueler, M., Hildebrandt, F., Moffat, J., Gingras, A.C., Raught, B., and Pelletier, L. (2015). A Dynamic Protein Interaction Landscape of the Human Centrosome-Cilium Interface. *Cell* 163, 1484-1499.
- Guzzo, C.M., Berndsen, C.E., Zhu, J., Gupta, V., Datta, A., Greenberg, R.A., Wolberger, C., and Matunis, M.J. (2012). RNF4-dependent hybrid SUMO-ubiquitin chains are signals for RAP80 and thereby mediate the recruitment of BRCA1 to sites of DNA damage. *Sci Signal* 5, ra88.
- Hang, J., and Dasso, M. (2002). Association of the human SUMO-1 protease SENP2 with the nuclear pore. *The Journal of biological chemistry* 277, 19961-19966.
- Hardeland, U., Steinacher, R., Jiricny, J., and Schar, P. (2002). Modification of the human thymine-DNA glycosylase by ubiquitin-like proteins facilitates enzymatic turnover. *The EMBO journal* 21, 1456-1464.
- Harder, Z., Zunino, R., and McBride, H. (2004). Sumo1 conjugates mitochondrial substrates and participates in mitochondrial fission. *Curr Biol* 14, 340-345.

- Harr, J.C., Luperchio, T.R., Wong, X., Cohen, E., Wheelan, S.J., and Reddy, K.L. (2015). Directed targeting of chromatin to the nuclear lamina is mediated by chromatin state and A-type lamins. *J Cell Biol* 208, 33-52.
- Hay, R.T. (2005). SUMO: a history of modification. *Molecular cell* 18, 1-12.
- Hay, R.T. (2013). Decoding the SUMO signal. *Biochemical Society transactions* 41, 463-473.
- Hecker, C.M., Rabiller, M., Haglund, K., Bayer, P., and Dikic, I. (2006). Specification of SUMO1- and SUMO2-interacting motifs. *The Journal of biological chemistry* 281, 16117-16127.
- Hendriks, I.A., D'Souza, R.C., Chang, J.G., Mann, M., and Vertegaal, A.C. (2015). System-wide identification of wild-type SUMO-2 conjugation sites. *Nat Commun* 6, 7289.
- Hendriks, I.A., and Vertegaal, A.C. (2016). A comprehensive compilation of SUMO proteomics. *Nat Rev Mol Cell Biol* 17, 581-595.
- Hickey, C.M., Wilson, N.R., and Hochstrasser, M. (2012). Function and regulation of SUMO proteases. *Nat Rev Mol Cell Biol* 13, 755-766.
- Hochstrasser, M. (2009). Introduction to intracellular protein degradation. *Chem Rev* 109, 1479-1480.
- Itahana, Y., Yeh, E.T., and Zhang, Y. (2006). Nucleocytoplasmic shuttling modulates activity and ubiquitination-dependent turnover of SUMO-specific protease 2. *Molecular and cellular biology* 26, 4675-4689.
- Johnson, E.S. (2004). Protein modification by SUMO. *Annu Rev Biochem* 73, 355-382.
- Johnson, E.S., and Blobel, G. (1997). Ubc9p is the conjugating enzyme for the ubiquitin-like protein Smt3p. *The Journal of biological chemistry* 272, 26799-26802.
- Johnson, E.S., Schwienhorst, I., Dohmen, R.J., and Blobel, G. (1997). The ubiquitin-like protein Smt3p is activated for conjugation to other proteins by an Aos1p/Uba2p heterodimer. *The EMBO journal* 16, 5509-5519.
- Jonikas, M.C., Collins, S.R., Denic, V., Oh, E., Quan, E.M., Schmid, V., Weibezahn, J., Schwappach, B., Walter, P., Weissman, J.S., and Schuldiner, M. (2009). Comprehensive characterization of genes required for protein folding in the endoplasmic reticulum. *Science (New York, N.Y.)* 323, 1693-1697.

Kagey, M.H., Melhuish, T.A., and Wotton, D. (2003). The polycomb protein Pc2 is a SUMO E3. *Cell* *113*, 127-137.

Kerscher, O. (2007). SUMO junction-what's your function? New insights through SUMO-interacting motifs. *EMBO Rep* *8*, 550-555.

Kerscher, O., Felberbaum, R., and Hochstrasser, M. (2006). Modification of proteins by ubiquitin and ubiquitin-like proteins. *Annu Rev Cell Dev Biol* *22*, 159-180.

Kessner, D., Chambers, M., Burke, R., Agus, D., and Mallick, P. (2008). ProteoWizard: open source software for rapid proteomics tools development. *Bioinformatics* *24*, 2534-2536.

Kim, J.H., Choi, H.J., Kim, B., Kim, M.H., Lee, J.M., Kim, I.S., Lee, M.H., Choi, S.J., Kim, K.I., Kim, S.I., Chung, C.H., and Baek, S.H. (2006). Roles of sumoylation of a reptin chromatin-remodelling complex in cancer metastasis. *Nature cell biology* *8*, 631-639.

Kupke, T., Di Cecco, L., Muller, H.M., Neuner, A., Adolf, F., Wieland, F., Nickel, W., and Schiebel, E. (2011). Targeting of Nbp1 to the inner nuclear membrane is essential for spindle pole body duplication. *The EMBO journal* *30*, 3337-3352.

Lahiri, S., Chao, J.T., Tavassoli, S., Wong, A.K., Choudhary, V., Young, B.P., Loewen, C.J., and Prinz, W.A. (2014). A conserved endoplasmic reticulum membrane protein complex (EMC) facilitates phospholipid transfer from the ER to mitochondria. *PLoS Biol* *12*, e1001969.

Lee, S., Henderson, M.J., Schiffhauer, E., Despanie, J., Henry, K., Kang, P.W., Walker, D., McClure, M.L., Wilson, L., Sorscher, E.J., and Zeitlin, P.L. (2014). Interference with ubiquitination in CFTR modifies stability of core glycosylated and cell surface pools. *Molecular and cellular biology* *34*, 2554-2565.

Li, S.J., and Hochstrasser, M. (1999). A new protease required for cell-cycle progression in yeast. *Nature* *398*, 246-251.

Li, S.J., and Hochstrasser, M. (2000). The yeast ULP2 (SMT4) gene encodes a novel protease specific for the ubiquitin-like Smt3 protein. *Molecular and cellular biology* *20*, 2367-2377.

Li, S.J., and Hochstrasser, M. (2003). The Ulp1 SUMO isopeptidase: distinct domains required for viability, nuclear envelope localization, and substrate specificity. *J Cell Biol* *160*, 1069-1081.

- Liu, G., Zhang, J., Larsen, B., Stark, C., Breitkreutz, A., Lin, Z.Y., Breitkreutz, B.J., Ding, Y., Colwill, K., Pasculescu, A., Pawson, T., Wrana, J.L., Nesvizhskii, A.I., Raught, B., Tyers, M., and Gingras, A.C. (2010). ProHits: integrated software for mass spectrometry-based interaction proteomics. *Nat Biotechnol* 28, 1015-1017.
- Liu, Y., Zhao, D., Qiu, F., Zhang, L.L., Liu, S.K., Li, Y.Y., Liu, M.T., Wu, D., Wang, J.X., Ding, X.Q., Liu, Y.X., Dong, C.J., Shao, X.Q., Yang, B.F., and Chu, W.F. (2017). Manipulating PML SUMOylation via Silencing UBC9 and RNF4 Regulates Cardiac Fibrosis. *Mol Ther* 25, 666-678.
- Mahadevan, K., Zhang, H., Akef, A., Cui, X.A., Gueroussov, S., Cenik, C., Roth, F.P., and Palazzo, A.F. (2013). RanBP2/Nup358 potentiates the translation of a subset of mRNAs encoding secretory proteins. *PLoS Biol* 11, e1001545.
- Mahajan, R., Delphin, C., Guan, T., Gerace, L., and Melchior, F. (1997). A small ubiquitin-related polypeptide involved in targeting RanGAP1 to nuclear pore complex protein RanBP2. *Cell* 88, 97-107.
- Makhnevych, T., Sydorsky, Y., Xin, X., Srikumar, T., Vizeacoumar, F.J., Jeram, S.M., Li, Z., Bahr, S., Andrews, B.J., Boone, C., and Raught, B. (2009). Global map of SUMO function revealed by protein-protein interaction and genetic networks. *Molecular cell* 33, 124-135.
- Martins, W.C., Tasca, C.I., and Cimarosti, H. (2016). Battling Alzheimer's Disease: Targeting SUMOylation-Mediated Pathways. *Neurochem Res* 41, 568-578.
- Matunis, M.J., Coutavas, E., and Blobel, G. (1996). A novel ubiquitin-like modification modulates the partitioning of the Ran-GTPase-activating protein RanGAP1 between the cytosol and the nuclear pore complex. *J Cell Biol* 135, 1457-1470.
- Matunis, M.J., Zhang, X.D., and Ellis, N.A. (2006). SUMO: the glue that binds. *Dev Cell* 11, 596-597.
- McCaffery, J.M., and Farquhar, M.G. (1995). Localization of GTPases by indirect immunofluorescence and immunoelectron microscopy. *Methods Enzymol* 257, 259-279.
- Mendler, L., Braun, T., and Muller, S. (2016). The Ubiquitin-Like SUMO System and Heart Function: From Development to Disease. *Circ Res* 118, 132-144.
- Meng, X., Clews, J., Kargas, V., Wang, X., and Ford, R.C. (2017). The cystic fibrosis transmembrane conductance regulator (CFTR) and its stability. *Cell Mol Life Sci* 74, 23-38.

Meszaros, N., Cibulka, J., Mendiburo, M.J., Romanauska, A., Schneider, M., and Kohler, A. (2015). Nuclear pore basket proteins are tethered to the nuclear envelope and can regulate membrane curvature. *Dev Cell* 33, 285-298.

Mikolajczyk, J., Drag, M., Bekes, M., Cao, J.T., Ronai, Z., and Salvesen, G.S. (2007). Small ubiquitin-related modifier (SUMO)-specific proteases: profiling the specificities and activities of human SENPs. *The Journal of biological chemistry* 282, 26217-26224.

Mukhopadhyay, D., and Dasso, M. (2007). Modification in reverse: the SUMO proteases. *Trends Biochem Sci* 32, 286-295.

Nayak, A., and Muller, S. (2014). SUMO-specific proteases/isopeptidases: SENPs and beyond. *Genome biology* 15, 422.

Neyret-Kahn, H., Benhamed, M., Ye, T., Le Gras, S., Cossec, J.C., Lapaquette, P., Bischof, O., Ouspenskaia, M., Dasso, M., Seeler, J., Davidson, I., and Dejean, A. (2013). Sumoylation at chromatin governs coordinated repression of a transcriptional program essential for cell growth and proliferation. *Genome Res* 23, 1563-1579.

Nishida, T., Kaneko, F., Kitagawa, M., and Yasuda, H. (2001). Characterization of a novel mammalian SUMO-1/Smt3-specific isopeptidase, a homologue of rat axam, which is an axin-binding protein promoting beta-catenin degradation. *The Journal of biological chemistry* 276, 39060-39066.

O'Riordan, C.R., Lachapelle, A.L., Marshall, J., Higgins, E.A., and Cheng, S.H. (2000). Characterization of the oligosaccharide structures associated with the cystic fibrosis transmembrane conductance regulator. *Glycobiology* 10, 1225-1233.

Ochaba, J., Monteys, A.M., O'Rourke, J.G., Reidling, J.C., Steffan, J.S., Davidson, B.L., and Thompson, L.M. (2016). PIAS1 Regulates Mutant Huntingtin Accumulation and Huntington's Disease-Associated Phenotypes In Vivo. *Neuron* 90, 507-520.

Odeh, H.M., Coyaud, E., Raught, B., and Matunis, M.J. (2018). The SUMO-Specific Isopeptidase SENP2 is Targeted to Intracellular Membranes via a Predicted N-Terminal Amphipathic alpha-Helix. *Molecular biology of the cell*, mbcE17070445.

Pedrioli, P.G. (2010). Trans-proteomic pipeline: a pipeline for proteomic analysis. *Methods Mol Biol* 604, 213-238.

Pichler, A., Gast, A., Seeler, J.S., Dejean, A., and Melchior, F. (2002). The nucleoporin RanBP2 has SUMO1 E3 ligase activity. *Cell* 108, 109-120.

Pickart, C.M., and Eddins, M.J. (2004). Ubiquitin: structures, functions, mechanisms. *Biochimica et biophysica acta* *1695*, 55-72.

Prunuske, A.J., Liu, J., Elgort, S., Joseph, J., Dasso, M., and Ullman, K.S. (2006). Nuclear envelope breakdown is coordinated by both Nup358/RanBP2 and Nup153, two nucleoporins with zinc finger modules. *Molecular biology of the cell* *17*, 760-769.

Qi, Y., Wang, J., Bomben, V.C., Li, D.P., Chen, S.R., Sun, H., Xi, Y., Reed, J.G., Cheng, J., Pan, H.L., Noebels, J.L., and Yeh, E.T. (2014). Hyper-SUMOylation of the Kv7 Potassium Channel Diminishes the M-Current Leading to Seizures and Sudden Death. *Neuron* *83*, 1159-1171.

Rajan, S., Plant, L.D., Rabin, M.L., Butler, M.H., and Goldstein, S.A. (2005). Sumoylation silences the plasma membrane leak K⁺ channel K2P1. *Cell* *121*, 37-47.

Richard, M., Boulin, T., Robert, V.J., Richmond, J.E., and Bessereau, J.L. (2013). Biosynthesis of ionotropic acetylcholine receptors requires the evolutionarily conserved ER membrane complex. *Proceedings of the National Academy of Sciences of the United States of America* *110*, E1055-1063.

Roux, K.J., Kim, D.I., and Burke, B. (2013). BioID: a screen for protein-protein interactions. *Curr Protoc Protein Sci* *74*, Unit 19 23.

Rytinki, M.M., Kaikkonen, S., Pehkonen, P., Jaaskelainen, T., and Palvimo, J.J. (2009). PIAS proteins: pleiotropic interactors associated with SUMO. *Cell Mol Life Sci* *66*, 3029-3041.

Sadler, J.B., Bryant, N.J., Gould, G.W., and Welburn, C.R. (2013). Posttranslational modifications of GLUT4 affect its subcellular localization and translocation. *Int J Mol Sci* *14*, 9963-9978.

Saitoh, H., and Hinchey, J. (2000). Functional heterogeneity of small ubiquitin-related protein modifiers SUMO-1 versus SUMO-2/3. *The Journal of biological chemistry* *275*, 6252-6258.

Sapay, N., Guermeur, Y., and Deleage, G. (2006). Prediction of amphipathic in-plane membrane anchors in monotopic proteins using a SVM classifier. *BMC Bioinformatics* *7*, 255.

Sarge, K.D., and Park-Sarge, O.K. (2011). SUMO and its role in human diseases. *Int Rev Cell Mol Biol* *288*, 167-183.

Satoh, T., Ohba, A., Liu, Z., Inagaki, T., and Satoh, A.K. (2015). dPob/EMC is essential for biosynthesis of rhodopsin and other multi-pass membrane proteins in *Drosophila* photoreceptors. *eLife* 4.

Schmidt, P.M., Sparrow, L.G., Attwood, R.M., Xiao, X., Adams, T.E., and McKimm-Breschkin, J.L. (2012). Taking down the FLAG! How insect cell expression challenges an established tag-system. *PLoS One* 7, e37779.

Schulz, S., Chachami, G., Kozaczekiewicz, L., Winter, U., Stankovic-Valentin, N., Haas, P., Hofmann, K., Urlaub, H., Ovaas, H., Wittbrodt, J., Meulmeester, E., and Melchior, F. (2012). Ubiquitin-specific protease-like 1 (USPL1) is a SUMO isopeptidase with essential, non-catalytic functions. *EMBO Rep* 13, 930-938.

Seeler, J.S., and Dejean, A. (2017). SUMO and the robustness of cancer. *Nat Rev Cancer* 17, 184-197.

Shen, T.H., Lin, H.K., Scaglioni, P.P., Yung, T.M., and Pandolfi, P.P. (2006). The mechanisms of PML-nuclear body formation. *Molecular cell* 24, 331-339.

Shin, E.J., Shin, H.M., Nam, E., Kim, W.S., Kim, J.H., Oh, B.H., and Yun, Y. (2012). DeSUMOylating isopeptidase: a second class of SUMO protease. *EMBO Rep* 13, 339-346.

Simon, D.N., Domaradzki, T., Hofmann, W.A., and Wilson, K.L. (2013). Lamin A tail modification by SUMO1 is disrupted by familial partial lipodystrophy-causing mutations. *Molecular biology of the cell* 24, 342-350.

Song, J., Durrin, L.K., Wilkinson, T.A., Krontiris, T.G., and Chen, Y. (2004). Identification of a SUMO-binding motif that recognizes SUMO-modified proteins. *Proceedings of the National Academy of Sciences of the United States of America* 101, 14373-14378.

Souquet, B., and Doye, V. (2015). Bending or Building: Multifaceted Functions of Amphipathic Helices in Basket Nucleoporins. *Dev Cell* 33, 626-628.

Steinacher, R., and Schar, P. (2005). Functionality of human thymine DNA glycosylase requires SUMO-regulated changes in protein conformation. *Curr Biol* 15, 616-623.

Tammsalu, T., Matic, I., Jaffray, E.G., Ibrahim, A.F.M., Tatham, M.H., and Hay, R.T. (2014). Proteome-wide identification of SUMO2 modification sites. *Sci Signal* 7, rs2.

Tanaka, K. (2009). The proteasome: overview of structure and functions. *Proc Jpn Acad Ser B Phys Biol Sci* 85, 12-36.

Tatham, M.H., Geoffroy, M.C., Shen, L., Plechanovova, A., Hattersley, N., Jaffray, E.G., Palvimo, J.J., and Hay, R.T. (2008). RNF4 is a poly-SUMO-specific E3 ubiquitin ligase required for arsenic-induced PML degradation. *Nature cell biology* *10*, 538-546.

Tatham, M.H., Jaffray, E., Vaughan, O.A., Desterro, J.M., Botting, C.H., Naismith, J.H., and Hay, R.T. (2001). Polymeric chains of SUMO-2 and SUMO-3 are conjugated to protein substrates by SAE1/SAE2 and Ubc9. *The Journal of biological chemistry* *276*, 35368-35374.

Teo, G., Liu, G., Zhang, J., Nesvizhskii, A.I., Gingras, A.C., and Choi, H. (2014). SAINTexpress: improvements and additional features in Significance Analysis of INTeractome software. *J Proteomics* *100*, 37-43.

Tu-Sekine, B., and Raben, D.M. (2012). Dual regulation of diacylglycerol kinase (DGK)-theta: polybasic proteins promote activation by phospholipids and increase substrate affinity. *The Journal of biological chemistry* *287*, 41619-41627.

Vollmer, B., Lorenz, M., Moreno-Andres, D., Bodenhofer, M., De Magistris, P., Astrinidis, S.A., Schooley, A., Flotenmeyer, M., Leptihn, S., and Antonin, W. (2015). Nup153 Recruits the Nup107-160 Complex to the Inner Nuclear Membrane for Interphasic Nuclear Pore Complex Assembly. *Dev Cell* *33*, 717-728.

Wasik, U., and Filipek, A. (2014). Non-nuclear function of sumoylated proteins. *Biochimica et biophysica acta*.

Wideman, J.G. (2015). The ubiquitous and ancient ER membrane protein complex (EMC): tether or not? *F1000Research* *4*, 624.

Wilke, M., Buijs-Offerman, R.M., Aarbiou, J., Colledge, W.H., Sheppard, D.N., Touqui, L., Bot, A., Jorna, H., de Jonge, H.R., and Scholte, B.J. (2011). Mouse models of cystic fibrosis: phenotypic analysis and research applications. *J Cyst Fibros* *10 Suppl 2*, S152-171.

Wilson, V.G. (2017). Introduction to Sumoylation. *Adv Exp Med Biol* *963*, 1-12.

Witty, J., Aguilar-Martinez, E., and Sharrocks, A.D. (2010). SENP1 participates in the dynamic regulation of Elk-1 SUMOylation. *Biochem J* *428*, 247-254.

Yang, Y., He, Y., Wang, X., Liang, Z., He, G., Zhang, P., Zhu, H., Xu, N., and Liang, S. (2017). Protein SUMOylation modification and its associations with disease. *Open Biol* *7*.

Yip, S.C., Cotteret, S., and Chernoff, J. (2012). Sumoylated protein tyrosine phosphatase 1B localizes to the inner nuclear membrane and regulates the tyrosine phosphorylation of emerin. *J Cell Sci* 125, 310-316.

Yun, C., Wang, Y., Mukhopadhyay, D., Backlund, P., Kolli, N., Yergey, A., Wilkinson, K.D., and Dasso, M. (2008). Nucleolar protein B23/nucleophosmin regulates the vertebrate SUMO pathway through SENP3 and SENP5 proteases. *J Cell Biol* 183, 589-595.

Yunus, A.A., and Lima, C.D. (2009). Structure of the Siz/PIAS SUMO E3 ligase Siz1 and determinants required for SUMO modification of PCNA. *Molecular cell* 35, 669-682.

Zhang, H., Saitoh, H., and Matunis, M.J. (2002). Enzymes of the SUMO modification pathway localize to filaments of the nuclear pore complex. *Molecular and cellular biology* 22, 6498-6508.

Zhang, X.D., Goeres, J., Zhang, H., Yen, T.J., Porter, A.C., and Matunis, M.J. (2008). SUMO-2/3 modification and binding regulate the association of CENP-E with kinetochores and progression through mitosis. *Molecular cell* 29, 729-741.

Zhang, Y.Q., and Sarge, K.D. (2008). Sumoylation regulates lamin A function and is lost in lamin A mutants associated with familial cardiomyopathies. *J Cell Biol* 182, 35-39.

CURRICULUM VITAE

HANA M. ODEH

143 E. North Ave, Apt. 3 - Baltimore, MD 21202
443-473-5611; hodeh2@jhmi.edu

EDUCATION

Doctor of Philosophy (PhD)

September 2018

Johns Hopkins School of Public Health, Baltimore MD – USA

Department of Biochemistry and Molecular Biology

Major: Biochemistry and Molecular Biology

Laboratory of Dr. Michael J. Matunis

Dissertation: Characterizing the regulation and function of the SUMO-specific isopeptidase SENP2

Master of Science (ScM)

August 2012

Johns Hopkins School of Public Health, Baltimore MD – USA

Department of Biochemistry and Molecular Biology

Major: Biochemistry and Molecular Biology – Focus on Reproductive and Cancer Biology

Laboratory of Dr. Barry Zirkin

Thesis: The regulation of the proliferation and differentiation of leydig stem cells in the adult testis

Bachelor of Science (BSc)

June 2008

University of Jordan, Amman – Jordan

Department of Biology

Major: Biological Sciences

HONORS AND AWARDS

Pierre Coulombe Travel Award

2018

Johns Hopkins School of Public Health

The American Society for Cell Biology Travel Award

2017

Sharon Krag Award for Excellence in Leadership

2015

Johns Hopkins School of Public Health

Delta Omega Scholarship Competition Award – Laboratory Category

2014

Johns Hopkins School of Public Health

J. William Fulbright Pre-Doctoral Student Scholarship Award

2010 – 2012

Jordanian-American Fulbright Commission for Educational Exchange

PUBLICATIONS

Odeh, H. M., Coyaud, E., Raught, B., and Matunis, M.J. (2018). The SUMO-specific isopeptidase SENP2 is targeted to intracellular membranes via a predicted N-terminal amphipathic α -helix. *Molecular Biology of the Cell*. 29(15):1878-1890

Odeh, H. M., Kleinguetl, C., Ge, R., Zirkin B. R., and Chen, H. (2014). Regulation of the proliferation and differentiation of leydig stem cells in the adult testis. *Biology of Reproduction*. 90(6):123

Gleason, J. E., Li, C. X., **Odeh, H. M.**, and Culotta, V. C. (2013). Species-specific activation of Cu/Zn SOD by its CCS copper chaperone in the pathogenic yeast candida

albicans. *Journal of Biological Inorganic Chemistry: JBIC: A Publication of the Society of Biological Inorganic Chemistry*. 19(4-5):595-603

Al-Aboudi, A., **Odeh, H.**, Khalid, A., Naz, Q., and Choudhary, M. I. (2009). Butyrylcholinesterase inhibitory activity of testosterone and some of its metabolites. *Journal of Enzyme Inhibition and Medicinal Chemistry*. 24(2), 553-558

PRESENTATIONS

Oral Presentations

Biochemistry and Molecular Biology Departmental Retreat, Notre Dame of Maryland University, Baltimore, MD, April 2018

Gordon Research Seminar on Protein Transport Across Cell Membranes, Galveston, TX, March 2018

The Northeast Nuclear Envelope Meeting, Yale University, New Haven, CT, September 2017

Hopkins Ubiquitin Club, Johns Hopkins School of Public Health, Baltimore, MD, March 2017 and April 2014

Biochemistry and Molecular Biology Departmental Retreat, Sheppard Pratt Conference Center, Towson, MD, March 2015

SUMO Meeting hosted by Dr. Mary C. Dasso, National Institute of Health, Bethesda, MD, August 2014

Poster Presentations

Gordon Research Conference on Protein Transport Across Cell Membranes, Galveston, TX, March 2018

The American Society for Cell Biology Annual Meeting, Philadelphia, PA, December 2017

Biochemistry and Molecular Biology Departmental Retreat, Eisenhower Complex, Gettysburg, PA, April 2017

NCI Symposium on Chromosome Biology, National Institute of Health, Bethesda, MD, November 2016 and April 2015

Biochemistry and Molecular Biology Departmental Retreat, Sheppard Pratt Conference Center, Towson, MD, April 2016

RESEARCH

Johns Hopkins School of Public Health

Baltimore, MD

Graduate Researcher; Advisor: Michael J. Matunis, PhD

2013 – 2018

Characterizing the localization and functions of the SUMO-specific isopeptidase SENP2

Developed a method for capturing SENP2 substrates (SUMO Capture) by generating inducible stable cell lines expressing various SENP2 mutants, Co-immunoprecipitation, and mass spectrometry

Identified a unique N-terminal amphipathic α -helix in SENP2 using site-directed mutagenesis, immunofluorescence microscopy, and subcellular fractionation
 Analyzed mass spectrometry data to define SENP2 binding partners
 Used protein affinity purification and liposome-binding methods to study SENP2-membrane interaction and regulation in vitro

Graduate Researcher; Advisor: Barry R. Zirkin, PhD 2011 – 2012

Regulation of the proliferation and differentiation of leydig stem cells in the adult testis
 Utilized rats as a model organism to study the proliferation and differentiation of leydig stem cells
 Studied the effects of platelet-derived growth factors (PDGFs) on leydig stem cell development by using isolated seminiferous tubules culture system
 Examined the proliferation of leydig stem cells using Click-iT EdU assay, and used radioimmunoassay to measure testosterone levels as an indicator for leydig stem cell differentiation

Biolab **Amman, Jordan**

Research Assistant; The Genographic Project 2009 – 2010

Study human ancestry and migratory history through analyzing patterns in DNA
 Developed consent forms and recruited participants for the Genographic Project
 Collected blood specimens and isolated DNA samples from individuals

University of Karachi – H.E.J. Research Institute of Chemistry **Karachi, Pakistan**

Research Assistant; Advisor: Amal Al-Aboudi, PhD Summer 2006

Testosterone metabolites and their activity as butyrylcholinesterase (BChE) inhibitors
 Tested several testosterone metabolites for their potency as BChE inhibitors using in vitro biochemical assays

TEACHING AND MENTORING

Johns Hopkins School of Public Health **Baltimore, MD**

Laboratory of Dr. Michael J. Matunis; Students trained:

Sharon Patray, Graduate rotation student for 7 weeks	2018
Ki'Juana Land, High school student (MERIT Program) for 5 weeks	2017
Zorawar Singh, Graduate student for 1 year	2016 – 2017
Danielle Bouchard, Graduate rotation student for 8 weeks	2015

Teaching Assistant; Graduate level courses:

Genomics in Public Health	Fall 2016
Principles of Cell Biology	Fall 2014
Biochemical and Biophysical Properties	2013 – 2014

Thread Program – Dunbar High School **Baltimore, MD**

Academic and personal mentor for high school students 2011 – 2018

Injaz Program – Public Middle Schools **Amman, Jordan**

Program provides training for a set of personal skills tailored for middle school students
 Course led and taught: Time management and problem-solving 2009 – 2010

RELEVANT EMPLOYMENT

Biolab	Amman, Jordan
Laboratory Technician; 45-50 hours/week	2008 – 2010
Checked-in patients and carried out phlebotomy procedures	
Executed and analyzed tests in several lab divisions including hematology, chemistry, bacteriology, and serology	
Operated and calibrated an assortment of laboratory testing equipment	
Confirmed test-result validity before reporting results to physicians and patients	
Prepared a comprehensive test guide and educational pamphlets for patients	
Trained and supervised new staff in several divisions	
University of Birmingham, School of Biosciences	Birmingham, England
Laboratory Technician; 35-40 hours/week	Summer 2007
Training at the Proteomics and Genomics service facility:	
Carried out PCR and real-time PCR reactions	
Prepared DNA samples and operated 3730 DNA Analyzer for DNA sequencing	

LEADERSHIP

Randallstown High School, STEM Fair	Baltimore, MD
Served as Judge for the Poster Competition	2017
Johns Hopkins School of Public Health	Baltimore, MD
The Biochemistry and Molecular Biology Departmental Retreat	2017
Served as Judge for oral presentations	
Delta Omega Poster Competition	2015
Served as Judge for the laboratory category	
Scientific Methods Workshop; Led by Tung-Tien Sun, PhD (NYU)	2014
Workshop tailored for pre-doctoral students, post-doctoral fellows	
Initiated and organized the first scientific methods workshop for all three lab-based science departments at school	
Student Assembly; Elected Department Student Representative	2012 – 2013
Served as member on the Community Affairs and the Communications Committees	
Student Assembly; Elected Vice-President of Social Affairs Committee	2011 – 2012
Organized school-wide social and cultural events	

REFERENCES

Michael J. Matunis, PhD
Professor and Interim Chair
Department of Biochemistry and Molecular Biology
Johns Hopkins School of Public Health
615 N. Wolfe Street, Room W8118
Baltimore, MD, 21205
410-614-6878
mmatuni1@jhu.edu